

UNIVERSITY OF NAPLES FEDERICO II

**PHD IN Chemical Sciences
XXVII CYCLE**

*Structure/activity evaluation of the bacterial
membrane constituents involved in the
immune system*

Alberto Maria Marzaioli

TUTOR
Dott.ssa Cristina De Castro

SUPERVISOR
Prof. Piero Pucci

Structure/activity evaluation of the bacterial membrane constituents involved in the immune system

Index

Part I: Introduction

Chapter I: Gram negative cell envelop; structure and functions of polysaccharide components of the outer membrane

1.1 Bacterial cell wall structure	8
1.2 Lipopolysaccharide; structure, function and biosynthesis	9
1.3 Lipid A; structure and biological activity	11
1.4 The Core oligosaccharide and O-specific Chain	14
1.5 Capsular polysaccharides (CPSs)	15

Part II: Results and discussion

Chapter II: Preparation of liposomes using oligosaccharides from *Rhizobiaceae* family

Introduction	18
2.1 Extraction purification and partially delipidation of LOS produced by <i>Rhizobium rubi</i> ^T	20
2.2 Preparation of liposomes	22
2.3 DLS and Cryo-TEM analyses of liposomes	23
2.3.1 DLS analyses	23
2.3.2 Cryo-TEM investigations	27
2.4 <i>In vitro</i> cytotoxicity tests	29
2.5 Conclusions	31

Chapter III: Identification and structural analysis of the Capsular polysaccharides from different clinical isolates of *Acinetobacter baumannii*, strains A74 , D36, F4, D78 and D46

<i>Introduction</i>	33
3.1 Isolation of different CPSs	34
3.2 Chemical and structural analyses of CPS from <i>A.baumannii</i> A74	34
3.2.1 Chemical analyses of CPS	35
3.2.2 NMR analyses of hydrolyzed CPS	36
3.3 Chemical and spectroscopical analyses of CPS from <i>A.baumannii</i> D36	44
3.3.1 Chemical analyses of CPS	45
3.3.2 NMR analyses of hydrolyzed CPS	47
3.3.3 Molecular mechanics calculations	50
3.3.4 NMR analysis of monosaccharide mixture	52
3.4 Chemical and spectroscopical analyses of CPS from <i>A.baumannii</i> F4	56
3.4.1 Chemical analyses of CPS	56
3.4.2 NMR analyses of CPS	57
3.5 Chemical and spectroscopical analyses of CPS from <i>A.baumannii</i> D46	61
3.5.1 Chemical analyses of CPS	61
3.5.2 NMR analyses of CPS	62
3.6 Chemical and spectroscopical analyses of CPS from <i>A.baumannii</i> D78	67
3.6.1 Chemical analyses of CPS	67
3.6.2 NMR analyses of CPS	69
3.7 Conclusions	74

Chapter IV: Identification and structural analysis of the Lipopolysaccharides from different bacteria present in C.S.C.M .Crypt Specific Core Microbiota

<i>Introduction</i>	77
4.1 Isolation and purification of LPS from <i>Stenotrophomonas BRT 12</i>	78
4.2 Chemical and structural analyses of LPS	79
4.2.1 Chemical analyses of LPS	79
4.2.2 NMR analyses of LPS	80
4.3 Isolation and purification of LPS from <i>Delphia 3OF</i>	84
4.3.1 Chemical analyses of LPS	84
4.3.2 NMR analyses of LPS	85
4.3.3 Structural characterization of Lipid-A	89
4.4 Isolation and purification LPS from <i>Acinetobacter 11G</i>	93

4.4.1 Chemical analyses of LPS	93
4.4.2 NMR analyses of LPS	94
4.5 Biological tests	98
4.6 Conclusions	101

Chapter V: Preparation of the building block for the synthesis of new glycoconjugates with potential activity against HIV-1

Introduction	104
5.1 Preparation of a carrier of chitoazido oligomers	106
5.1.1 Hydrolysis of chitosan polymers and derivatization of free amino function with an azide group	107
5.1.2 Chromatographic purification of different chito-oligomers	109
5.1.3 NMR analysis of different chito-oligomers	110
5.2 Conversion of yeast mannan polysaccharide in mannose oligosaccharides with a thiopropargyl linker at anomeric position	115
5.2.1 Acetolysis of yeast mannan	116
5.2.2 Preparation of thiomannopropargyl-oligosaccharides	116
5.2.3 Purification of different mannose oligosaccharides	117
5.2.3.1 Silica gel chromatography of the fully acetylated mixture and RP8-HPLC purification of deacetylated fractions (Method A)	117
5.2.3.2 Deacetylation of the oligosaccharide mixture and RP8-HPLC purification (Method B)	118
5.2.3.3 Deacetylation, size exclusion chromatography and RP8-HPLC purification of oligosaccharide mixture (Method C)	118
5.2.4 NMR analysis of different mannose oligosaccharides obtained	120
5.3 Conclusions	124

Part III: Experimental

Chapter VI: Experimental method

6.1 General (NMR, MALDI; GC-MS, DLS, CROMATOGRAPHIC PURIFICATION, HPLC)	128
6.2 Cell membrane constituents extraction.	129
6.2.1 <i>Rhizobium rubi</i> ^T	129
6.2.1.1 De-O-acylation of LOS from <i>Rhizobium rubi</i> ^T	130
6.2.2 <i>Acinetobacter baumannii</i> clinical isolates A74, D36, D78, D46, F4	131

6.2.3 <i>Acinetobacter parvus</i> 11G, <i>Stenotrophomonas maltophilia</i> (BRT112), <i>Delfia acidovorans</i> (30F)	132
6.2.3.1 <i>Acinetobacter parvus</i> 11G	132
6.2.3.2 <i>Stenotrophomonas maltophilia</i> (BRT112)	132
6.2.3.3 <i>Delfia acidovorans</i> (30F)	133
6.3 Methyl glycosides acetylated M.G.A. and fatty acid methyl esters F.A.M.E.	134
6.4 Partially methylated alditol acetates A.A.P.M ⁵ .	134
6.5 Octyl glycosides acetylated	135
6.6 Mild acid hydrolysis of CPSs	135
6.6.1 Mild hydrolysis and purification of CPS from <i>Acinetobacter baumannii</i> A74	136
6.6.2 Mild hydrolysis and purification of CPS from <i>Acinetobacter baumannii</i> D36	136
6.6.3 Mild hydrolysis and purification of CPS from <i>Acinetobacter baumannii</i> D78	137
6.7 Computational analysis	137
6.8 Total delipidation of different LPSs	138
6.9 Isolation of Lipid A from different bacteria and O-chain from different bacteria	138
6.10 Preparation of Liposomes ToThyRu/POPC/LOS	139
6.11 Hydrolysis of chitosan polymer and reduction of anomeric function	139
6.12 Azidation of chitosan free amino function	140
6.13 Chromatographic purification chito oligomers	140
6.14 Acetolysis of mannan polymer	141
6.15 Preparation of thiomannopropargyl-oligosaccharides	141
6.16 Purification of different mannose oligosaccharides	142
6.16.1 Silica gel chromatography of the fully acetylated mixture and RP8-HPLC purification of deacetylated fractions	142
6.16.2 Deacetylation of the oligosaccharide mixture and RP8-HPLC purification	
6.16.3 Deacetylation, size exclusion chromatography and RP8-HPLC purification of oligosaccharide mixture	

Part I: Introduction

Chapter I: Gram negative cell envelop; structure and functions of polysaccharide components of the outer membrane

1.1 Bacterial cell wall structure

All living organisms are classified into three macro-groups namely *Archea*, *Bacteria* and *Eukaryotes*. *Archea* and *Bacteria* are also classified as Prokaryotes, which differ from Eukaryotes for the lack of nucleus¹. Typically, *Archea* group includes all microorganisms that live in habit conditions that are unusual for the other microorganisms, such as critical pH values, high salinity or pressure. *Bacteria* are a group of microorganisms that are divided into two subclasses, Gram-negative and Gram-positive, depending on the different behaviour to colorimetric Gram test. This different response to Gram test is directly related to a different organization of the cell wall structure between the two microorganisms. Gram-positive bacteria cell walls are made up of a bilayered phospholipidic membrane surrounded by a thick layer of peptidoglycan (PGN). On the other hand Gram-negative bacteria produce a thin layer of peptidoglycan followed by an additional asymmetric phospholipidic bilayered membrane, the outer membrane (OM). The inner surface of this membrane is constituted by glycerophospholipids while the external part is composed of trans-membrane proteins and, for 75%, by lipopolysaccharides (LPSs)² (figure 1.1). Bacteria can also produce a third glycopolymer, the capsule polysaccharide (CPS), an high molecular weight polymer constituted by an oligosaccharide repeating unit, which presents different sugars joined together by specific linkages.

Surrounding the external surface of cell membrane PGN, LPSs and CPSs are strongly involved in different mechanisms, like adhesion, colonization and infection of host

organisms, thus the knowledge of oligosaccharidic moiety is fundamental to understand bacterial infection mechanism.

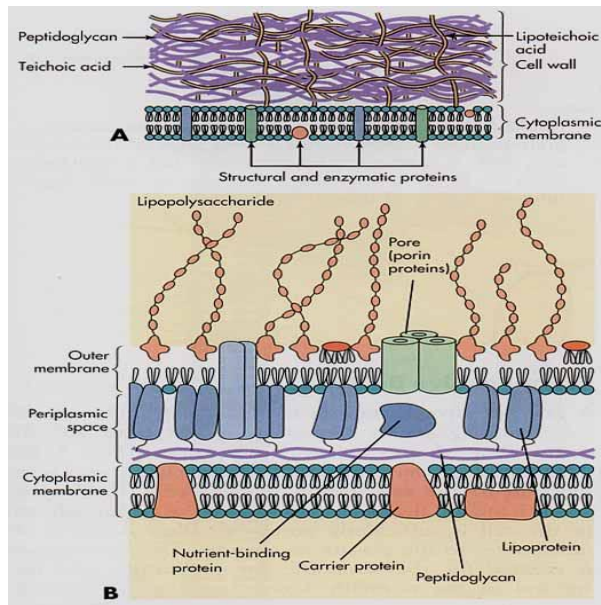


Figure 1.1: Structural differences between Gram positive (A) and Gram negative (B) cell envelope.

1.2 Lipopolysaccharide; structure, function and biosynthesis

Lipopolysaccharides are amphiphilic molecules, marker for Gram-negative microorganisms, and essential for bacterial survival. Structurally LPS can be divided in three regions, each of which has a different biological property: an external polysaccharide (**O-chain**), which is covalently linked to an oligosaccharide part (**core**), in turn, linked to a glycolipid portion (**Lipid A**). The O-chain polysaccharides, when present, are usually characterized by regular polysaccharide with repeating units consisting up to eight monosaccharides. Core region is composed by one to three residues of 2-keto-3-deoxy-D-manno-octulosonic acid (Kdo) a distinctive acid monosaccharide for all bacterial Core oligosaccharide, and heptose and hexose. Lipid-A is the highest conserved moiety in LPSs, produced by different species belonging to

the same bacterial genus. It is composed by a disaccharide backbone of glucosamine phosphorylated and acylated with a variable number and type of fatty and hydroxyl-fatty acid chains² (figure 1.2).

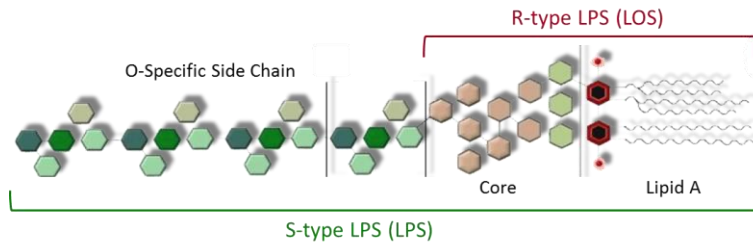


Figure 1.2: Gram negative bacteria LOS and LPS structure.

The biosynthesis of LPS is a complex process involving various steps that starts in the plasma membrane and finishes with the translocation of LPS to the outer membrane. In general, the Core oligosaccharide is assembled on Lipid-A, while O-antigen is independently assembled and then linked to Lipid-A-Core oligosaccharide. The lipid-A biosynthesis has been elucidated for *Escherichia coli*⁴(figure 1.3). All the steps are catalyzed by an enzyme that is present in a single copy in the whole genome. In the first step the UDP-GlcNAc acyltransferase (LpxA) promotes the acylation of nucleotide UDP-GlcNAc on C-3 of GlcNAc with a 3-hydroxymyristic acid. Different enzymes catalyze the tetra acylation of glucosamine disaccharide backbone; at this not yet complete Lipid-A two Kdo residues are then added forming Kdo₂-IV_A. This is further acylated to obtain hexa acylated lipid-A.

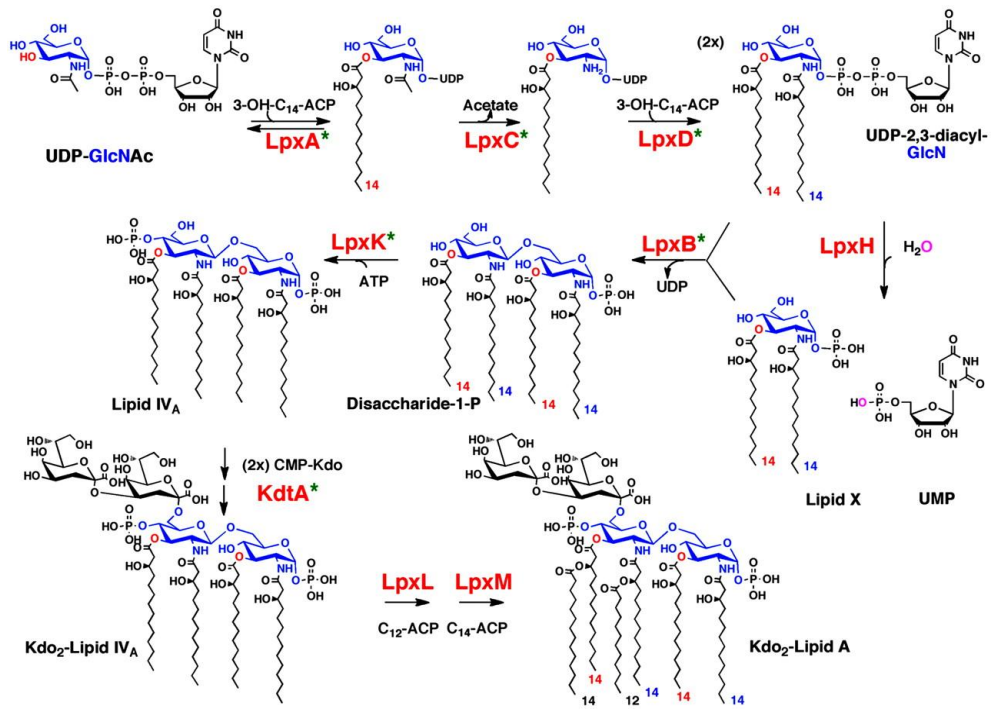


Figure 1.3: Biosynthetic pathway of Kdo₂-lipid A in *E. coli* K12

1.3 Lipid-A; structure and biological activity

Lipid A is the most conservative portion of LPS: its structure is conserved, with a few variations, among different bacterial strains that belong to the same family. Generally its structure is composed of a disaccharide of glucosamine, GlcN, β -1,6-linked. The reducing glucosamine (GlcN I) is phosphorylated at reducing position, while the non-reducing (GlcN II) presents a phosphate group at position 4. Both GlcN residues are acylated with primary 3-hydroxy fatty acids at positions 2 and 3 and hydroxyl group can be further acylated by second acyclic chains⁵(figure 1.4).

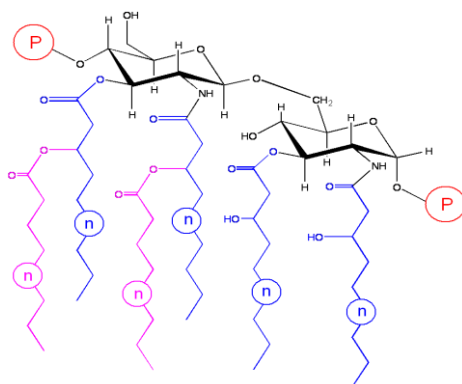


Figure 1.4: Schematic representation of Lipid A structure

Biologically, Lipid A is the real endotoxin moiety of LPS because it is recognized by innate immune system receptors from the pattern recognition receptors (PRRs), as pathogen associated molecular pattern (PAMPs). The inflammation mechanism (figure 1.5) involves interaction between Lipid A and Toll-like receptors 4 (TLR4); this is a complex mechanism that requires several accessory molecules^{6,7}. Initially, LPS is linked to a serum protein, LBP (lipid binding protein), that forms a complex with the Lipid A moiety of LPS, removing it from the outer membrane and therefore delivering the LPS to the glycoprotein mCD14. mCD14 mediates interaction of LPS with TLR4-MD2 complex (MD2 is a glycoprotein essential for the formation of

complex between LPS and TLR4). Interaction of LPS with TLR4 triggers the inflammatory cascade, leading to the production of several effectors molecules, such as cytokines and interleukins.

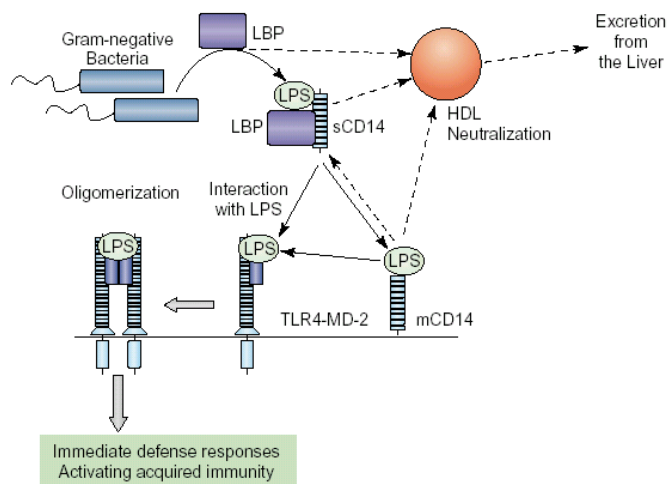


Figure 1.5: Gram negative infection: LPS recognition

It has been demonstrated that the bioactivity of lipid A is strictly dependent on its primary structure: variation in number, distribution of fatty acids or presence of polar groups strongly influence the three-dimensional arrangements and biological properties of these endotoxins. Lipid A, indeed, may act as agonistic or antagonistic molecule. In the latter case, in moderate concentration, it does not cause an inflammatory response. A lipid-A with agonistic action, instead, stimulates inflammatory response that can induce septic shock and cellular death. The toxicity of these molecules is dependent by their capacity of interaction with innate immune system receptors. These interactions are correlated, principally, to two structural parameters: the molecular shape of endotoxin and the tilt angle between the disaccharide backbone and the acyl chains (figure 1.6). The former reflects the three-dimensional structure assumed by LPS in the lipid bilayer and how it is exposed toward the external environment; while the tilt angle reveals the inclination of lipid A in respect to membrane surface⁸. These physical parameters reflect the exposure of

hydrophobic task to the receptors, thus the endotoxin affinity for the hydrophobic binding site of the innate immune receptors.

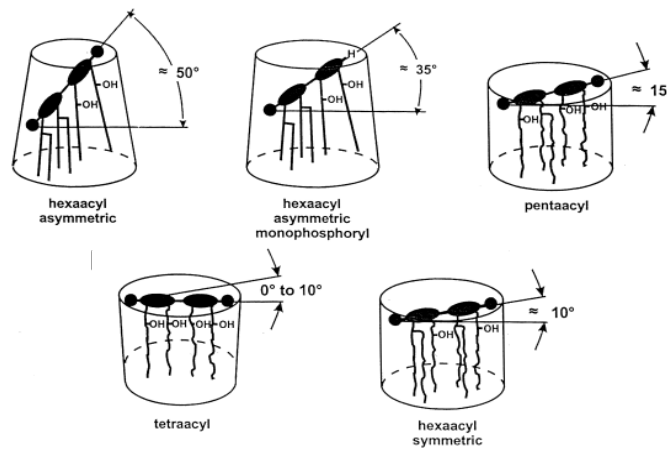


Figure 1.6: The inclination of sugar backbone in respect to the membrane surface (tilt angle) depends on the number and the distribution of acyl chains.

1.4 The Core oligosaccharide and *O*-specific chain

The core is composed of oligosaccharidic moiety, which include up to fifteen residues, directly linked to C-6 of Glc II. It is divided into two regions: the Inner core directly linked to Lipid A and the Outer-core that provides an attachment site for the *O*-chain. The Inner core is more conservative and presents always a peculiar residue, the Kdo which is directly involved in the linking with lipid A; often there are also heptose residues functionalized by phosphate, phosphoethanolamine. The Outer core region is the most exposed portion, often branched, and is characterized by high structural variability with respect to the inner core. It is commonly composed by neutral sugars, however it might contain also amino and acid residues.

In the rough bacteria the core oligosaccharide is the most exposed portion and it is recognized by adaptive immune system.

The *O*-chain is the polymeric portion of LPS and is produced only in the smooth-type bacteria. Its molecular weight can reach up to 60 kDa and the repeating unit contains

different kinds of monosaccharides often decorated by non carbohydrate substituent. The location of *O*-chain at the cell surface places it at the interface between the bacterium and its environments; variations of the structure can be used to modulate the response of the bacterium to external factors. It has also a protective role by preventing phagocytosis up-taking and by masking bacterial virulence factors from host recognition.

1.5 Capsular polysaccharides (CPSs)

Bacteria can also produce an additional external polysaccharide. It can be directly linked to bacterial cells membrane, capsular polysaccharide (CPS), or does not present visible means of attachment to cell membrane, exopolysaccharide (EPS). In contrast to *O*-Chain, CPSs are characterized by differ type of linkage to cell surface and size, and tend to form a thick layer which surrounds cell membrane, masking *O*-chain to the immune system receptors.

Capsular polysaccharides are CPSs, they have a high molecular weight and they are generally composed of repeating oligosaccharides in which different sugars are connected by specific linkages and sometimes can be functionalized by organic or inorganic molecules. This results in multiple serotypes established for many bacterial species and implies an enormous variability of serotypes for many bacterial species.

Capsule Polysaccharides are not ubiquitous structures, but they can be found on the cell surface of both Gram-positive and Gram-negative bacteria and they often constitute the outermost layer of the cell. The polysaccharide capsule is not essential for bacterial to survival, but it performs many important functions. Consequently to its location, CPS might mediate direct interactions between the bacterium and its immediate environment and might protect the cell from it. In addition, since Capsule Polysaccharides are highly hydrated molecules with 95% of water, they can prevent

bacterial cell desiccation. One more function of Capsule Polysaccharides is to promote the formation of a biofilm that assists the colonization process and the adherence of bacteria to several surfaces. Surrounding bacterial cell membrane CPS could be directly involved in bacterium-host interactions; in many phytopathogenic bacteria, indeed, the expression of CPSs is essential for virulence⁹.

The polysaccharidic capsule often results immunogenic in humans, representing good candidates for the development on new vaccines¹⁰. In addition, they are not-toxic, easy to be isolated and purified with high yield, and have conserved and chemically definite structures. To date several vaccines based on the CPS of *Neisseria meningitidis*, *Streptococcus pneumoniae* and *Haemophilus influenzae* type b have been developed¹¹. However, the immune response generated by CPS is T-independent (TI) with no immunologic memory and produces an inadequate response in infants, which are the most vulnerable to bacterial infections. To overcome this limitation a new class of glycoconjugate vaccines were developed, in which capsular polysaccharide is linked to a protein carrier generating a T-dependent (TD) response

References

- ¹ Madigan M, Artiko MA, and Parker J.; *Biology of microorganism*. Pearson education international, **2003**
- ² Alexander C., and Rietschel ET; Bacterial lipopolysaccharides and innate immunity, *J. Endotoxin Res*, **2001**; Vol.7, pp. 167-202.
- ³ Raetz C.R., and Whitfield C.; Lipopolysaccharide endotoxins. *Annu. Rev. Biochem.*; **2002**, Vol. 71, pp. 635-700.
- ⁴ Li C., Guan Z., Liu D., and Raetz C.R.; Pathway for lipid A biosynthesis in *Arabidopsis thaliana* resembling that of *Escherichia coli*; *PNAS*; **2011**; Vol. 108 (28); pp. 11387-11392.
- ⁵ Zähringer U., Lindener B., Desjardins E., Sweet R.W., Robinson J., Hendrickson W.A., and Sodroski J.G.; Chemical structure of Lipid A: recent advances in structural analysis of biologically active molecules; *Endotoxin in Health and Disease*; **1999**; pp. 93-114.
- ⁶ Kyoshi T., and Shizuo A.; Toll-like receptors in innate immunity; *International immunology*, **2005**; Vol. 17 (1), pp.1-14.
- ⁷ Kensuke M.; Innate recognition of lipopolysaccharide by Toll-like receptor 4-MD-2; **2004**; *TRENDS in Microbiology*; Vol.12 (4); pp.186-192.
- ⁸ Seydel U., Oikawa M., Fukase K., Kusumoto S., and Brandenburg K.; Intrinsic conformation of lipid A responsible for agonist and antagonistic activity; *Eur. J. Biochem.*; **2000**; Vol. 267; pp.3032-3039.
- ⁹ Roberts I.S.; The biochemistry and genetics of capsular polysaccharide production in bacteria; *Annu. Rev. Microbiol.*; **1996**; Vol. 50; pp.285-315.
- ¹⁰ Peeters C.C., Lagerman P.R., De Weers O., Oomen L.A., Hoogerhout P., Beurret M., Poolman J.T., and Reddin K.M.; Preparation of polysaccharide-conjugate vaccines; *Methods Mol. Med.*; **2003** ; Vol. 87; pp. 153-174.
- ¹¹ Pon R.A., and Jennings H.J.; Carbohydrates-Based Antibacterial Vaccines, *Carbohydrate-Based Vaccines and Immunotherapies*: John Wiley & Sons, Inc.; **2009**; pp.117-166.

Chapter II: Preparation of liposomes using oligosaccharides from *Rhizobiaceae* family

Introduction

This topic is developed in collaboration with Prof. L. Paduano's team. The aim of this project is to use oligosaccharides from bacteria to functionalize Ru(III)-liposome, in order to increase their life-time in the body and to promote, eventually, a target specific delivery.

Ruthenium complexes have attracted much interest as a promising alternative to platinum, showing a remarkable antitumor and antimetastatic activity (some of these complexes are in II clinical trial) ¹.

In this context, liposomes and nanoparticles containing Ru(III) complexes appear perfect candidate for the drug delivery and theranostic for the following different reasons²:

- 1) Transport larger amounts of metal inside the blood stream;
- 2) They are “stealth” to the human immune system, specifically increasing the complex permanence time in the blood;
- 3) Are selective toward cancer cells recognized by protein receptors specifically over-expressed by cancer tissues.

It is known that when these aggregates are decorated with amphiphilic molecules, they show both enhanced biocompatibility and half-time life in blood stream³.

This project is introduced on the basis of this context: functionalize Ru-based liposomes with an amphiphilic molecule produced by bacteria that belongs to *Rhizobiaceae* family. This class of bacteria produces LPS without inflammatory

activity on human cells. In particular, lipooligosaccharide by *Rhizobium rubi*^T was selected because this bacterium produces a LOS, which displays on the outer core the human Lewis B domain⁴. In this context, a partially delipidated derivative was used and liposomes with up to 40% of LOS were obtained and analyzed: Cryo-TEM and DLS analyses showed that they present a "monomodal hydrodynamic rays (R_H)" distribution and a classical spherical structure.

Future *in vivo* experiments will disclose the perception of these aggregates to prove if the occurrence of the Lewis B epitope enhances the compatibility of these particles, as surmised⁵. Preliminary biological tests show that these aggregates decorated with LOSs from *Rhizobium rubi*^T show similar toxicity of POPC-Ru(III)-complex.

Ru(III)-liposomes with different percentage of LOS were formulated following lipid film method. These aggregates were composed by three different components:

1. Ru(III) complex: ToThyRu
2. POPC (1-palmitoyl-2-oleylphosphatidylcholine)
3. Partially delipidated LOS from *Rhizobium rubi*^T

ToThyRu [(3-(4-pyridylmethyl)-3'-*O*-oleyl-5'-*O*-(benzyloxy)hexaethylene glycol-acetyl-thymidine-RuCl₄DMSO)-Na⁺, figure 2.1) is an amphiphilic-Ru complex that is able to form supramolecular aggregates. It is composed by a core of pyrimidine deoxyribo-Thymidine. The ribose is functionalized on the secondary hydroxyl groups with fatty acids chains to confer amphiphilicity and resistance to these aggregates to enzymatic degradation. Finally, nucleobase is linked to a pyridine, which is able to chelate the Ru (III) complex⁶. ToThyRu mixed with POPC forms variety of supramolecular system such as liposomes and cubic phase. It is well known that when these supramolecular aggregates are decorated with amphiphilic molecules, they show a more marked biocompatibility and half-time life. It is the role of LOS from *Rhizobium rubi*^T, a natural amphiphilic molecule, able to self-assemble liposome with ToThyRu and POPC⁶.

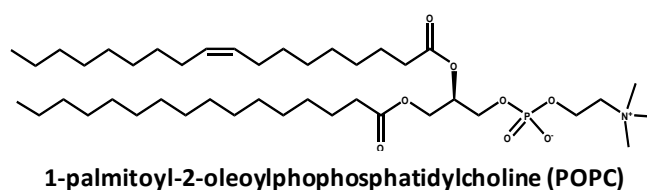
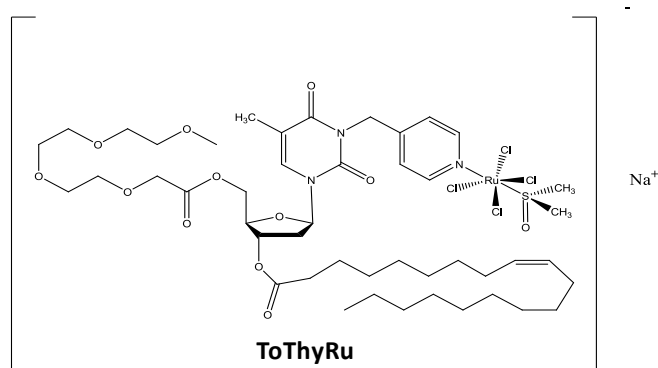


Figure 2.1: Structure of ToThyRu and POPC reagents

2.1 Extraction purification and partially delipidation of LOS produced by *Rhizobium rubi*^T

Rhizobium rubi^T cells were extracted according to PCP and hot water-phenol extractions; LOS was recovered in the PCP phase. SDS-PAGE gel shows mobility that is typical of a low molecular weight molecule, characteristic of lipooligosaccharide species.

The structure of core oligosaccharide produce by *Rhizobium rubi*^T was already studied by Gargiulo *et al*⁴., and was chosen for the decoration of liposomes because it produces an oligosaccharide with a terminal part presenting a tetrasaccharide composed by Fuc, Gal and GlcNAc linked in the same way of Lewis B domain (figure 2.2).

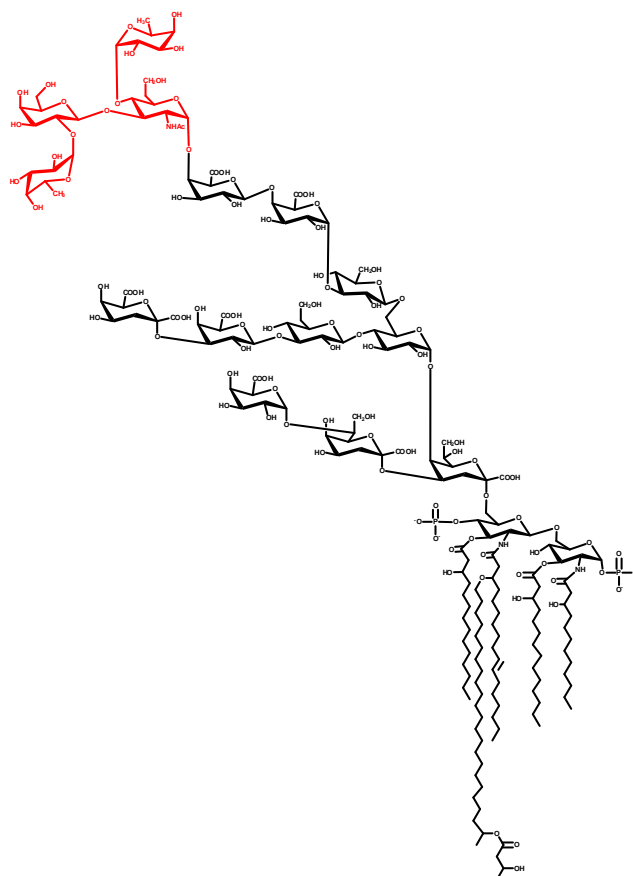


Figure 2.2: Structure of LOS produced by *Rhizobium rubi*^T; in red is evidenced tetrasaccharide unit identical to human Lewis B domain.

In order to verify purity grade of LOS, chemical analyses were done. The figure 2.3 shows the chromatogram of acetylated methyl glycosides obtained by LOS. As shown in the figure, it is possible to identify all monosaccharides reported for these molecules⁴.

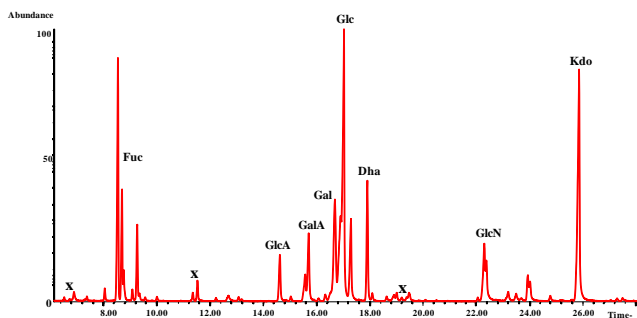


Figure 2.3: Chromatographic profile of acetylated methyl glycosides obtained by LOS of *Rhizobium rubi*^T

Since preliminary preparation of liposome with pure LPS produced a poly modal liposome distribution pure LOS was partially delipidated with hydrazine to obtain a de-*O*-LOS (figure 2.4).

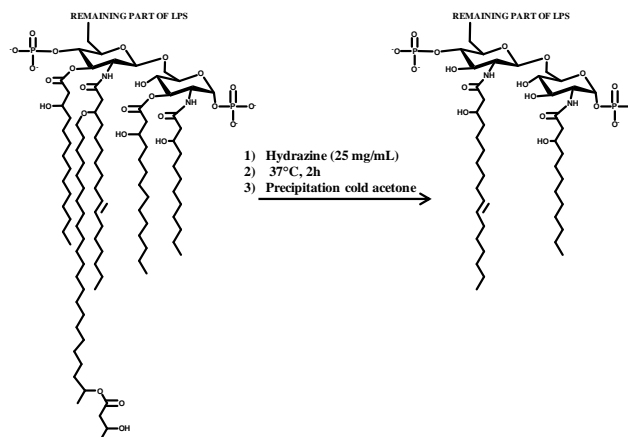


Figure 2.4: Schematic representation of mechanism of de-*O*-lipidation of LOS from *Rhizobium rubi*^T.

2.2 Preparation of liposomes

Ru-containing samples have been prepared by dissolving a suitable amount of the Ru-complex in pure chloroform, in order to get a concentration of 1 mg/mL. For pseudo-ternary systems containing POPC, an appropriate amount of this phospholipid was added to the Ru-complex solution, in order to have the pre-fixed molar ratio. LOS was dissolved in a solution of CHCl₃:MeOH:H₂O (15:8:2) to get again a solution 1 mg/mL. Sonication and slight warming favoured sample dissolution. These solutions were transferred, in a fixed ratio, in a round-bottom glass tube and through evaporation of the solvent and vacuum desiccation a thin lipid film was obtained. The samples have been hydrated with water or FBS (section 6.10), the solutions were vortexed and the suspension was sonicated and repeatedly extruded through polycarbonate membranes, for at least 15 times. The molar ratio of Ru was 10%, while the amount of POCP and LOS was changed to obtain different liposomes with different percentage of LOS; as showed in table 2.1.

Molar ratio	ToThyRu	POPC	LOS
ToThyRu:POPC	10	90	0
ToThyRu:POPC:LOS	10	85	5
ToThyRu:POPC:LOS	10	70	20
ToThyRu:POPC:LOS	10	60	30
ToThyRu:POPC:LOS	10	50	40

Table 2.1: Composition of different liposomes formulatates

2.3 DLS and Cryo-TEM analyses of liposomes

2.3.1 DLS analyses

The size of aggregates was obtained by DLS measurement, which was carried out in the range 45°-110° using a concentration of samples of 1 mg/mL.

The fluctuations of the scattered light, as a time function, are originated by Brownian motion of the particles present in the solution that randomly changes their position over time. In a dynamic light scattering experiment, it is important to define the auto-correlation function of the electric field of the scattered light in time:

$$g^{(1)}(\tau) = \langle E_s(t) \times E_s(t + \tau) \rangle = \lim_{t \rightarrow \infty} \frac{1}{t} \int_0^t E_s(t) \times E_s(t + \tau) \delta t$$

However, the electric field magnitude was impossible to determine instrumentally. In fact, it is more simple to introduce the intensity autocorrelation function of scattered light $g^{(2)}(\tau)$:

$$g^{(2)}(\tau) = \langle I_s(t) \times I_s(t + \tau) \rangle$$

In case of mono-dispersed systems, the expressions of the two auto-correlation functions are the following:

$$g^{(1)}(q; \tau) = \exp(-q^2 \times D \times \tau)$$

$$g^{(2)}(q; \tau) = 1 + \alpha[\exp(-q^2 D \tau)]^2$$

Where q is scattering vector and D is diffusion coefficient. Plotted $\ln(g^{(1)}(\tau))$ as a function of τ , we obtain a straight line to a negative slope, the value of which, in both cases, is given by:

$$q^2 \times D = \frac{1}{\tau} = \Gamma$$

The parameter Γ depends on the angle of observation (θ appears in the definition of the scattering vector, q). However, the system in question is not mono-dispersed; Γ is expressed in series of powers of q^2 :

$$\Gamma = a_0 + a_1 q^2 + a_2 q^4 + \dots$$

The first term of the series is considered zero, the second coefficient represents the diffusion coefficient (D), while the third coefficient is connected to the poly-dispersity of the system under examination (P). The next higher order terms are neglected. So, considering a series of measures at different angles, it is possible to report the results on a graph like Γ vs q^2 . For particles that in solution give aggregates of spherical shape; it is possible to derive the hydrodynamic radius R_H , using the Stokes-Einstein relation:

$$D = \frac{kt}{6\pi\eta R_H}$$

The equation reported above for mono-dispersed systems was applied for all liposomes obtained; in order to evaluate the effect of the *Rubi*^T-LOS on the liposome structure, also analyses on liposomes formulated without LOS were done. Figure 2.4 shows hydrodynamic rays distribution for different system; by the interpolation of distribution it was possible to obtain data, as reported in Table 2.2.

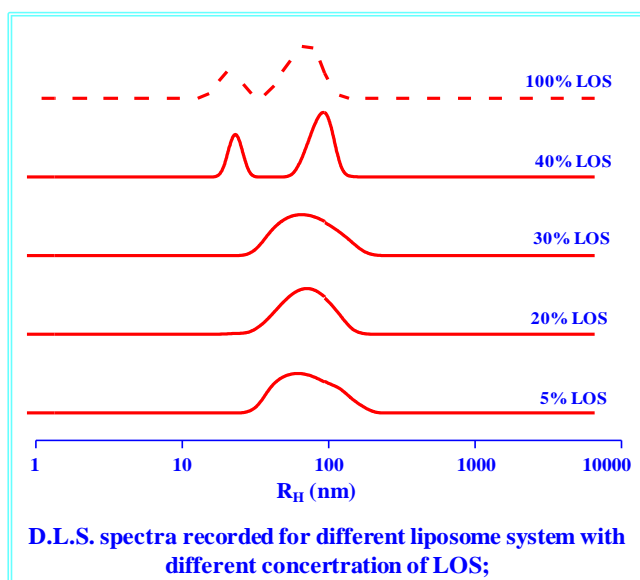


Figure 2.4: Hydrodynamic rays distribution at 25°C and $\theta=90^\circ\text{C}$ for the different liposomic systems.

Samples	% of LOS	$D \pm \text{error} (\text{cm}^2/\text{s})$	$R_H \pm \text{error} (\text{nm})$
POPC	0	$6.3 \cdot 10^{-8} \pm 0.8 \cdot 10^{-8}$	38.8 ± 4.9
ThoThyRu:POPC	0	$2.9 \cdot 10^{-8} \pm 0.1 \cdot 10^{-8}$	82.9 ± 0.4
ThoThyRu:POPC:LOS	5	$2.8 \cdot 10^{-8} \pm 0.1 \cdot 10^{-8}$	87.4 ± 1.9
ThoThyRu:POPC:LOS	20	$2.9 \cdot 10^{-8} \pm 0.1 \cdot 10^{-8}$	82.8 ± 1.6
ThoThyRu:POPC:LOS	30	$3.1 \cdot 10^{-8} \pm 0.1 \cdot 10^{-8}$	79.4 ± 1.5
ThoThyRu:POPC:LOS	40	$3.8 \cdot 10^{-8} \pm 0.2 \cdot 10^{-8}$	66.2 ± 3.8
ThoThyRu:POPC:LOS	100	$3.5 \cdot 10^{-8} \pm 0.1 \cdot 10^{-8}$	69.6 ± 2.6

Table 2.2: Diffusion coefficient and hydrodynamic rays obtained from DLS analyses for different ToThyRu:POPC:LOS systems in water.

Hydrodynamic rays of aggregates with increasing of LOS concentration tend to decrease. The slight size reduction of aggregates can be attributed to sterically hindered, caused by the high volume occupied by polar heads of LOS and the increase of negative charge on the liposomal surface. The results show a monomodal hydrodynamic rays distribution, unless of the sample ToThyRu:POPC:LOS 10:50:40 which presents a bimodal distribution. The smaller population, about 13 nm, describes

the presence of micelle aggregates, this tendency of LOS to form micelles in solution was also demonstrated by DLS analysis LOS, 1 mg/mL, in water (figure 2.4).

In order to analyze the aggregates in a physiological environment fetal bovine serum (FBS) was chosen as a biological matrix. As the starting serum solution contained same proteins that caused scattering, this solution was dialyzed, to avoid aggregates in the same range of liposomes.

As a result, the serum solution showed the same characteristics of pH and ionic strength compared to the starting solution, without interferences. The treated serum was used for hydration of the lipid films of ThoThyRu:POPC:LOS 10:70:20 and compared with the same systems in water. Table 2.3 and figure 2.5 demonstrate that liposomes present similar hydrodynamic rays distribution in both the solvent.

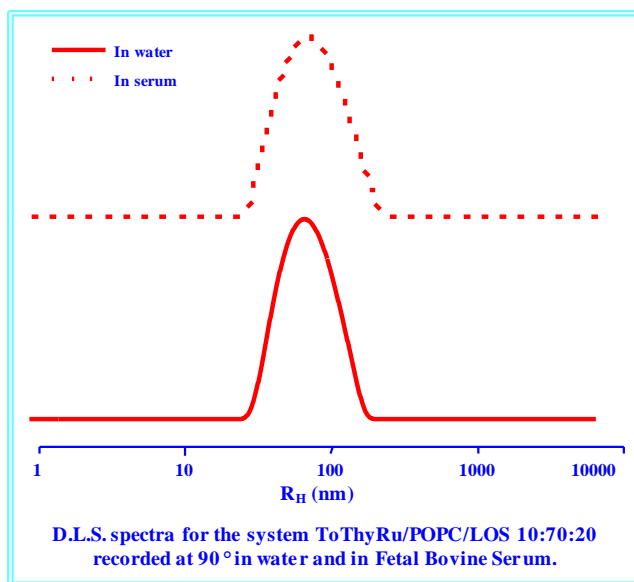


Figure 2.5: : Hydrodynamic rays distribution at 25°C and $\theta=90^\circ$ for the system ThoThyRu:POPC:LOS 10:70:20 in aqueous solvent (continue line) and in fetal serum bovine (dotted line).

Samples	SOLVENT	D ± error (cm ² /s)	R _H ± error (nm)
ThoThyRu:POPC:LOS (20%)	H ₂ O	2.9·10 ⁻⁸ ± 0.1·10 ⁻⁸	82.8 ± 1.6
ThoThyRu:POPC:LOS(20%)	FBS	3.4·10 ⁻⁸ ± 0.1·10 ⁻⁸	71.4 ± 0.8

Table 2.2: Diffusion coefficient and hydrodynamic rays obtained from DLS analyses ThoThyRu:POPC:LOS (20%) hydrated in water and in fetal serum bovine.

2.3.2 Cryo-TEM investigations

The shape and size distribution of liposomal systems were observed through Cryo-TEM technique, in order to obtain high-resolution images directly in their original environment. The samples investigated by electron microscopy were prepared with lipid film method. About 50 µl of liposomes solution were placed on a grid containing a film of carbon. Subsequently, the solution was dried with a filter paper and then frozen by placing the grid in a container of ethane (-184 °C). The grid with the frozen sample was placed in the sample holder. Figure 3.6 shows Cryo-TEM image for ThoThyRu:POPC:LOS 10:85:5 and confirms that this aggregates presents a monomodal hydrodynamic rays distribution.

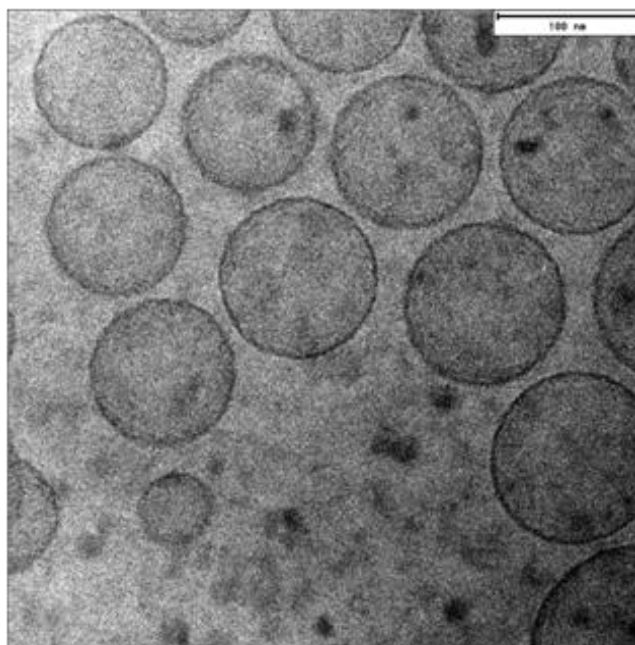


Figure 2.6: Cryo-TEM image for system ThoThyRu:POPC:LOS 10:85:5.

2.4 *In vitro* cytotoxicity tests

The *in vitro* cytotoxicities of different aggregates of MCF-7 cancer cells (human breast adenocarcinoma cancer cell line) and J774 (murine macrophages) have been determined by MTT (3-(4,5-dimethyl-2-thiazolyl)-2,5-diphenyltetrazolium bromide) assay and total cell count. Figure 2.7 shows toxicological tests on different Ru-aggregates. Firstly toxicity of POCP was analyzed and predictably liposomes composed exclusively of POCP showed no significant interference with the cell viability and cell proliferation. Starting from these preliminary experiments, the cells were then treated for 48h (MCF-7) and 24h (J774) with different concentrations (10, 25, 50, and 100 μ M) of POPC:LOS (90:10), POPC:ToThyRu (90:10) and POPC:ToThyRu:LOS (70:10:20). The evaluation of the “cell survival index” suggests that liposomes formulated with LOS produce cytotoxic effect substantially similar to that composed by only POPC and ToThyRu on MCF-7 line cells. On J774 line cells, instead, when LOS was added, the aggregates show more marked toxicity. In order to verify if there is a part of LOS that could enhance toxicological power, the same tests were conducted on dephosphorylated LOS, on Lipid A and Core region. Figure 2.8 shows the results on the different cellular lines and the different parts of LOS show similar activities on the same cell line and in both case a vitality greater than 50% is observed.

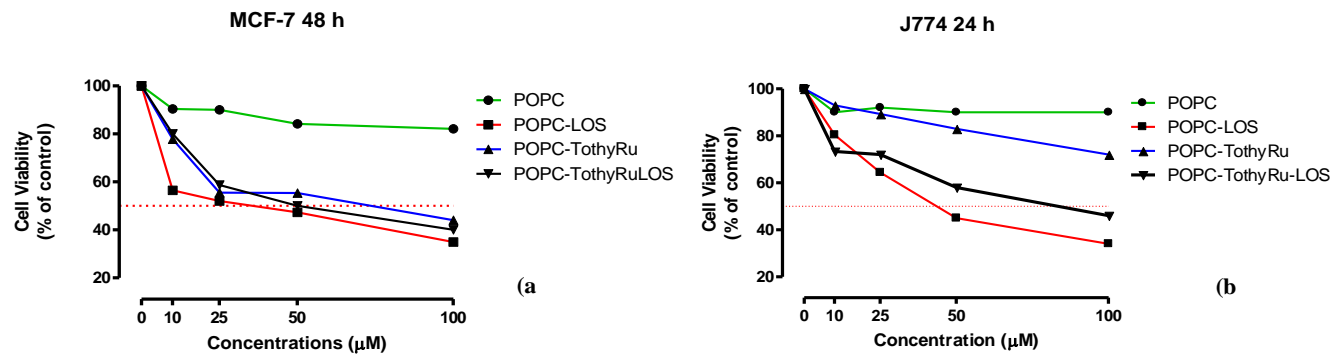


Figure 2.7: Concentration/effect curves and cell survival index. Cell survival index, evaluated by MTT assay and total cell count, in MCF-7 (part a) and J774 (part b) cell lines incubated with different Ru-containing formulations. Data are expressed as percentage of untreated control cells. Biological tests were performed by Prof. Carlo Irace from department of pharmacology of University of Naples.

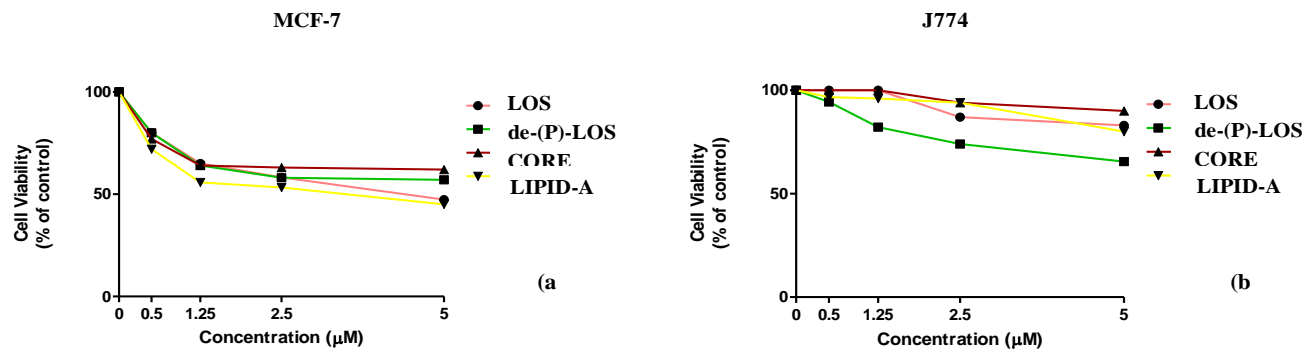


Figure 3.8: Concentration/effect curves and cell survival index. Cell survival index, evaluated by MTT assay and total cell count, in MCF-7 (part a) and J774 (part b) cell lines incubated with different part of LOS: LOS, dephosphorylated LOS (de-(P)-LOS), Core region and Lipid-A. Data are expressed as percentage of untreated control cells. Biological tests were performed by Prof. Carlo Irace from department of Pharmacology of University of Naples.

2.5 Conclusions

The aim of this project was to study the formulation and physical-chemical characterization of supramolecular aggregates based on Ru (III) complex and lipooligosaccharide (LOS), which have antitumor activity. The idea is to analyze new liposomal class systems containing, for the first time, a LOS (lipooligosaccharide), partially delipidated, to make it "stealth" against the immune system. The presence of LOS in the liposomal bilayer gives different structural and functional properties than classical liposomes formulation. The idea infers from the ability to create a membrane that shows the same characteristics of low permeability and high resistance, typical of the cell wall of Gram-negative bacteria, in order to increase the stability and lifetime of aggregates. The supramolecular systems analyzed are structurally characterized by the presence of amphiphilic molecules: a zwitterionic lipid, POPC; a Ru(III) complex ToThyRu, and lipooligosaccharide produced by *Rhizobium rubi*^T. The latter, since preliminary formulations with native LOS have led to obtaining poly-modal distribution of liposomes, was partially delipidated by hydrazine.

All liposomal systems have been investigated through combined experimental strategy, including dynamic light scattering (DLS), Cryo-TEM analyses and biological tests.

In this context, the results suggest that the LOS insertion in the liposomal formulation changes the size and structure of aggregates but not their cytotoxicity.

References

- ¹ Vaccaro M., Del Litto R., Mangiapia G., Carnerup A.M., D'Errico G., Ruffo F., and Paduano L.; Lipid based nanovectors containing ruthenium complexes: a potential route in cancer therapy; *Chem. Commun.*; **2009**; Vol.11, pp. 1404-1406.
- ² Sava G., Bergamo A., Zorzet S., Gava B., Casarsa C., Cocchietto M., Furlani A., Scarcia V., Serli B., Lengo E., Alessio E., and Mestroni G.; Influence of chimica stability on the activity of the antimetastasis ruthenium compound NAMI-A; *Eur.J. Cancer*; **2002**; Vol. 38 (3); pp. 427-435.
- ³ D'Errico G., Silipo A., Mangiapia G., Vitiello G, Radulescu A., Molinaro A., Lanzetta R., and Paduano L.; Characterization of liposomes formed by lipopolysaccharides from *Burkholderia cenocepacia*, *Burkholderia multivorans* and *Agrobacterium tumefaciens*: from the molecular structure to the aggregate architecture; *Phys. Chem. Chem. Phys.*; **2010**; Vol.1; pp. 1–12.
- ⁴ Gargiulo V., Garozzo D, Lanzetta R., Molinaro A., Sturiale L.; De Castro C., and Parrilli, M.; *Rhizobium rubi*^T: a Gram-negative phytopathogenic bacterium expressing the Lewis B Epitope on the Outer Core of its lipooligosaccharide fraction; *ChemBioChem*; **2008**, Vol. 9, pp. 1830 – 1835.
- ⁵ De Castro C., Fregolino E., Gargiulo V., Lanzetta R., and Parrilli M.; A novel capsular polysaccharide from *Rhizobium rubi* strain DSM 30149; *Carbohydrate Research*; **2008**, Vol. 343, pp. 1482-1485.
- ⁶ Mangiapia G., D'Errico G., Simeone L., Irace C., Radulescu A., Di Pascale A., Colonna A., Montesarchio D., and Paduano L.; Ruthenium-based complex nanocarriers for cancer therapy; *Biomaterials*; **2012**; Vol. 33, pp. 3770-3782.

Chapter III: Identification and structural analysis of the Capsular polysaccharides from different clinical isolates of *Acinetobacter baumannii*, strains A74, D36, F4, D78, D46

Introduction

This work is in collaboration with dr. J. Kenyon at the University of Sydney, she works on the elucidation of genes responsible for LPS and CPS biosynthesis in *Acinetobacter* bacteria, a Gram-negative species relevant in nosocomial infections. The final purpose of this work is the understanding of how these bacteria trigger inflammation and how they escape the host immune system, together with the idea to understand the biosynthetic pathway of CPS.

Acinetobacter baumannii causes in immuno-compromised patients severe nosocomial, bloodstream, pneumonia and septicemia¹. This class of bacteria presents a particularly property of resistance to the most commonly used antibiotics. It produces lipopolysaccharides (LPSs) and capsular polysaccharides (CPSs)² which display a crucial role in the pathogenicity mechanism. CPSs are high molecular weight polymers constituted by an oligosaccharide repeating unit in which different sugars are connected together by specific linkages.

The primary role of CPS is to protect bacterial cell from external environment and to prevent its desiccation. Furthermore, capsular polysaccharides promoting formation of biofilms show a fundamental role in the bacteria adhesion and host colonization. The knowledge of CPS structure is fundamental for the elucidation of infection mechanism and for the development of new glycoconjugates vaccines.

So far, attention was focused on five different strains of *Acinetobacter baumannii* isolated from different Australian hospitals: *A. baumannii* A74, D36, F4, D46 and D78. The structures of CPSs produced by these different strains of *Acinetobacter baumannii* were resolved on the basis of chemical and spectroscopical analyses.

3.1 Isolation of different CPSs

Capsular polysaccharides produced by different strains of *Acinetobacter baumannii* were found in the water phase of hot water-phenol extraction. They were purified from proteins, nucleic acid and LPS by enzymatic hydrolysis and centrifugation.

3.2 Chemical and structural analyses of CPS from *A. baumannii* A74³

Acinetobacter baumannii A74 produces a branched capsular polysaccharide constituted by D-glucose (D-Glcp), D-galactose (D-Galp), *N*-acetyl-D-glucosamine (D-GalpNAc) and pseudaminic acid (Pse5Ac7Ac) linked as shown in figure 4.1. The complete oligosaccharidic sequence was elucidated on the basis of chemical and spectroscopical analyses.

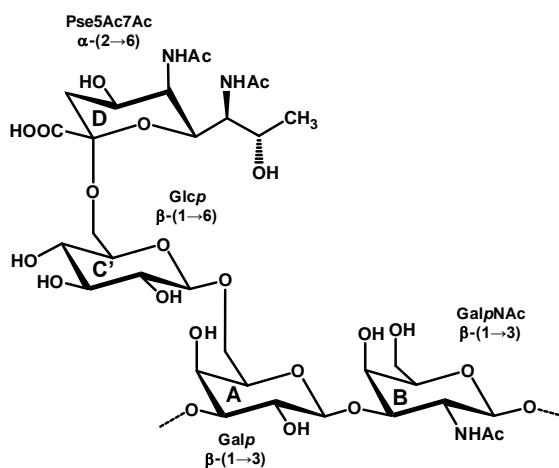


Figure 3.1: Structure of the repeating unit of the CPS from *A. baumannii* A74. Labels reflect those reported in Table 3.1

3.2.1 Chemical analyses of CPS

Acinetobacter baumannii A74 cells were extracted according to PCP and hot water-phenol extractions. CPS was recovered in the water phase and purified from nucleic acid, proteins and LOS by enzymatic treatment and centrifugation (section 6.7). SDS-PAGE gel, stained with alcian blue and silver nitrate, shows the presence of a polysaccharide molecule with a molecular weight greater than LPS of *Escherichia coli* 055:B5 used as standard (figure 3.2)

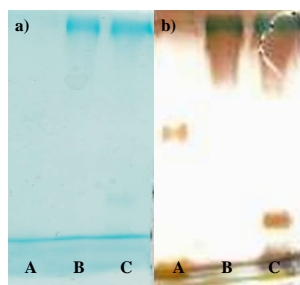


Figure 3.2: SDS-PAGE (stacking gel 5%, separating gel 12.5%) stained with alcian blue, **a**, and alcian blue and silver nitrate, **b**, of **A** standard of *E. coli* 055:B5, **B** 10 μ g. of crude material obtained in water phase, and **C** 10 μ g of enzyme treated water phase.

Chemical analysis disclosed the occurrence of three different hexoses: glucose, galactose and galactosamine, all with the D configuration and linked at position 6, 3, 6 and 3, respectively. An additional component was detected in the acetylated methyl glycosides mixture, with the fragmentation pattern compatible with that of a 5,7-diacetamido-3,5,7,9-tetraoxo-2-keto-nonulosonic acid, later identified as pseudaminic acid (5,7-diacetamido-3,5,7,9-tetraoxo-2-keto-L-glycero-L-manno-nonulosonic acid). Kdo, the marker of lipopolysaccharide, was not found or it was below the detection limit of the instrument⁴.

First NMR inspection of the CPS returned a proton spectrum with very broad signals (figure 3.3 part a), specifically the anomeric protons were at high field suggesting the occurrence of sugars β configured only. The spectrum also contained three N-acetyl signals at ca. 2 ppm, two protons of a deoxy position at 1.60 and 2.15 ppm and one

methyl group at 1.15 ppm, these last three signals together with two of the N-Acetyl groups were consistent with Pse. Nevertheless, the quality of the 2D NMR spectra was poor and prevented any structural assignment. Assuming that Pse was internal to the polysaccharide chain, CPS was treated with 1% AcOH in order to cleave selectively the backbone at level of the Pse residue (section 6.6.1), and to obtain a depolymerized product with improved spectroscopic properties. The acid treated polysaccharide fulfilled this last expectation (figure 3.3 part b); even though it was later found that Pse was not an internal residue but a terminal substituent. Pse was removed only partially creating some heterogeneity in the polymer; nevertheless, this did not prevent the interpretation of the NMR spectra and determination of the polysaccharide structure was accomplished.

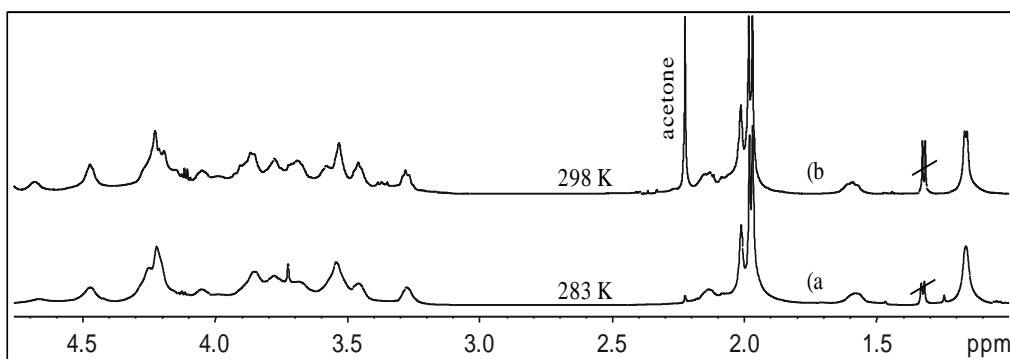


Figure 3.3: ^1H NMR spectra (600 MHz, D_2O) of CPS after a) enzymatic purification and b) after mild acid hydrolysis. Signals of impurities are crossed and the temperatures used are indicated on the spectra

3.2.2 NMR analyses of hydrolyzed CPS

The ^1H NMR spectrum (figure 3.3 part b) contained two signals in the anomeric region (5.00–4.00 ppm) in an approximate ratio of 1:2; these signals were labelled with letters (A–C) in the order of their decreasing chemical shifts, and letter **D** was assigned to Pse residue.

Analysis of the 2D NMR spectra of the polysaccharide permitted the assignment of all proton and carbon chemical shifts (Table 3.1, structure in figure 3.1)

As for **A**, the anomeric proton resonated at 4.68 ppm, indicating the β configuration of the anomeric centre, also confirmed by the *inter* residues NOEs with H-3 and H-5. In the TOCSY spectrum (figure 3.5 part b), H-1 of **A** had only three correlations due to the null H-4/H-5 coupling, typical of the *galacto* ring stereochemistry, C-2 resonated at 52.7 ppm indicating a nitrogen bearing carbon, and H-2 chemical shift (4.05 ppm) proved the acetylation of the amino function. Therefore, **A** was a N-acetylated β -galactosamine and the low field shift of its C-3 signal (80.7 ppm) with respect to the standard value (72.3 ppm) proved glycosylation at this position (figure 3.4)⁵.

With regard to the broad signal at ca. 4.50 ppm, TOCSY spectrum was not informative because it contained the correlations from **B** and **C** residues; conversely, information were recovered from H-2 protons of these units because these did not overlap with any other signal in the spectrum (Inset in figure 3.5 shows COSY spectrum detailing the H-1/H-2 cross peaks of **C** and **B** residues).

With regard to **B**, its H-2 (3.59) displayed on three cross peaks in TOCSY spectrum, with H-2, H-3 and H-4, as occur for a *galacto* configured residue; complete identification of protons H-5 and H-6 was possible on the basis of NOESY correlations. Residue **B**, indeed, was a galactose, β configured on the basis of the diagnostic anomeric signal chemical shift (4.48 ppm) and because H-1 showed the expected NOEs with H-3 and H-5; carbon chemical shift indicated that **B** was substituted at both O-3 and O-6.

With regard to **C**, a close view to H-1/H-2 cross peak in the COSY spectrum (inset in figure 3.5) evidenced that it was composed by two different residues, labelled **C** and **C'**, with the second resonating at a higher field. Following COSY spectrum connectivities, it resulted that **C** and **C'** had the same H-2 and H-3 protons, but differed for H-4 (figure 3.5 part b). H-4 of **C** appeared in the not-crowded region of the spectrum (3.37 ppm) and its TOCSY connectivities were used to discriminate the

other protons of this unit from those of **C'**. This signal displayed in TOCSY spectrum five distinct cross peaks instead of six, suggesting that two ring protons of this residue overlapped: of these five densities, three were assigned to H-1/H-4, H-2/H-4 and H-3/H4 correlations, and therefore attention was focused on the other two left, which connect H-4 to the signals at 3.92 and 3.70 ppm. In the gHSQC spectrum (figure 4.4) these signals belonged to a hydroxyl-methyl carbon at 62.1 ppm, given as C-6 of **C**. H-6 protons displayed a correlation with signal at 3.45 ppm which overlapped with H-3 and was assigned to H-5.

C was identified as glucose on the basis of the excellent magnetization propagation seen for proton H-4 in the TOCSY spectrum; starting from this proton, indeed, is possible to identify all protons of the ring. β configuration of the anomeric centre was supported by the low field chemical shift of the anomeric proton and by the large $^3J_{H1-H2}$ value (8.3 Hz).

With regard to **C'** analysis started from H-4 signal at 3.54 ppm which present a correlation with signal at 3.67 ppm assigned to H-6 on the basis of its carbon chemical shift at 63.4 ppm; this modest chemical shift at low field was diagnostic of the occurrence of a ketose residue. H-6' chemical shift was found by analyzing of gHSQC spectrum that correlate with the same carbon signal of H-6. H-5 (3.53 ppm), instead, was inferred at the end of the analysis because its carbon was the only one left unattributed in the gHSQC spectrum.

Consequently, **C'** signals were also identify as a glucose residue, β configured at the anomeric centre. **C** and **C'** residues differed at C-6 position: this carbon atom was found at 62.1 ppm in **C**, indicating a not substituted residue, while C-6 of **C'** was at 63.4 ppm due to the presence of a ketose at C-6 position; this result is in agreement with the occurrence of a 6-linked glucose in the chemical analysis of the intact CPS.

Assignment of **D** started from the diastereotopic methylene protons at high field (2.15 and 1.60 ppm), which correlated in the COSY spectrum with H-4 (4.26 ppm) and with a further signal in the TOCSY spectrum, at 4.23 ppm and assigned to H-5. The other

resonances of the nonulosonic acid were determined by starting from the methyl signal at 1.15 ppm; the gHMBC spectrum correlated this methyl group with a carbon at 68.1 ppm assigned to C-8 and with a carbon at 54.9 given to C-7; the corresponding protons were found in the gHSQC spectrum at 4.24 and 4.20 ppm, respectively, and COSY spectrum linked H-7 to H-6 which was at 3.85 ppm. Determination of all the carbon chemical shift of **D** evidenced that both its amino groups were N-acetylated, as confirmed by the long range correlation of H-5 and H-7 with a carbonyl (175.9 and 175.0, respectively), and comparison of the carbon chemical shifts of this sugar with those published^{6,7} identified this residue as an unsubstituted pseudaminic acid, α configured at the anomeric centre.

Sequence among the residues was inferred analysing the NOESY spectrum (figure 3.4 part a), which displayed these key correlations: H-1 of **A** with H-3 and H-4 of **B**; H-1 of **B** with H-3 of **A**; H-1 of **C'** with both H-6 and H-4 of **B**. NOEs from **C** were barely visible, but this was due to the low amount of this residue with respect to **C'**, as deduced comparing the intensity of its H-4 (3.37 ppm) with the signal at 3.28 ppm which included H-2 protons from both **C** and **C'**. It was assumed that this residue was linked in the same fashion as **C'**. As for residue **D**, meaningful NOEs were not detected in the NOESY spectrum and it was placed at O-6 of **C'** because of the mild chemical shift displacement of this carbon atom. The not-substituted glucose **C** was an artefact due to the partial removal of **D** during the mild acid hydrolysis treatment of the CPS. These data, combined with the linkage analysis and with the carbon chemical shift analysis permitted the elaboration of the structure of the repeating unit of the polysaccharide, shown in figure 3.1 chemical shifts are reported in Table 3.1. The CPS has backbone where Gal and GalNAc alternate and are β -(1 \rightarrow 3) linked, further elongated at C-6 with α -Pse-(2 \rightarrow 6)- β -Glc disaccharide.

As showed in figure 3, part a, besides the NOEs listed above, this other effects were detected: H-1 of **A** with its own H-4 and H-6. H-1 of **C'** with H-5 of A (or with its H-6'', which is coincident); for this correlation it was not possible to find an explanation

and assuming that spin diffusion effects were minimized, our hypothesis is that they arise from the secondary conformation of the polymer.

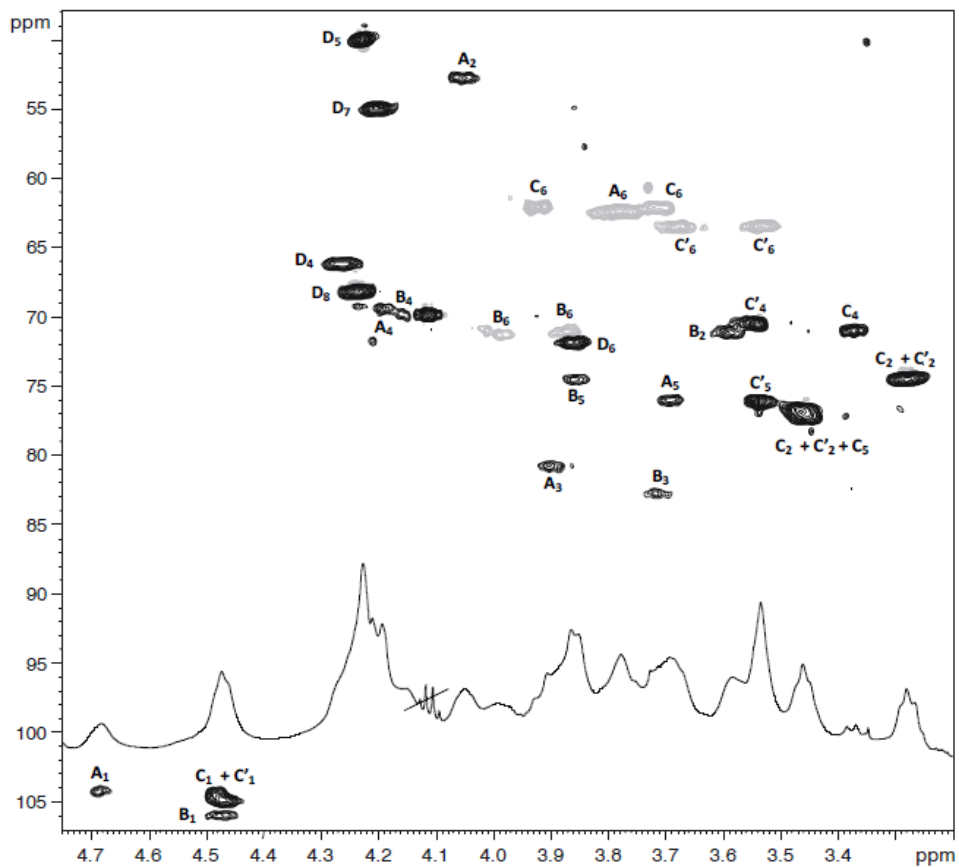


Figure 3.4:(600 MHz; 298 K): zoom of gHSQC (black) and HMBC (grey) spectra of acid hydrolyzed CPS from baumannii A74. Attribution of most of the cross peaks is indicated near the corresponding density.

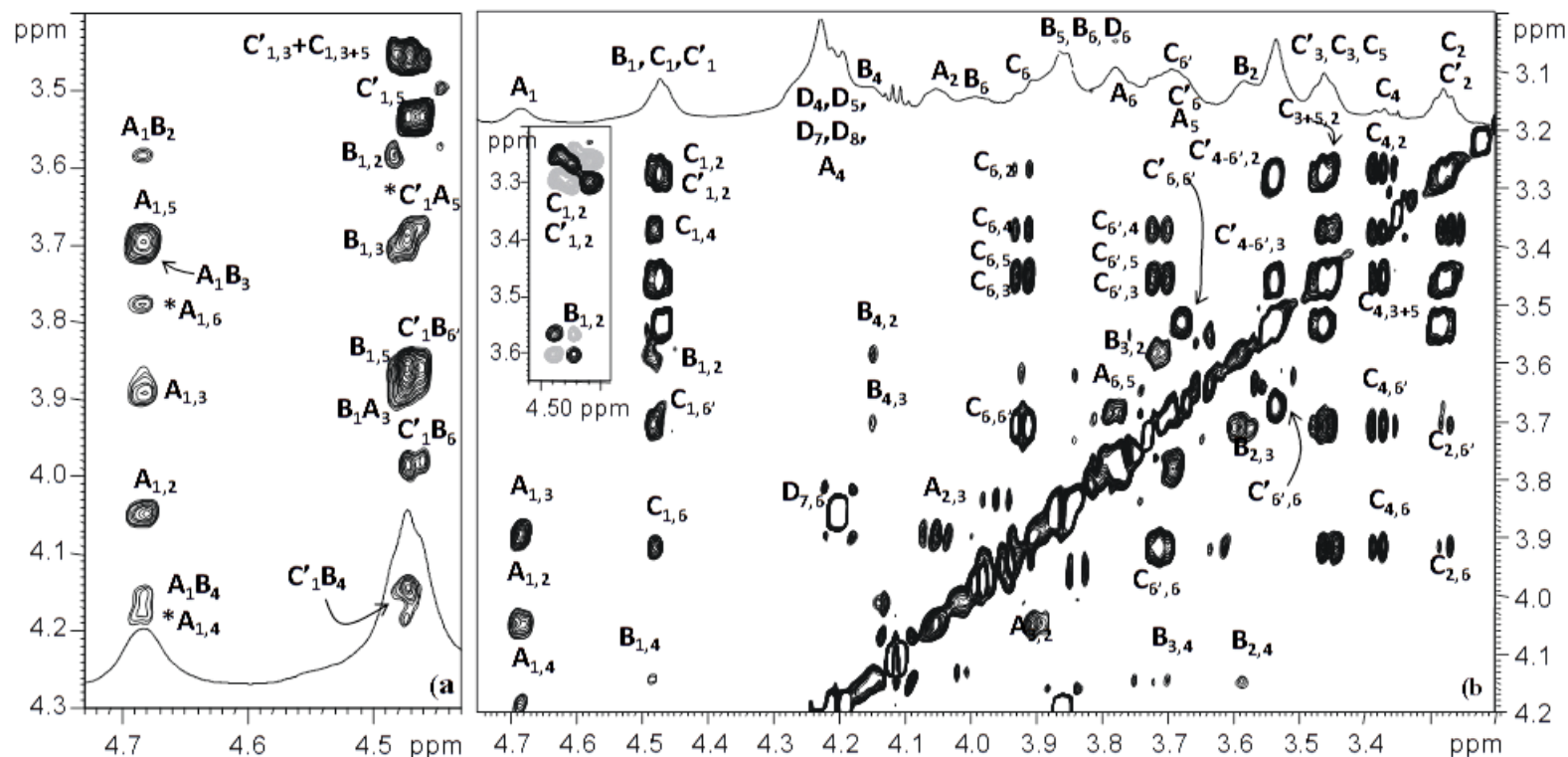


Figure 3.5: (600 MHz, 298 K) Expansion of NOESY (part a) and TOCSY (part b) spectra of CPS from *A. baumannii* A74. Attribution of most of the cross peaks is indicated nearby the corresponding density. Inset: COSY spectrum detailing the H-1/H-2 cross peaks of C group of signals (upper part) and B residue (lower part). The C group of signals includes two anomeric protons, C and C': these are related to a glucose unit that is not stoichiometrically substituted at C-6 by Pseudaminic acid, as effect of the mild acid hydrolysis of the CPS. When Pse is present, glucose is substituted at O-6 and its anomeric signal is C'. NOE effect marked with an asterisk is not deductable from the primary structure of the CPS; it could be due to spin diffusion phenomena or, more probably, from the secondary conformation of the polysaccharide.

		1	2	3	4	5	6	6'
A	¹ H	4.68	4.05	3.90	4.19	3.70	3.78 x 2	-
3-β-GalNAc	¹³ C	104.2	52.7	80.7	69.4	76.0	62.3	-
B	¹ H	4.48	3.59	3.72	4.15	3.86	3.98	3.86
3,6-β-Gal	¹³ C	105.9	71.1	82.7	69.8	74.5	71.1	-
C	¹ H	4.48	3.28	3.46	3.37	3.45	3.92	3.70
t-β-Glc	¹³ C	104.8	74.4	76.9	70.9	77.2	62.1	-
C'	¹ H	4.47	3.28	3.46	3.54	3.53	3.67	3.53
6-β-Glc	¹³ C	104.8	74.4	76.9	70.5	76.0	63.4	
		3	4	5	6	7	8	9
D	¹ H	2.15; 1.60	4.26	4.23	3.85	4.20	4.24	1.15
t-α-Pse	¹³ C	36.6	66.1	50.0	71.8	54.9	68.1	16.9

Table 3.1. Proton (600 MHz) and carbon (150 MHz) chemical shifts of CPS obtained by *A. baumannii* A74, measured at 298 K. Spectra were calibrated with respect to internal acetone (¹H: 2.225 ppm, ¹³C: 31.45 ppm). Structure of the repeating unit of the CPS is in figure 3.1.

3.3 Chemical and spectroscopical analyses of CPS from *A.baumannii* D36⁸

Acinetobacter baumannii D36 produces a branched capsular polysaccharide constituted by D-glucose (D-Glcp), *N*-acetyl-D-galactosamine (D-GalpNAc), *N*-acetyl-D-fucosamine (D-FucpNAc) and *L*-glycero-*L*-altro nonulosonic acid (Aci5NAc7NAc) linked, as shown in figure 3.6. The complete oligosaccharidic sequence was elucidated on the basis of chemical and spectroscopical analysis.

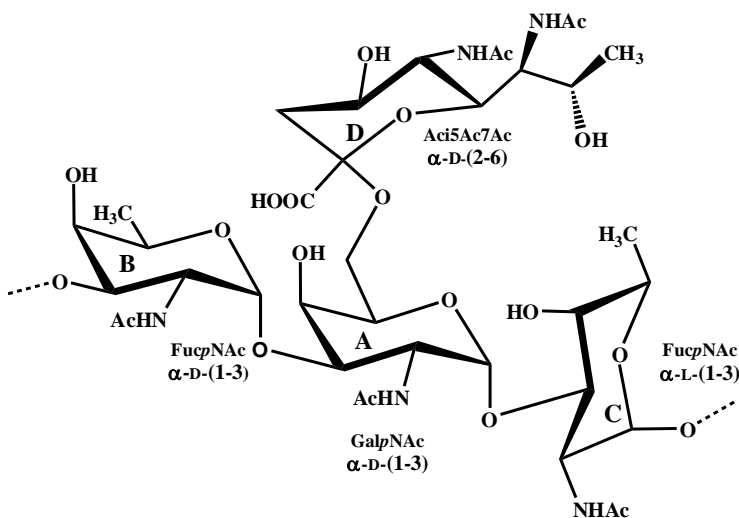


Figure 3.6: Structure of the repeating unit of the CPS from *A. baumannii* D36. Labels reflect those reported in Table I.

CPS produced by *A.baumannii* D36 presents particular 2-nonulosonic acid *L*-glycero-*L*-altro isomers (Aci5Ac7Ac). Although this monomer was obtained by synthetic approach and totally characterized⁴ this is the first case in which this residue was isolated as a component of a glycoconjugates produced by bacterium. It was reported that 2-nonulosonic acid are fundamental constituents of bacterial glycoconjugates and show particular roles in immune recognition and epitope specificity. 5,7-diamino-2-nonulosonic acid are directly involved in gastrointestinal tract colonization; *H. pylori* and *C. jejuni*, flagellated bacteria, present flagellins heavily *O*-glycosylated with nonulosonic acid and this functionalization is

fundamental for colonization mechanism. In addition, pseudoaminic acid is a constituent of O-specific chain polysaccharide (OPSS) of *P. aeruginosa*, *S. Boydii*⁹ and in CPSs of *A. Baumannii*¹. Legionaminic acid occurs in OPSSs of different bacteria strains like *P. fluorescens*, *L. pneumophila*¹⁰, and *A. baumannii*. 5NAc7NAcNONIA is a constituent of LPS produced by two different strains of *Vibrio parahaemolyticus* and it is directly involved in the serological activity of this bacteria¹¹.

3.3.1 Chemical analyses of CPS

CPS from *A. baumannii* D36 was isolated after enzymatic hydrolysis of the crude material present water phase of hot phenol/water extraction. SDS-PAGE gel, stained with alcian blue and silver stain, showed the presence of a polysaccharide with a molecular weight greater than LPS of *Escherichia coli* 055:B5 used as standard. Chemical analysis disclosed the presence of two different amino sugars: fucosamine and galactosamine, linked at position 3 and at positions 3 and 6 respectively as deduced by applying the methylation protocol for neutral sugar². Octyl glycoside analysis shows that galactosamine presents D configuration while fucosamine was present in the two possible configuration D and L. Analysis of methyl glycoside acetylated mixture also shows that a 5,7-diacetamido-3,5,7,9-tetradecoxy-2-keto-nonulosonic acid, later identified by NMR analysis and by its optical rotation as 5,7-diacetamido-3,5,7,9-tetradecoxy-L-glycero-L-altro non-2-ulosonic acid residue, is present. Substitution pattern for this residue was not determined by GC-MS analysis because the protocol used was not suitable for acid residues.

Pure CPS proton spectrum (figure 3.7 part a) presents very broad signals; it is possible to indentify two anomeric signals at low field, ca 5 ppm, suggesting an α configuration, three different signal at ca 2 ppm attributable to N-acetyl groups,

and a signal at ca 1.2 ppm belonged to methyl groups of FucNAc and *L-glycero-L-althro* residue. Analysis of 2D-NMR spectra of polymer did not lead to any conclusive information because of their poor quality, signal densities were generally rather broad and mostly lost in the baseline noise. One information was found by the analysis of gHSQC spectrum of CPS (spectrum not shows); this contains a carbon signal of a hydromethylene group at 64 ppm, this value compared to typical value (60-62 ppm) indicated a glycosylation with a ketose residue; therefore combining this information with those obtained by chemical analysis, it was deduced that nonulosonic acid was linked as terminal residue to C-6 of GalNAc.

Starting from this information, to improve the spectra resolution, enzyme treated CPS was hydrolyzed with a solution of AcOH 6% (section 6.6.2). Acid treated mixture was purified on a BioGel P-10 column using NH_4HCO_3 50mM as eluent and using a RID as detector. Chromatographic profile shows the presence of two different species. They were collected, freeze dried and analyzed by $^1\text{H-NMR}$ (figure 3.7 part b and c); in the void volume of column was eluted a linear oligosaccharide in which nonulosonic residue was totally removed. The second species instead, result to be a monosaccharide mixture containing *L-glycero-L-althro-5,7-diacetammido-3,5,7,9-tetradecoxy-2-nonulosonic acid*.

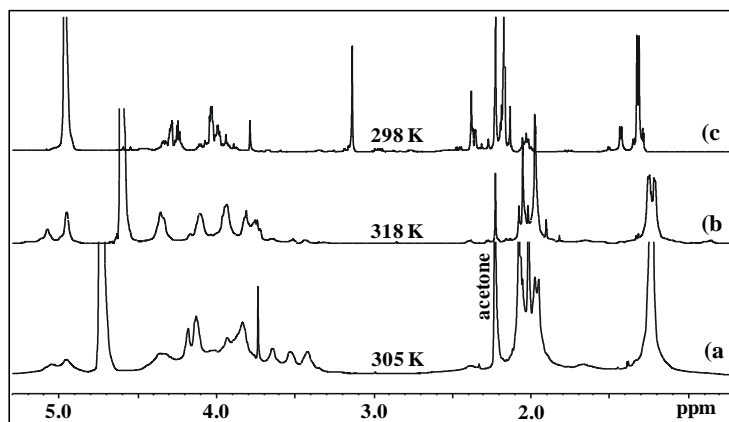


Figure 3.7: ^1H NMR spectra (600 MHz, D_2O) of CPS after (a) enzymatic purification (b) and (c) after mild acid hydrolysis chromatographic purification. Spectra temperatures used are indicated on the spectra

3.3.2 NMR analyses of hydrolyzed CPS

Analysis of 2D spectra of acid treated CPS permitted the assignment of all proton and carbon chemical shift (Table 3.2, structure figure 3.6). Proton at 5.01 ppm was assigned to residue **A** and its chemical shift suggests a α configuration. This proton presents only three TOCSY (figure 3.9 part b) correlations with protons H-2 and H-3 and H-4 respectively, due to the null H-4/H-5 coupling, characteristic of *galacto*-configured sugars. Proton and carbon chemical shift of C-2 also underline that it is directly linked to an N-acetyl group. Complete proton and carbon assignment of this residue was possible starting from H-3 and following NOE correlation. Therefore residue **A** was identified as a N-acetyl α -galactosamine; the low chemical shift of its C-3 at 73.8 ppm confirms glycosylation at this position as showed by methylation analyses.

The broad signal at ca 4.9 ppm contains H-1 signals from both **B** and **C** sugars; complete proton assignment was possible starting from H-2 signal, which did not overlap with outer signals in this spectrum. These residues, as showed by TOCSY propagation from H-2, result to be *galacto* configured sugars. C-2 signals resonated at ca 49.3 ppm indicating a nitrogen-bearing carbon, and H-2 at 4.35 ppm proved

the acetylation of amino group. This signal showed correlation with two protons at 3.81 ppm and 4.09 ppm, identified as H-3 of residue **B** and residue **C** respectively. TOCSY and NOESY analyses showed that these residues are N-Acetyl fucosamine and permitted the allocation of all carbons and protons chemical shift. Oligosaccharide sequence was resolved on the basis of NOESY correlations, while HMBC did not contain any useful information. H-1 of residue **A** shows a NOE correlation with H-3 and H-4 of residue **C** (figure 3.8 part b); this had to be linked to **B** which in turn had to be linked to **A**. Combining results obtained by chemical and NMR analyses, it was possible to obtain the complete oligosaccharidic sequence as follows:

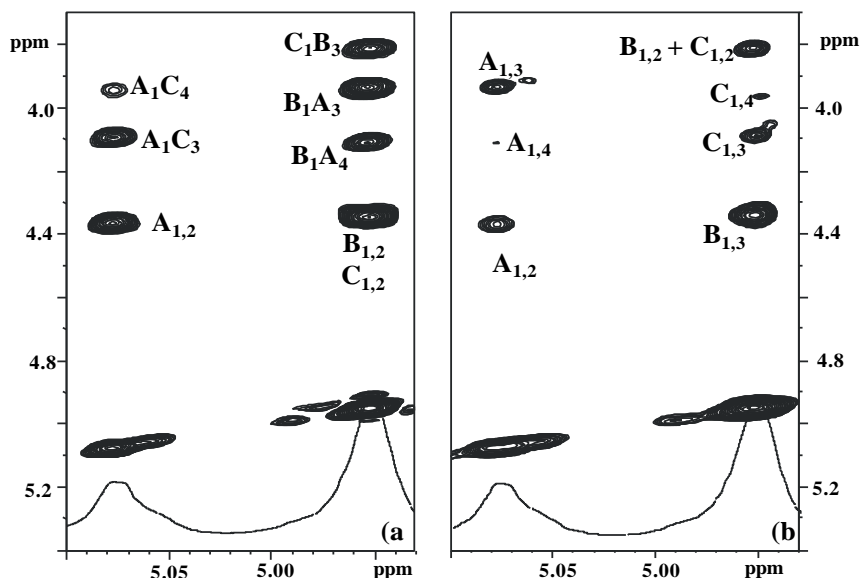


Figure 3.8: (600 MHz, 318 K) Expansion of the NOESY (a) and TOCSY (b) spectra of CPS from *A. baumannii* D36. Attribution of most of the cross peaks is indicated near the corresponding density.

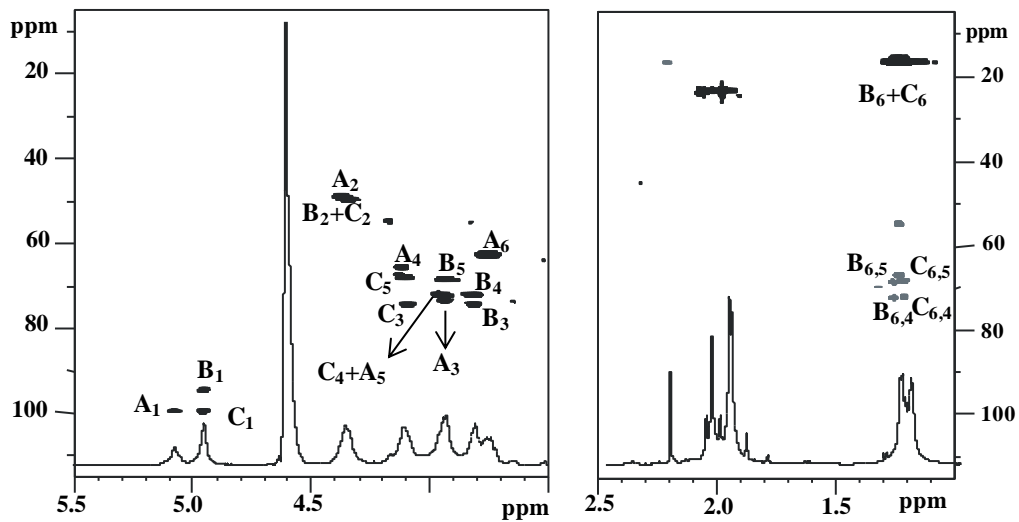


Figure 3.9: (600 MHz; 318K): zoom of gHSQC (black) overlap to HMBC (grey) spectra of acid treated CPS from *A. baumannii* D36. Attribution of most of the cross peaks is indicated near the corresponding density.

		1	2	3	4	5	6
A	¹ H	5.08	4.37	3.40	4.12	3.93	3.76 x 2
3-α-D-GalNAc	¹³ C	99.6	49.8	73.5	65.6	72.5	62.6
B	¹ H	4.95	4.35	3.81	3.81	3.94	1.25
3-α-D-FucNAc	¹³ C	94.7*	49.3	74.3	72.2	68.5	16.5
C	¹ H	4.95	4.34	4.09	3.96	4.10	1.22
3-α-D-FucNAc	¹³ C	99.8*	49.3	74.3	72.1	68.2	16.5

Table 3.2: Proton (600 MHz) and carbon (150 MHz) chemical shifts of acid hydrolyzed CPS obtained by *A. baumannii* D36, measured at 318 K. Spectra were calibrated with respect to internal acetone (¹H: 2.225 ppm, ¹³C: 31.45 ppm). Structure of the repeating unit of the CPS is in figure 4.6.* attribution interchangeable.

3.3.3 Molecular mechanics calculations

Determination of fucosamine C residue absolute configuration by Molecular Mechanic calculation approach.

Since octyl glycoside analysis shows the presence of both 3 linked D and L α -FucNAc, molecular mechanic analyses were performed on the different possible glycosidic junctions. We investigated the conformational space for the glycosidic angles of pure hydrolyzed CPS by MD simulations with Macromodel Software 9.3 using MM3* force field. Two different disaccharides, α -D-GalpNAc-(1 \rightarrow 3)- α -L-FucpNAc (referred as DG-LF) and α -D-GalpNAc-(1 \rightarrow 3)- α -D-FucpNAc (referred as DG-DF), were built, and for each of them, flexible maps were obtained by incrementally changing the two dihedral angles, Φ and Ψ , by steps of 20° in order to evaluate their preferential conformation. As a result, two flexible maps were obtained (Figure 3.10) and the ensemble of conformers generated by the program for each disaccharide entity was used to simulate the NOEs and the averaged inter-

proton distances. Starting from minimum, in these maps optimal dihedral angles were obtained, if two forms were possible the lowest energy was considered, and minimized again with the MM3* force field. The two structures were built up taking the *N*-Acetyl group in the typical *trans* disposition.

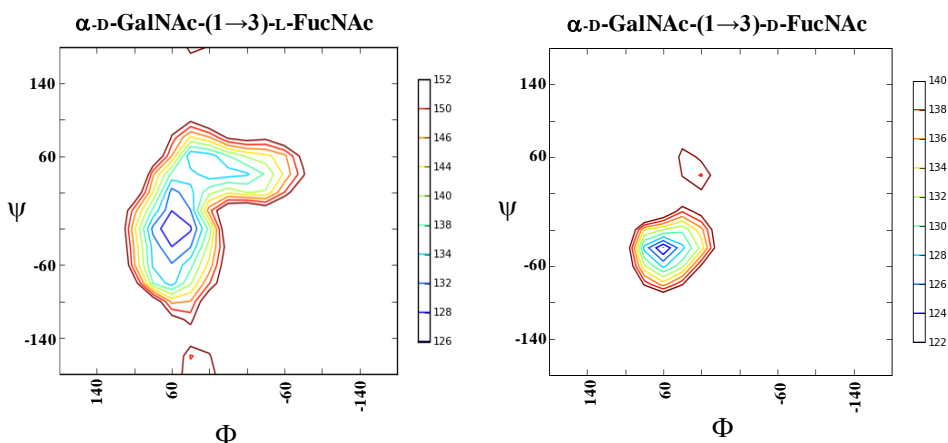


Figure 3.10: MAESTRO flexible maps calculated for the different glycosidic junction.

These results were used to simulate inter residue $\langle r^{-6} \rangle$ distances NOEPROM. Table 3.3 shows calculated inter-proton distances compared to experimental distances. Distance analysis started from H-1 proton of residue A, which present clear correlation with H-3 and H-4 of residue C (figure 3.5 part a). Integration of these NOE correlations permits to obtain inter residue distances¹². Comparison of these results with those obtained from NOESY spectrum indicated that D-GalNAc is linked on C-3 of an L-FucNAc. As showed in Table 3.3, in this case simulated distances are in agreement with those obtained from NOESY spectrum extrapolation; on contrary the other possible disaccharide, DG-DF, shows inter residual distances non compatible with results obtain by NOESY spectrum analysis.

Distance Å	Exp.	Calc	Calc.
		DG-LF	DG-DF
A1-C3	2.69	2.45	2.78
A1-C4	3.76	3.43	2.23

Table 3.3: Experimental (NOESY estimate error 5-10%) and calculated (from MD simulation) inter-proton distances for the different glycosidic junction. Because of severe overlap, only distances experimentally derivate from NOE contact are reported

3.3.4 NMR analysis of monosaccharide mixture

gHSQC spectrum (figure 3.11 part a) of monosaccharide mixture show the presence of several signals; interesting is the high field region between 37 ppm and 44 ppm ca that is attributable to H-3 methylenic carbons of four different nonulosonic residues; these residues were labeled (**D-G**).

NMR analysis started from these signals. Diastereotopic protons at 1.88 and 2.21 were assigned to H-3 methylenic protons of residue **D** (C-3 at 40.4 ppm). These were coupled in COSY spectrum (not shown) with H-4 (3.88 ppm) while TOCSY spectrum (not shown) displayed from H-3 with a proton at 4.14 ppm later identified as H-7. Analysis of HMBC spectrum, figure 3.11, disclosed that H-3 protons correlated with C-2 (97.9 ppm), C-1 (177.3 ppm), C-4 (69.0 ppm) and with a carbon at 55.6 ppm later identify as C-5. Starting from C-9 signal, at 1.16 ppm and 19.7 ppm respectively, is possible, via long range correlation, to identify C-8 (67.6) and C-7 (55.1). The same approach was followed for the other residues.

Identification of different residue was done by comparing proton and carbon chemical shift with those present in bibliography³. In this way residues **D** and **F** were identified as sodium form of α and β anomers of *L-glycero-L-altro*-nonulosonic acid respectively on the basis of $J_{H,H}$ coupling constant, proton and carbon chemical shift⁶.

As for residue **E**, carbon and proton chemical shifts were not found in bibliography. This residue was again in pyranose form, since was present a correlation H-6/C2, but the $^2J_{H3,H3'}$, $^3J_{H3,H4}$ and $^3J_{H3',H4}$ values (14.7, 6.3 and 4.9 Hz respectively) diverged consistently from those of **A** (12.9, 3.9 and 4.3 Hz) and **C** (12.7, 4.5 and 11.2 Hz) for which the ring conformation is a 2C_5 chair.

Interesting is that H-5 was found at 4.18 ppm, shifted at a lower field respect H-5 of **D** (3.88 ppm) and **F** (3.83 ppm) suggesting that, as for Kdo residues, this group was transformed into an acetimido one forming an 1,5 intramolecular lactam. It was reported, indeed, for Kdo that acid conditions can promote intramolecular cyclization between anomeric acidic function and nitrogen of -Nac group on C-5. More bibliography data report that in this case Kdo adopts a skew-boat conformation with a $^3J_{H3,H3'} = 14.5$ Hz; value that is rather close to that found for **E** (14.7 Hz)¹³. The other Kdo coupling constants values ($^3J_{H3,H4}$ and $^3J_{H3',H4}$) diverge from those of **B**, but this can be due a different skew conformation of the pyranose ring of **B** induced by the sequence and by the different stereochemistry the three atoms C-4/C-5/C-6 with respect to those of Kdo. In general, acidic conditions promote formation of intramolecular lactones when the appropriate structural requirements are met, and for **B** an imidolactam is supposed; the reactivity of an acetamido function in this reaction is not unexpected as documented by the formation of cyclic succinimido or aspartimido intramolecular derivatives¹⁴.

With regard to residue **G**; its HMBC spectrum presents a correlation between H-3 protons and a carbon at 205 ppm attributable to a keto form of anomeric signal. The chemical shift of C-4 (71.4 ppm) and C-8 (71.7 ppm) diverged from those of acetaminic residue and displaced at lower field, as if both O-substituted. A possible explanation is given looking reactivity of ulosonic acids after prolonged mild acid treatments. Kdo, indeed, upon prolonged mild acid treatment transforms into it 4,7- and 4,8-anhydro derivatives; the 4,7-anidro is less plausible, as for acinetaminic acid, because cyclization process would involve the poorly nucleophilic acetamido

function at C-7¹⁵. In contrast, formation of the 4,8-anhydro is operated by hydroxyl at C-8 as occur for Kdo. This hypothesis was supported by the analysis of scalar coupling constants; the large value of ${}^3J_{H4,H5}$ (9.7 Hz) indicated the these protons were in trans diaxial position, as occurred for H-7 and H-8 (${}^3J_{H7,H8}$ = 10.4 Hz) while the small value of ${}^3J_{H5,H6}$ indicated that H-6 was in equatorial position of the six-membered ring. These values of scalar coupling constants is in agreement with structure hypothesized for 4,8-anhydroderivative of acinetaminic acid. Chemical shifts of all residues are reported in Table 3.4, structures in figure 3.11 part b.

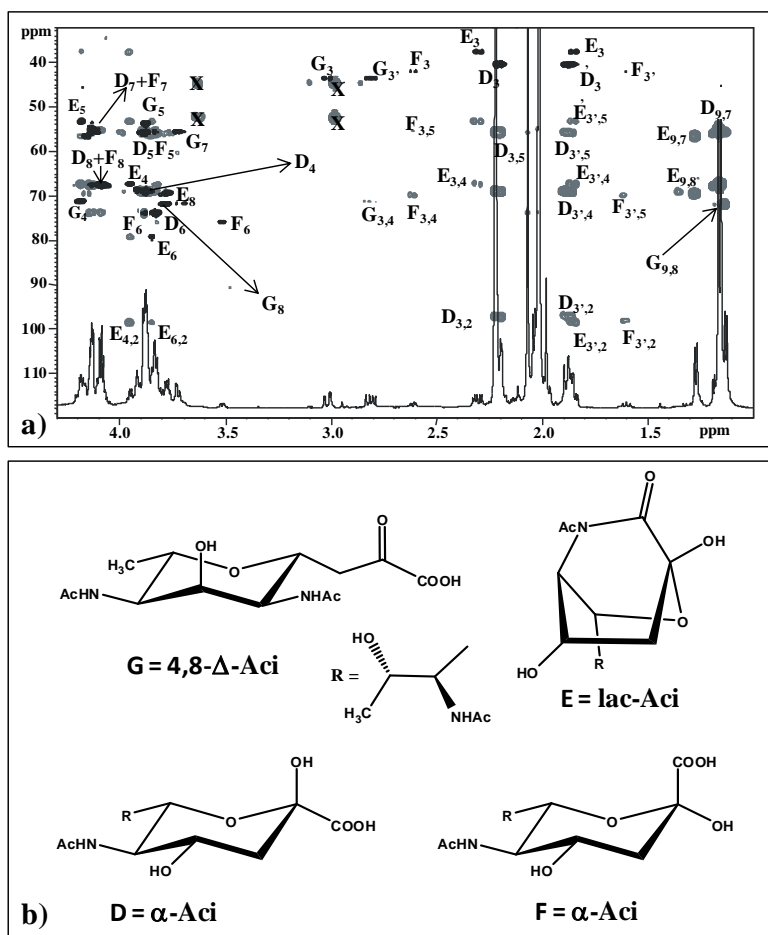


Figure 3.11: Part a: (600 MHz; 398K); zoom of gHSQC (black) overlap to HMBC (grey) spectra of monosaccharide mixture obtained by acid treatment of CPS from *A. baumannii* D36. Attribution of most of the cross peaks is indicated near the corresponding density.

Part b: Structures of the 5,7-diacetamido derivatives of acinetaminic acid obtained after acid hydrolysis. Capital letters refer to those used for NMR attribution. α -Aci: α anomer of Aci; β -Aci: β anomer; lac-Aci: 1,5-lactam form of β -Aci; 4,8- Δ -Aci: 4,8-anhydro form of Aci.

		1	2	3	4	5	6	7	8	9
D	¹ H	-	-	2.21-1.88	3.88	3.88	3.83	4.13	4.09	1.16
α-Aci	¹³ C	177.3	97.9	40.4	69.0	55.6	73.8	55.1	67.6	19.7
E	¹ H	-	-	2.30-1.85	3.95	4.18	3.84	4.15	3.77	1.27
lac-Aci	¹³ C	176.8	98.7	37.6	67.2	53.1	79.1	56.4	69.4	19.3
F	¹ H	-	-	2.61-1.60	3.79	3.83	3.52	4.10	4.06	1.19
β-Aci	¹³ C	175.9	98.2	41.9	69.7	55.7	75.8	55.7	67.5	19.6
G	¹ H	-	-	3.02-2.81	4.19	3.87	3.92	3.73	3.79	1.13
4,8-Δ-Aci	¹³ C	-	205.3	43.55	71.2	53.7	68.4	55.4	71.7	18.6

Table 3.4: Proton (600 MHz) and carbon (150 MHz) chemical shifts of different Acinetaminic residues (Aci, is used as abbreviation of Aci5Ac7Ac) obtained by acid treatment of CPS from *A. baumannii* D36, measured at 318 K. α-Aci: α anomer of Aci; β-Aci: β anomer; lac-Aci: 1,5-lactam form of β-Aci; 4,8-Δ-Aci: 4,8-anhydro form of Aci.

3.4 Chemical and spectroscopical analyses of CPS from *A.baumannii* F4

Acinetobacter baumannii F4 produces a linear capsular polysaccharide constituted by D-galactose (D-Galp), N-acetyl-D-galactosamine (D-GalpNAc) and pseudoaminic (Pse5NAc7NAc) acid linked as showed in the figure 3.12. The complete oligosaccharidic sequence was resolved on the basis of chemical and spectroscopical analysis.

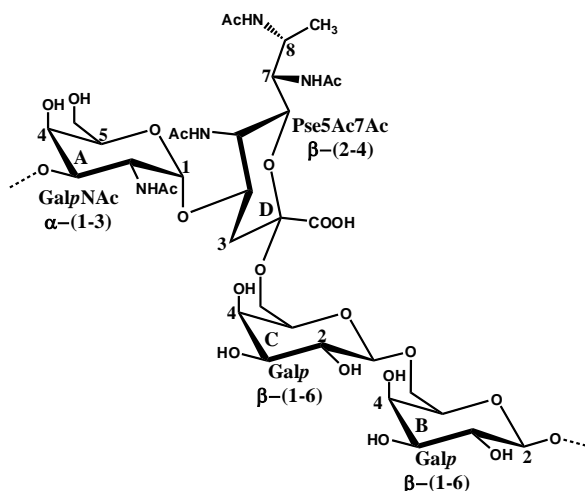


Figure 3.12: The structure of the repeating unit of the CPS from *A. baumannii* F4. For each residue, the chemical structure is drawn together with its abbreviated name, the label used in Table 3.5.

3.4.1 Chemical analyses of CPS

Pure CPS from *Acinetobacter baumannii* F4 was isolated after enzymatic treatment of the crude material present in the water layer of the hot water phenol extraction. In order to eliminate any LOS contamination, this was ultracentrifuged; CPS was found in the supernatant while LOS was found in the precipitate. The polysaccharide was labelled below pure-CPS.

Chemical analysis disclosed the occurrence of Gal and GalNAc, linked at position 6 and position 3 respectively following methylation protocol for neutral sugars².

An additional component was detected in the acetylated methyl glycosides mixture, with the fragmentation pattern compatible with that of a 5,7-diacetamido-3,5,7,9-tetra-deoxy-2-keto-nonulosonic acid, later identified as pseudaminic acid (5,7-diacetamido-3,5,7,9-tetra-deoxy-2-keto-L-glycero-L-manno-nonulosonic acid)¹.

First NMR inspection of the pure CPS returned a proton spectrum with well-defined signals (figure 3.13). It was possible to identify a signal at 5.04 ppm attributable to an anomeric proton having a α configuration and two signals at 4.47 ppm and 4.42 ppm respectively attributable to two different anomeric protons with a β configuration. The spectrum contained also three N-acetyl signals at ca. 2 ppm, two protons of a deoxy position at 1.63 and 2.55 ppm and one methyl group at 1.21 ppm, these last three signals together with two of the N-Acetyl groups were consistent with Pse.

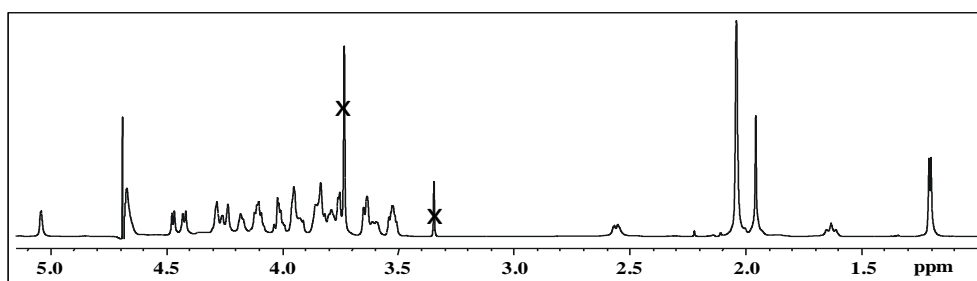


Figure 3.13: ¹H NMR spectrum (600 MHz, D₂O, 310K) of pure-CPS after. Signals of impurities are crossed and the temperatures used are indicated on the spectra.

Since also 2D NMR spectra showed a good quality, pure CPS was directly analyzed for the structural assignment.

3.4.2 NMR analyses of CPS

The ¹H NMR spectrum, as shown in figure 3.13, contained three signals in the anomeric region (5.00–4.00 ppm) in an approximate 1:1:1 ratio; these signals were labelled with a letter (A–C) in the order of their decreasing chemical shifts, and D was given to Pse residue.

Analysis of the 2D NMR spectra of the polysaccharide permitted the assignment of all proton and carbon chemical shifts (Table 3.5).

For **A** H-1 in the TOCSY spectrum had only two correlations due to the null H-4/H-5 coupling typical of the *galacto* ring stereochemistry H-5 was identified because of the *intra*-residue H-5/H-3 and H-5/H-4 cross peaks present in the NOESY spectrum. C-2 resonated at 49.9 ppm indicating a nitrogen bearing carbon, and H-2 chemical shift (4.27 ppm) proved the acetylation of the amino function. Therefore, **A** was a N-acetylated α -galactosamine and the low field shift of its C-3 signal (78.9 ppm) with respect to the standard value (72.3 ppm)³ confirmed glycosylation at this position.

With regard to residue **B**, its H-1 (4.47 ppm) shows only three cross peaks in the TOCSY (not shown) spectrum with H-2, H-3, H-4, as occurs for a *galacto*-configured residue, for which magnetization is not propagated further than H-4.

This residue was identified as β -galactose on the basis of anomeric chemical shift and because this proton showed the expected NOEs with H-3 and H-5; more and C-6 carbon chemical shift, at 71.0, proved glycosylation at this position.

The same behaviour was found for residue **C**, which was identified as a β galactose. With regard to glycosylation position, C-6 carbon chemical shift is at 65.2 ppm; this modest shift at low fields was diagnostic of the occurrence of ketose sugar.

Assignment of **D** started from the diastereotopic methylene protons at high field (2.55 and 1.63 ppm), which correlated in the COSY spectrum with H-4 (3.86 ppm) and with a further signal in the TOCSY spectrum, at 4.29 ppm and assigned to H-5. The resonances of the other protons were determined by starting from the methyl signal at 1.21 ppm. The HMBC spectrum correlated this methyl group with a carbon at 70.2 ppm assigned to C-8 and with a carbon at 54.9 given to C-7; the corresponding protons were found in the gHSQC spectrum at 4.10 and 4.01 ppm, respectively, and COSY spectrum linked H-7 to H-6 which was at 4.06 ppm.

Determination of all the carbon chemical shift of **D** evidenced that both its amino groups were N-acetylated, as confirmed by the long range correlation of H-5 and H-7 with a carbonyl (175.3 and 174.9, respectively), and comparison of the carbon chemical shifts of this sugar with those published identified this residue as Pseudaminic acid β configured at the anomeric centre⁴. C-4 chemical shift, 73.1 ppm suggests a glycosylation at this position. HMBC spectrum analysis permitted also the identification of C-2 and C-1 at 102.8 ppm and 174.2 ppm respectively.

Oligosaccharide sequence was elucidated by the analysis of long range correlation; HMBC spectrum (figure 3.14), indeed, shows a correlation between C-1 of residue **A** and C-4 of residue **D**, more starting from anomeric signals of residue **B** and **C** is possible to find a correlation with C-3 of residue **A** and C-6 of **B** respectively. These results were confirmed by the analysis of NOESY spectrum, which displayed these key correlations: H-1 of **A** with H-3 and H-3' of **D**, H-1 of **B** with H-3 and H5 of **A**, H-1 of **C** with H-6 of **B**.

These data, combined with the linkage analysis and with the carbon chemical shift analysis allowed elaboration of the structure of the repeating unit of the polysaccharide, reported in figure 3.12.

		1	2	3	4	5	6	6'
A	^1H	5.04	4.27	3.85	4.24	4.18	3.76	3.76
3- α -GalpNAc	^{13}C	96.7	49.9	78.9	69.9	72.3	62.9	-
B	^1H	4.47	3.35	3.64	3.95	3.83	3.81	4.11
6- β -Galp	^{13}C	105.1	72.0	73.9	70.1	75.1	71.0	-
C	^1H	4.42	3.55	3.64	3.95	3.79	3.60	3.93
6- β -Galp	^{13}C	105.8	72.0	73.9	70.1	74.8	65.2	-
		3	4	5	6	7	8	9
D	^1H	1.63; 2.56	3.86	4.29	4.06	4.01	4.10	1.21
4- β -Pse	^{13}C	34.4	73.1	48.8	74.8	54.9	70.2	18.3

Table 3.5: Proton (600 MHz) and carbon (150 MHz) chemical shifts of CPS obtained by *A. baumannii* F4, measured at 310 K. Spectra were calibrated with respect to internal acetone (^1H : 2.225 ppm, ^{13}C : 31.45 ppm). Structure of the repeating unit of the CPS is in figure 3.12.

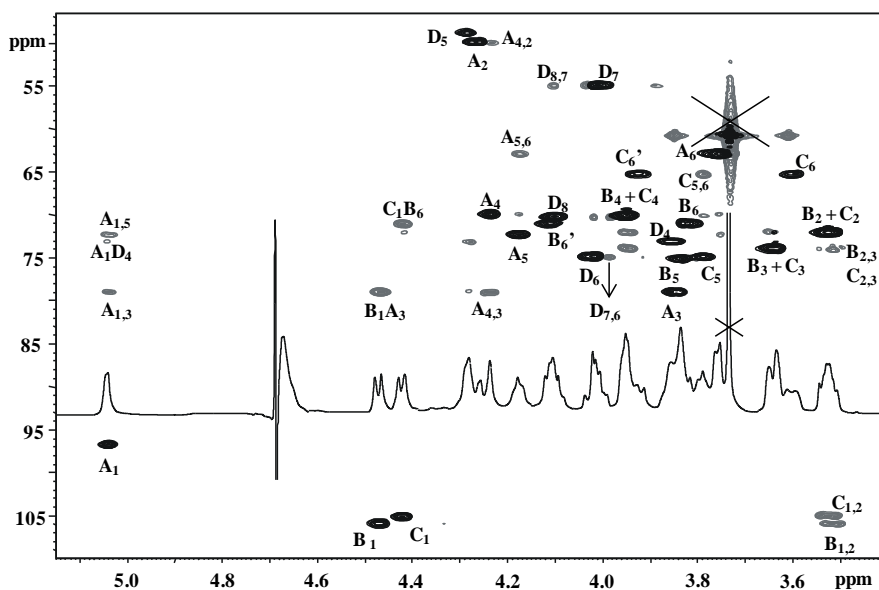


Figure 3.14: (600 MHz, D_2O , 298 K) Expansion of gHSQC spectrum (black) overlapped to HMBC spectrum (grey) of pure CPS from *A. baumannii* F4. Attribution of most of the cross peaks is indicated nearby the corresponding density. The structure of the repeating unit of the CPS is reported in Figure 4.14 together with the labels used.

3.5 Chemical and spectroscopical analyses of CPS from *A. baumannii* D46

A. baumannii D46 CPS is a branched polysaccharide with a backbone composed by GalNAc, Gal and Glc residues, all of them D configured (Figure 3.15). Its structure was resolved on the basis of the NMR and chemical analyses

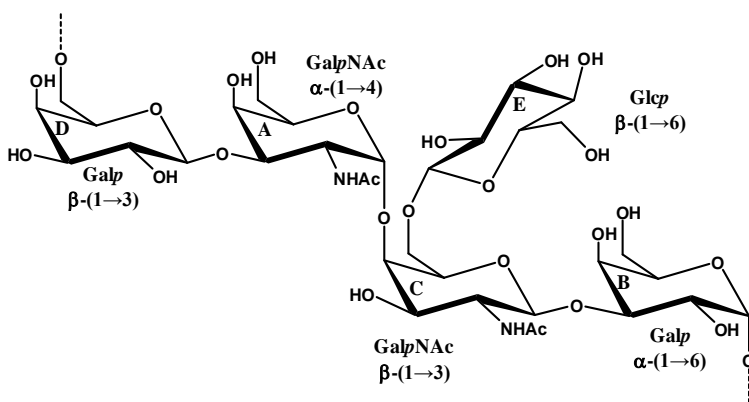


Figure 3.15: The structure of the repeating unit of the CPS from *A. baumannii* D46. For each residue, the chemical structure is drawn together with its abbreviated name and the label used in Table 3.6.

3.5.1 Chemical analyses of CPS

CPS produced by *Acinetobacter baumannii* D46 was obtained after enzymatic treatment of the crude material present in the water phase of hot water phenol extraction. In order to eliminate LOS contamination enzymatic treated polysaccharide was ultracentrifuged, CPS was found in the supernatant (figure 3.16 part a). and labelled pure-CPS.

Chemical analyses disclosed the occurrence of Gal, Glc and GalNAc, all of them with a D configuration. The methylation protocol for neutral sugars reveals a terminal Glc, two different Gal residues, linked at position 4 and position 6 respectively and two GalNAc residues: one linked at position 3 and another linked at positions 4 and 6². Kdo, the marker of lipopolysaccharide, was not found.

First NMR inspection of the pure CPS returned a proton spectrum with well defined signals (figure 3.16 part a). It was possible to identify two signals at 5.03 ppm and 4.97 ppm, attributable to two anomeric protons having α configuration and three signals at 4.70 ppm, 4.56 ppm and 4.42 ppm, attributable instead to three anomeric protons having a β configuration. The spectrum also contains two N-acetyl signals at 2 ppm.

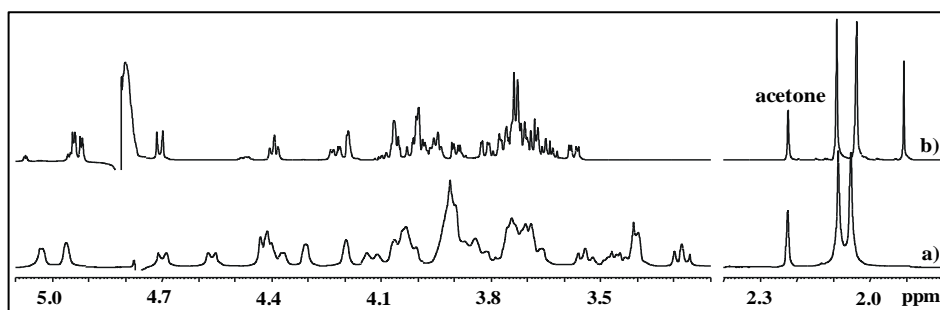


Figure 3.16: ^1H NMR spectra of CPS after (a) enzymatic purification and ultracentrifugation (400MHz, 298K) and (b) after smith degradation (600 MHz, 298K). Spectra were calibrated with acetone as internal standard (2.225 ppm).

3.5.2 NMR analyses of CPS

The ^1H NMR spectrum (figure 3.16 part a) contains five signals in the anomeric region (5.30–4.00 ppm) in an approximate 1:1 ratio; each signal is labelled with a letter (A–E) in the order of their decreasing chemical shifts.

The 2D NMR spectra analysis of the polysaccharide permitted the complete assignment of proton and carbon chemical shifts (Table 3.6, structure in figure 3.15). According to the Table 3.6, the A proton resonates at 5.03 ppm, indicating the α configuration of the anomeric centre. In the TOCSY spectrum, H-1 of A has correlations only with protons H-2, H-3 and H-4 the absence of other correlation can be the consequence of a peak cancellation due to a small $J_{3,4}$ coupling constant characteristic of a *galacto* ring stereochemistry. The NOESY spectrum allowed the complete attribution of ring protons. The gHSQC techniques used to assign the

corresponding ^{13}C ; in particular, the C-2 resonates at 49.8 ppm suggesting the presence of a nitrogen bearing carbon, and the H-2 chemical shift (4.38 ppm) proves the acetylation of the amino function. Moreover, **A** is a *N*-acetylated α -galactosamine and the low field shift of its C-3 signal (78.7 ppm) in comparison to the standard value (72.3 ppm)³ confirms the glycosylation at this position, figure 3.17. In the residue **B**, the H-1 (4.97 ppm) shows only two cross peaks in the TOCSY spectrum with protons H-2 and H-4, H-3 resonated at the same value of H-2, as is typical in a *galacto* configuration of sugar ring. The complete assignment was possible by the analysis of NOESY and HMBC spectra. This residue is identified as α -galactose on the basis of anomeric chemical shift, according to the C-3 carbon chemical shift at 80.5 ppm that proves glycosylation at this position.

The same behaviour is found for residue **C**, which is identified as a β -GalNAc: C-2 chemical shift at 53.8 ppm indicates a nitrogen bearing carbon. The glycosylation in the C-4 and C-6 position is confirmed by the carbon chemical shift at 77.1 and 69.2 ppm respectively.

Residue **D** shows, again, the classical behaviour of a galactose residue. H-1 shows three TOCSY correlations with protons H-2, H-3 and H-4 respectively; complete assignment was possible by the analysis of NOESY spectrum. Chemical shift of C-6 at 67.3 ppm confirms the glycosylation at this position.

Residue **E** is identified as a terminal glucose. It is possible to identify all proton ring starting from the anomeric signal at 4.42 ppm and by COSY and TOCSY correlations. The methylation analysis, with the comparison between the carbons chemical shift and those reported in bibliography³, proves that the residue **E** is an external residue.

Oligosaccharide sequence was elucidated on the basis of NOESY correlations, which displayed these key correlations: H-1 of **A** with H-4 of **C**, H-1 of **B** with H-6' and H-6 of **D**, H-1 of **C** with H-3 and H-4 of **B**, H-1 of **D** with H-3 and H-4 of

A; H-1 of **E** with H-6 and H-6' of **C**; HMBC spectrum (figure 3.17) shows correlation between C-1 of **E** and C-6 of **C**.

These data, combined with the linkage analysis and with the carbon chemical shift analysis permitted the elaboration of the structure of the repeating unit of the polysaccharide, reported in figure 3.15.

To confirm the oligosaccharidic sequence, a periodate degradation was performed¹⁶. The ¹H NMR spectrum (figure 3.16 part b) of degraded product contains three signals in the anomeric region (5.30–4.00 ppm) in an approximate 1:1 ratio; each signal is labelled with a letter (**A–C**) in the order of their decreasing chemical shifts. The analysis of 2D spectra of oligosaccharide (Figure 3.18 gHSQC spectrum) permitted the complete assignment of proton and carbon chemical shift (Table 3.7, structure in figure 3.19) and confirmed the structure of pure CPS, as reported in figure 3.15.

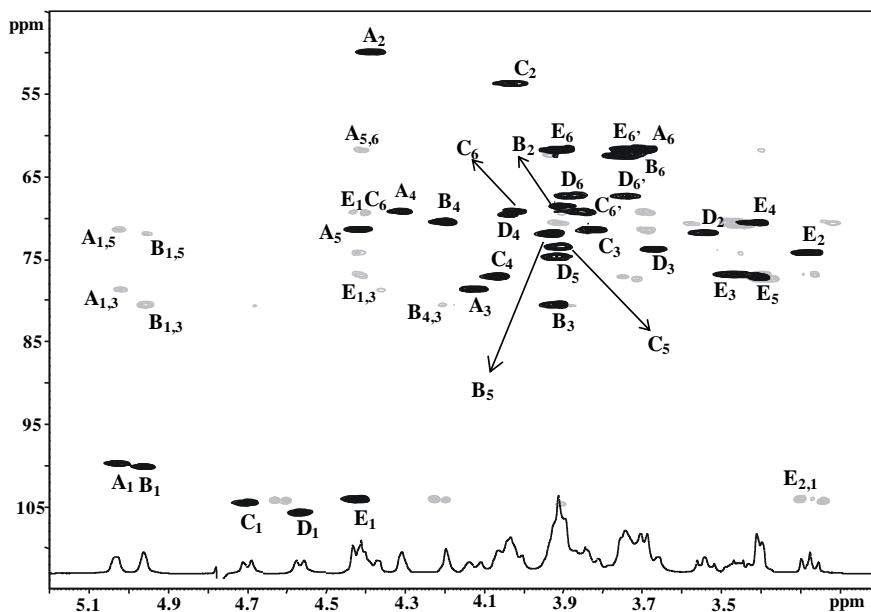


Figure 3.17: (400 MHz, D₂O, 298 K) Expansion of gHSQC spectrum (black) overlapped to HMBC spectrum (grey) of pure CPS from *A. baumannii* D46. Attribution of most of the cross peaks is indicated nearby the corresponding density. The structure of the repeating unit of the CPS is reported in Figure 3.15 together with the labels used.

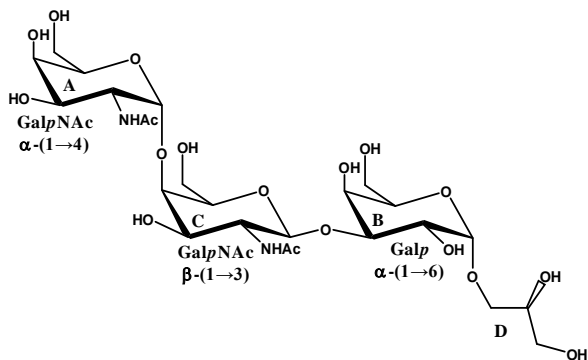


Figure 3.18: The structure of the oligosaccharide obtained by Smith degradation of the pure CPS from *A. baumannii* D46. For each residue, the chemical structure is drawn together with its abbreviated name and the label used in Table 3.7.

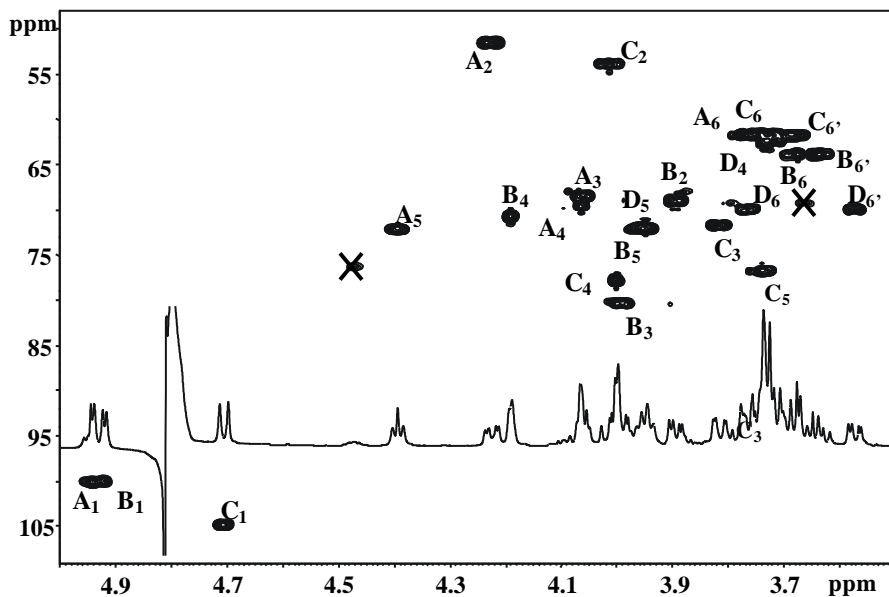


Figure 3.19: (600 MHz, D₂O, 298 K) Expansion of gHSQC spectrum of oligosaccharide obtained by Smith degradation of pure CPS from *A. baumannii* D46. Attribution of most of the cross peaks is indicated nearby the corresponding density. The structure of the repeating unit of the oligosaccharide is reported in Figure 5 together with the labels used. The signals crossed are impurity.

		1	2	3	4	5	6	6'
A	¹ H	5.03	4.38	4.13	4.31	4.41	3.70	3.70
3-α-GalpNAc	¹³ C	99.8	49.8	78.7	69.2	71.4	61.6	-
B	¹ H	4.97	3.91	3.91	4.20	3.93	3.91	3.75
3-α-Galp	¹³ C	100.2	68.5	80.5	70.4	71.8	62.2	-
C	¹ H	4.70	4.03	3.83	4.06	3.90	4.01	3.85
4-6-β-GalpNAc	¹³ C	104.5	53.8	71.4	77.1	73.4	69.1	-
D	¹ H	4.56	3.54	3.64	4.03	3.91	3.88	3.74
6-β-Galp	¹³ C	105.7	71.6	73.7	69.7	74.8	67.3	-
E	¹ H	4.42	3.28	3.47	3.40	3.40	3.91	3.74
t-β-GlcP	¹³ C	104.1	74.2	76.8	70.5	77.1	61.6	-

Table 3.6: Proton (400 MHz) and carbon (100 MHz) chemical shift of CPS obtained by *A. baumannii* D46, measured at 298 K. Spectra were calibrate with respect to internal acetone (¹H: 2.225 ppm; ¹³C: 31.45 ppm). Structure of the repeating unit of the CPS is in figure 3.15.

		1	2	3	4	5	6	6'
A	¹ H	4,95	4,02	4,06	4,06	4,4	3,78*2	-
t-α-GalpNAc	¹³ C	100,1	53,9	68,5	69,4	72,0	61,6	-
B	¹ H	4,92	3,9	3,99	4,19	3,94	3,96	3,63
3-α-Galp	¹³ C	100,1	68,9	80,3	70,7	71,9	63,8	-
C	¹ H	4,71	4,01	3,82	4	3,74	3,69*2	-
4-β-GalpNAc	¹³ C	104,8	53,9	71,7	77,9	71,9	61,6	-
D	¹ H	-	-	-	3,73*2	3,97	3,76	3,57
glycerol	¹³ C	-	-	-	62,5	71,9	69,9	-

Table 3.7: Proton (600 MHz) and carbon (150 MHz) chemical shift of oligosaccharide obtained by periodate oxidation of pure CPS from *A. baumannii* D46, measured at 298 K. Spectra were calibrate with respect to internal acetone (¹H: 2.225 ppm; ¹³C: 31.45 ppm). Structure of the repeating unit of the oligosaccharide is in figure 3.18.

3.6 Chemical and spectroscopical analyses of CPS from *A.baumannii* D78

The structure of capsular polysaccharide (CPS) produced by *Acinetobacter baumannii* D78, a nosocomial pathogen, was elucidated by means chemical and spectroscopical analysis.

A. baumannii D78 produces a branched polysaccharide constituted by GalpNAc, QuipNAc and PyrGalpNAc, all of them D configured (figure 3.20)

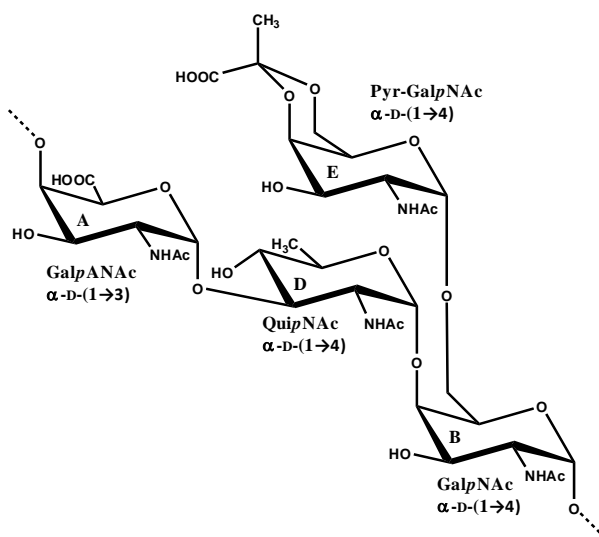


Figure 3.20: The structure of the repeating unit of the CPS from *A. baumannii* D78. For each residue, the chemical structure is drawn together with its abbreviated name and the label used in Table 3.8.

3.6.1 Chemical analyses of CPS

CPS produced by *Acinetobacter baumannii* D78 was obtained by enzymatic treatment of crude material present in water phase of hot phenol-water extraction. Enzyme treated material was ultracentrifuged two times, to eliminate LOS contamination, and CPS was found in supernatant.

Chemical analysis disclose the presence of QuiNAc, GalNAc, all of them D configured, as deducible, applying methylation protocol for neutral sugar², linked at position 4 and at positions 4 and 6 respectively. Also a GalNAcA and a Pyr-GalNAc were found and the linkage position was identified by the analyses of NMR spectra.

Kdo, the marker of lipopolysaccharide, was not found or it was below the detection limit of the instrument.

First NMR inspection of the pure CPS returned a proton spectrum with broad signals (figure 3.21 part b), however it was possible to identify four anomeric protons, in the region between 5.40 and 4.70, and four N-acetyl signals at ca. 2 ppm. In the aliphatic proton region, between 1,0 ppm and 1,5 ppm, resonate two different methyl signals: one at ca. 1.2 ppm attributable to the methyl group of QuiNAc; the second, at 1.5, attributable instead, to a methyl group of a pyruvic acid.

Since 2D spectra of pure-CPS do not present well defined signals, a mild acid hydrolysis was performed, in order to eliminate pyruvic acid (section 6.6.3). As showed by integration of methyl signals, only the 40% of pyruvic acid was hydrolysed (figure 3.21) obtaining a polysaccharide composed of an alternation of pyruvated and not pyruvated forms. However it was possible to resolve the structure of both by the analysis of 2D spectra. Starting from this information, it was possible to assign also the spectrum and to resolve the structure of native polysaccharide (figure 3.20).

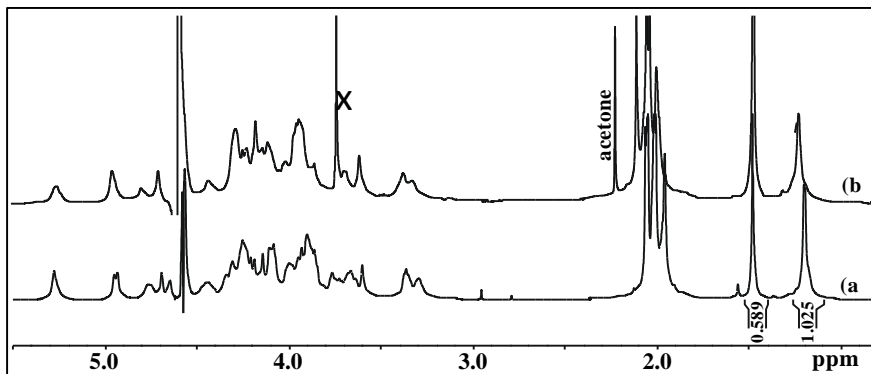


Figure 3.21: ^1H NMR spectra (600 MHz, 318K, D_2O) of CPS after a) after mild acid hydrolysis and b) enzymatic purification. Signals of impurities are crossed.

3.6.2 NMR analyses of CPS

The ^1H NMR spectrum of acid treated polysaccharide (figure 3.21 part a) contained five signals in the anomeric region (5.30–4.00 ppm) in an approximate 1:1 ratio; these signals were labelled with a letter (A–E) in the order of their decreasing chemical shifts.

Analysis of the 2D NMR spectra of the polysaccharide permitted the assignment of all proton and carbon chemical shifts (Table 3.8, structure in figure 3.20).

As for **A**, the proton resonated at 5.27 ppm, indicating the α configuration of the anomeric centre. In the TOCSY spectrum (figure 3.22 part b), H-1 of **A** had only three correlations with protons H-2, H-3 and H-4 as occurs for a *galacto*-configured residue. Complete attribution of ring protons was possible by the analysis NOESY spectrum (figure 3.22 part b) and gHSQC was used to assign the corresponding ^{13}C ; particularly C-2 resonating at 50.0 ppm suggest the presence of a nitrogen bearing carbon, and H-2 chemical shift (4.24 ppm) proved the acetylation of the amino function. HMBC spectrum showed a correlation between C-5 and a density at 172 ppm suggesting the presence of an acid group at position C-6 as anticipated by MGA analysis. Therefore, **A** was a N-acetylated α -

galactosaminuronic residue and the low field shift of its C-4 signal (77.6 ppm) with respect to the standard value³ confirmed glycosylation at this position, figure 4.

With regard to residue **A'**, its H-1 (5.27 ppm) showed only two cross peaks in the TOCSY spectrum with protons H-2, H-3 and H-4 indicating, also in this case, a *galacto* configuration of sugar ring. Total assignment was possible by the analysis of NOESY and HMBC spectra. This residue also appeared to be a 4-GalNAcA residue.

Residue **B** was identified as a α -GalNAc, C-2 chemical shift at 50.8 ppm indicates a nitrogen bearing carbon. With regard to glycosylation position C-4 and C-6 carbon chemical shift at 67.5 ppm and 63.9 ppm respectively proved glycosylation at these positions. The same behaviour was found for residue **C**, indeed, its H-1 presents only TOCSY correlation with protons H-2 and H-3/H-4, characteristic of *galacto* configured ring and carbon chemical shifts of C-4 and C-6, respectively at 67.5 ppm and 63.9 ppm confirming glycosylation at these positions, as showed also by methylation analysis.

Residue **D** was identified as a α -QuiNAc, starting from anomeric signal, at 4.75 ppm, following COSY and TOCSY correlation it was possible to identify all protons ring. C-2 chemical shift, 53.6 ppm, demonstrated a nitrogen bearing carbon, while C-3 resonating at 80.0 ppm confirmed glycosylation at this position.

Residue **E** was identified as a terminal GalNAc-Pyr residue; in the high field region of ¹H spectrum, it was possible to find at 1.54 ppm a singlet attributable to a methyl group. In HMBC spectrum is possible to identify a correlation between this substituent and two densities at 101 ppm and 176 ppm, respectively, attributable to a quaternary carbon and acid group of a pyruvic substituent¹⁷. Anomeric proton of this residue shows TOCSY correlation only with H-2, H-3 and H-4, indicating a *galacto* configuration of carbohydrate ring. The assignment was possible using NOESY and HMBC spectrum. The configuration of acetal carbon atoms was possible on the basis of bibliography data¹²; chemical shifts of CH₃ substituent,

indeed, at 1.54 ppm and at 26 ppm and the absence of NOESY correlations between this and other ring protons confirm an axial orientation of methylenic group.

With regards to residue **F**, it was identified as a terminal GalNAc on the basis of TOCSY correlations and bibliography data.

The order of residue was inferred analyzing NOESY spectrum (figure 3.22 part a), that displayed these key correlations: H-1 of **A** with H-3 of **D** and H-1 of **A'** with H-3 of **D**; H-1 of **B** with H-4 of **A**; H-1 of **C** with H-4 of **A'**; H-1 of **D** with H-4 of **C** and with H-4 of **B**; H-1 of **E** with H-6 and H-6' of **B** and H-1 of **F** with H-6 and H-6' of **C**. The presence of two different oligosaccharides is related to a partially hydrolysis of pyruvic substituent as showed also from integration of $^1\text{H-NMR}$ spectrum (figure 3.21 part a).

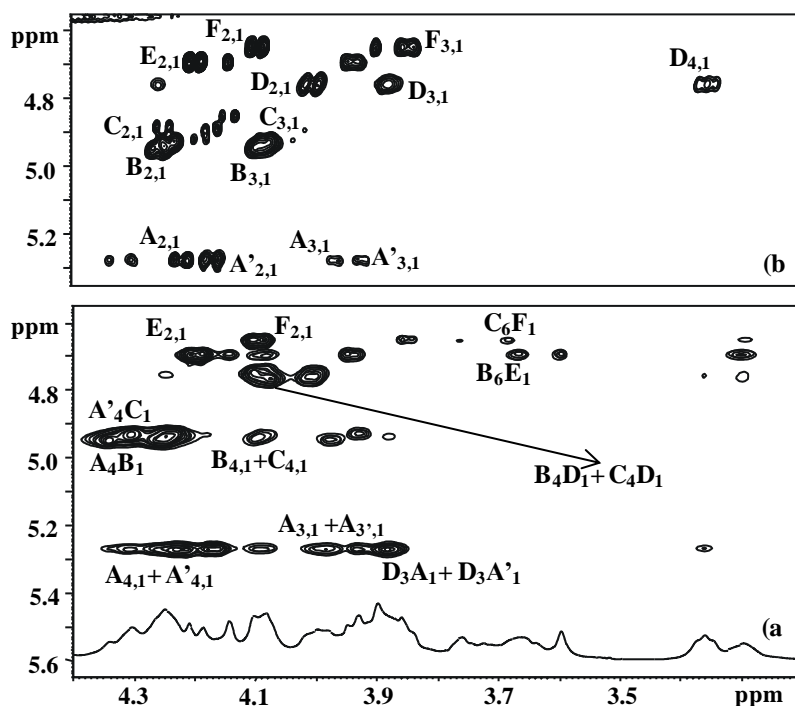


Figure 3.22: (600 MHz, 318 K, D_2O) Expansion of NOESY (a) and TOCSY (b) spectra of acid treated CPS from *A. baumannii* D78. Attribution of most of the cross peaks is indicated nearby the corresponding density. Letter labels reflect those reported in Table 3.8.

Starting from the information obtained from the analysis of spectra of acid treated CPS; it was possible to resolve broadly the spectra of a pure-CPS and to obtain its structure as reported in figure 3.20.

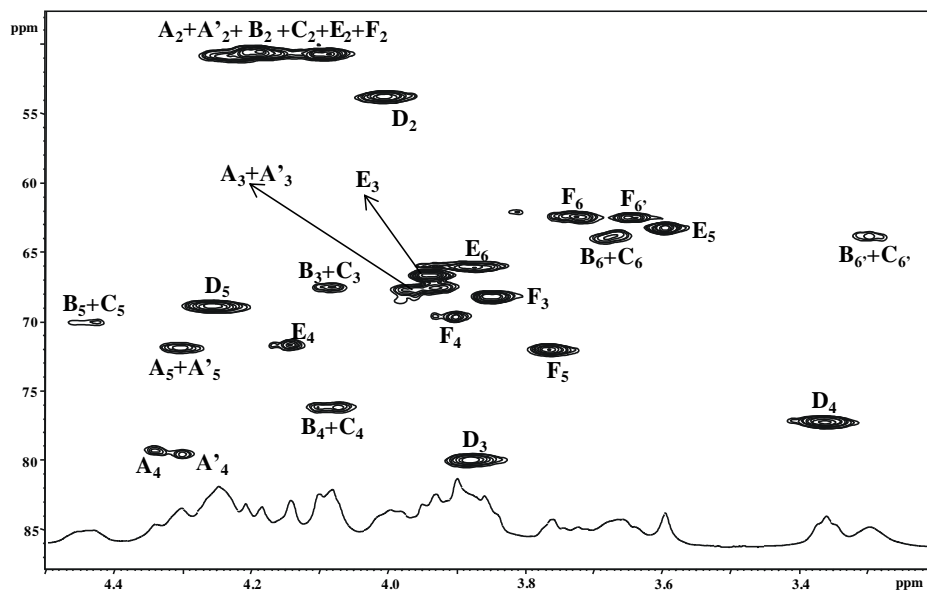


Figure 3.23: (600 MHz, D₂O, 318 K) Expansion of gHSQC spectrum acid treated CPS from *A. baumannii* D78. Attribution of most of the cross peaks is indicated nearby the corresponding density. The structure of the repeating unit of the CPS is reported in Figure 1 together with the labels used.

		1	2	3	4	5	6	6'
A	¹ H	5.27	4.24	3.97	4.34	4.30	-	-
4- α -GalpANAc	¹³ C	100.0	50.0	67.7	79.2	71.6	173	-
A'	¹ H	5.27	4.16	3.92	4.29	4.28	-	-
4- α -GalpANAc	¹³ C	100.0	50.0	67.3	79.6	71.5	173	-
B	¹ H	4.95	4.26	4.08	4.10	4.44	3.67	3.29
4-6- α -GalpNAc	¹³ C	99.8	50.8	67.5	76.0	70.1	63.9	-
C	¹ H	4.92	4.24	4.08	4.10	4.44	3.67	3.29
4-6- α -GalpNAc	¹³ C	99.8	50.8	67.5	76.0	70.1	63.9	-
D	¹ H	4.75	4.01	3.87	3.36	4.26	1.21	-
4- α -QuiPNAc	¹³ C	98.9	53.6	80.0	77.3	69.0	17.2	-
E	¹ H	4.69	4.20	3.91	4.14	3.60	3.88*2	-
<i>t</i> -Pyr- α -GalNAc	¹³ C	97.9	50.6	67.7	71.8	63.1	66.0	-
F	¹ H	4.65	4.08	3.84	3.90	3.76	3.73	3.64
<i>t</i> - α -GalNAc	¹³ C	97.6	50.8	68.2	69.2	71.8	62.6	-
Pyruvate	¹ H	1.54	-	-	-	-	-	-
	¹³ C	26.0	101	176	-	-	-	-

Table 3.8: Proton (600 MHz) and carbon (150 MHz) chemical shifts of oligosaccharidic mixture obtained by mild hydrolysis of pure CPS from *A. baumannii* D78, measured at 298 K. Spectra were calibrated with respect to acetone as internal standard (¹H: 2.225 ppm, ¹³C: 31.45). Structure of the repeating unit of the CPS is in figure 3.20.

3.7 Conclusions

This work was conducted in collaboration with dr. J. Kenyon at the University of Sidney. The principal aim of this collaboration was the elucidation of biosynthetic pathway of CPSs produced by different nosocomial strains of *Acinetobacter baumannii*. In this contest fundamental is the knowledge of CPS polysaccharide structure; so far this work was conducted on five different strains of *Acinetobacter baumannii* isolate from different Australian hospitals: *A. baumannii* A74, D36, F4, D46 and D78. The analysis of different CPSs structures was performed on the basis of chemical and spectroscopical data.

Starting from enzyme treated polysaccharides chemical analyses disclosed the presence of sugars reported in table 3.9.

Strain	RESIDUES				
A74	3-D-β-GalpNAc	3,6-D-β-Galp	6-D-β-Glc	<i>t</i> -α-Pse5Ac7Ac	-
D36	3-α-D-FucpNAc	3-L-α-FucpNAc	3,6-D-α-GalpNAc	<i>t</i> -α-Aci5Ac7Ac	
F4	3-D-α-GalpNAc	6-D-β-Galp	6-D-β-Galp	2-β-Pse5Ac7Ac	-
D46	6-D-β-Galp	3-D-α-GalpNAc	4,6-D-β-GalpNAc	<i>t</i> -β-D-Glcp	3-D-α-Galp
D78	4-D-α-GalApNAc	3-D-α-Quip	4,6-D-α-GalpNAc	<i>t</i> -Pyr-D-α-GalpNAc	

Table 3.9: monosaccharides identified in different strain of *A.baumannii*

NMR analyses allowed the establishment of the CPS repeating unit for all these strains. Interesting was the presence in all the polysaccharides of *galacto* configured residues and in three of them of a 5,7-diamino-2-nonulosonic acid isomers. *A. baumannii* D36 produced a CPS containing an L-*glycero*-L-*altro* nonulosonic acid (Aci5NAc7NAc) stereoisomer which was for the first time isolated by a bacterial source⁸.

References

- ¹ Van Looveren M., and Goossens H.; Antimicrobial resistance of *Acinetobacter* spp. in Europe. *Clin. Microbiol. Infect.* **2004**, Vol. 10 (8), pp. 684-704
- ² Fregolino E., Fugazza G., Galano E., Gargiulo V., Landini P., Lanzetta R., Linder B., Pagani L., Parrilli M., and Holst O.; Complete lipooligosaccharide structure of the clinical isolate *Acinetobacter baumannii*, Strain SMAL; *Eur. J. Org. Chem.*; **2010**; Vol. 7; pp. 1375-1352.
- ³ Kenyon J.J., Marzaioli A.M., Hall R.H., and De Castro C.; Structure of the K2 capsule associated with the KL2 gene cluster of *Acinetobacter baumannii*; *Glycobiology*; **2014**; Vol. 26 (6); pp. 554-563.
- ⁴ De Castro, C., Parrilli, M., Holst, O., and Molinaro, A.; Chapter Five - Microbe-Associated Molecular Patterns in Innate Immunity: Extraction and Chemical Analysis of Gram-Negative Bacterial Lipopolysaccharides. *Methods in Enzymology* , 2010; Vol.480, pp. 89-115: Academic Press.
- ⁵ Bock K., and Pederden C.; Carbon-13 nuclear magnetic resonance spectroscopy of monosaccharides; *Adv. Carbohydr. Chem. Biochem.*; **1983**; Vol.41; pp. 27-66.
- ⁶ Tsvetkov Y.E., Shashkov A.S., Knirel Y. A., and Zähringer U.; Synthesis and NMR spectroscopy of nine stereoisomeric 5,7-diacetamido-3,5,7,9-tetraoxynon-2-ulosonic acids; *Carbohydr. Res.*; Vol.335; pp. 221-234.
- ⁷ Perepelov A. V., Shashkov A. S., Tomshich S. V., Komandrova N. A., and Nedashkovskaya O. g. I.; A pseudoaminic acid-containing O-specific polysaccharide from a marine bacterium *Cellulophaga fucicola*. *Carbohydrate Research*, **2007** 342(10), pp. 1378-1381.
- ⁸ Kenyon J.J., Marzaioli A.M., De Castro C., and Hall R.H.; 5,7-di-*N*-acetyl-acinetaminic acid - a novel non-2-ulosonic acid found in the capsule of an *Acinetobacter baumannii*; *Glycobiology*; **2014**; doi: 10.1093.
- ⁹ Knirel Y.A., Shevelev S.D., Perepelov A.V.; Higher aldulosonic acid: components of bacterial glycans; *Mendeleev Commun.*; **2011**; Vol. 21; pp. 173-182.
- ¹⁰ Knirel Y. A., Kocharova N. A., Shashkov A. S., Dmitriev B. A., Kochetkov N. K., Stanislavsky E. S., and Mashilova G. M.; Somatic antigens of *Pseudomonas aeruginosa*; *Eur. J. Biochem.*; **1987**; Vol.163; pp. 639-652.
- ¹¹ Hashii N., Isshiki Y., Igushi T., Kondo S.; Structural characterization of the carbohydrate backbone of lipopolysaccharide of *Vibrio parahaemolyticus* O-untypeable strain KX-V212 isolated from a patient. *Carbohydr. Res.*; **2003**; Vol. 338; pp. 2711-2719.
- ¹² Kessel H.; Griesinger C, Joerg. Lautz J. , Mueller A, Van Gunsteren W.F., and Berendsen G.C.; Conformational dynamics detected by nuclear magnetic resonance NOE values and J coupling constants; *J. Am. Chem. Soc.*, **1988**, Vol. 110 (11), pp.3393-3396.

- ¹³ Auzanneau F., Charon D, and Szabó L.. Synthesis of 1,5-lactones of 3-deoxy-Dmanno-2-octulopyranosonic acid (Kdo); *Carbohydr. Res.*; **1988**; Vol. 179; pp. 125-136.
- ¹⁴ Kondakova A. N., Linder B., Fudala R., Senchenkova S. N., Moll H., Shashkov A. S., Kaca W., Zahringer U., Knirel Y. A.; New structures of the O-specific polysaccharides of *Proteus*. 4. Polysaccharides containing unusual acidic N-acyl derivatives of 4-amino-4,6-dideoxy-D-glucose; *Biochemistry*; Vol. 69; pp.1271-1282.
- ¹⁵ Volk W. A., Salomonsky N. L., and Hunt D.; *Xantomonas sinensis* cell wall lipopolysaccharide : isolation of 4,7-anhydro and 4,8-anhydro-3-deoxy-octulosonic acid following acid hydrolysis of *Xantomonas sinensis* lipopolysaccharide; *The journal of biological chemistry*; **1972**; Vol. 242 (12); pp.3881-3887.
- ¹⁶ Hay G.W., Lewis B.A., and Smith F.; Periodate oxidation of polysaccharides: general procedures, *Methods Carbohydrate Chemistry*, **1965**, Vol. 5, pp. 357-361: Academic Press.
- ¹⁷ Garegg P.J., and Lindberg; Preparation and N.M.R. studies of pyruvic acid and related acetals of pyranosides: configuration at the acetal carbon atoms; *Carbohydr. Res.*; **1979**; Vol. 77; pp.71-78.

Chapter IV: Identification and structural analysis of the Lipopolysaccharides from different bacteria present in C.S.C.M. (Crypt Specific Core Microbiota)

Introduction

This work was conducted in collaboration with Prof. Sansonetti of Pasteur Institute of Paris, which isolated different type of bacteria from the crypt of healthy mice. Intestinal crypt is the place in the intestine where cells replication happens and, on the contrary of the intestinal lumen, was considered a sterile environment. These regions of intestine shielded against bacteria colonization by the combination of various defenses strategies like the mucus at the top of the crypt and by a rich cocktail of antimicrobial molecules.

Prof. Sansonetti introduced the concept of Crypt-Specific Core Microbiota (C.S.C.M.) indicating a panel of different bacteria capable to colonize murine colonic crypt¹.

The existence of CSCM opens many questions, and the main point regards the role of bacterial CPSs and LPSs in the host immune system evasion of these bacteria. In this project, I have isolated all these molecules (LPS and CPS (when present)) from three different CSCM strains: *Acinetobacter parvus* 11G, *Stenotrophomonas maltophilia* BRT12, *Delftia acidovorans* CM30F. In this context the structure of the *O*-antigen from LPS produced by *Stenotrophomonas* and *Delftia* and the structure of LOS produced by *Acinetobacter parvus* 11G were resolved.

These molecules were tested on different cells in order to verify their inflammatory power and if did exist a competition between the different molecules which could explain how this bacteria can survive in colonic intestinal crypt.

4.1 Isolation purification and characterization of the LPS produced by *Stenotrophomonas maltophilia* BRT 12.

Stenotrophomonas maltophilia is an aerobic, non-fermentative, motile, Gram-negative bacterium, which was initially classified as *Pseudomonas maltophilia*. It is an opportunistic pathogen causing bacteremia, pneumonia, and intra-abdominal and mucocutaneous infections in debilitated and immunocompromised patients².

In this work the structure of LPS *Stenotrophomonas maltophilia* strain BRT12 was discussed. This bacterium produces a branched capsular polysaccharide constituted by D-mannose (D-Man_p), L-rhamnose (L-Rhap), and L-fucose (L-Fuc_p) linked as shown in figure 4.1.

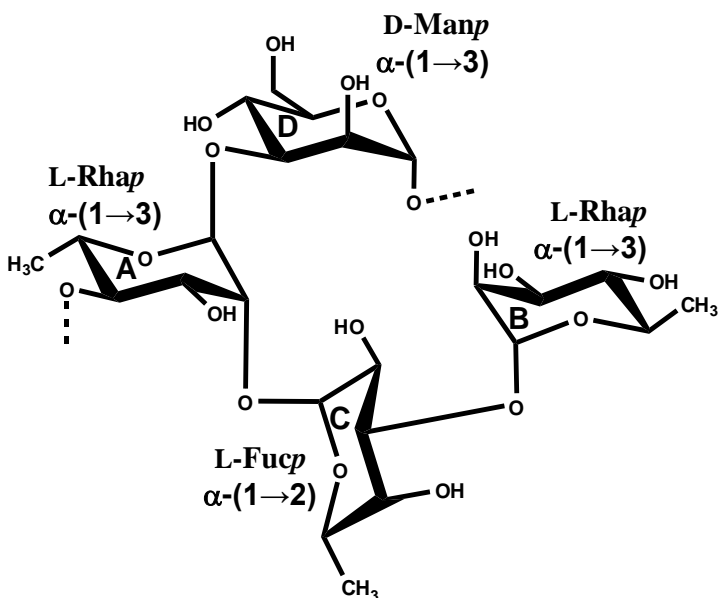


Figure 4.1: Structure of the repeating unit of the O-Chain of LOS from *S. maltophilia* BRT12. Labels reflect those reported in Table 4.1

4.2 Chemical and structural analyses of LPS

4.2.1 Chemical analyses of LPS

Cells of *Stenotrophomonas maltophilia* BRT12 were extracted according to the PCP and hot water–phenol extractions and LPS was found in the precipitate of PCP extraction; precipitation of LPS in this phase could be related to its lipophilic nature. SDS-PAGE analysis showed the characteristic ladder pattern of LPS molecules (figure 4.2).

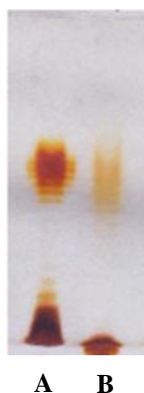


Figure 4.2: SDS-PAGE (stacking gel 5%, separating gel 12%) stained with silver nitrate of **A:** standard of *E. coli* O55:B5 (12 µg) and precipitate of PCP extraction **B** (12 µg)

Chemical analyses disclosed the occurrence of several monoses, Kdo was found, but as main components D-mannose (D-Man_p), L-rhamnose (L-Rhap), and L-fucose (L-Fuc_p) were found attributable as constituents of *O*-Chain repeating unit. Methylation analysis detected the presence of 2,4 and terminal rhamnose, 3-fucose and 3-mannose³.

LPS was treated with a solution of AcOH 1% to separate Lipid-A from Core region breaking bond between Kdo and C-6 of Glc-(II) of Lipid-A.

Fatty acid methyl esters analysis, performed on Lipid-A showed the presence of several fatty acids; as showed in figure 4.3.

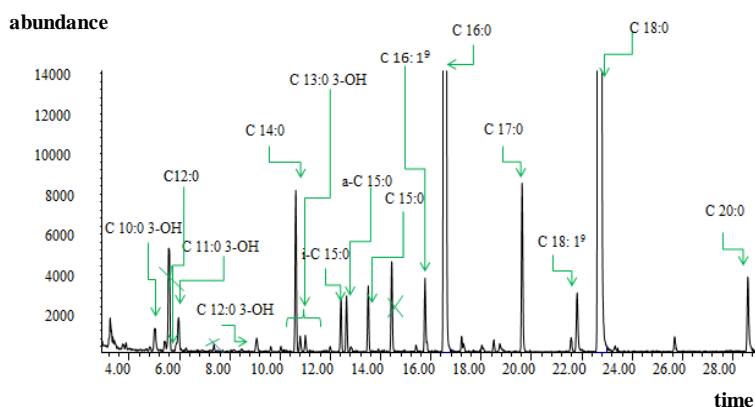


Figure 4.3: Fatty Acid Methyl Esters chromatogram for *Stenotrophomonas maltophilia* BRT12.

4.2.2 NMR analysis of LPS

^1H -NMR spectrum of acid treated LPS disclosed the diagnostic signals relative to the repeating unit of the *O*-Chain (figure 4.4): three protons in the anomeric area (in ratio 1:2:1 respectively) and three doublets in high field region of spectrum attributable to methyl signals of 6-deoxy-hexose residues. All residues were labelled in order of decreasing chemical shift with a letter (**A-D**) and the analysis of the homo- and heteronuclear 2D spectra led to assignment of all proton and carbon chemical shifts (table 4.1).

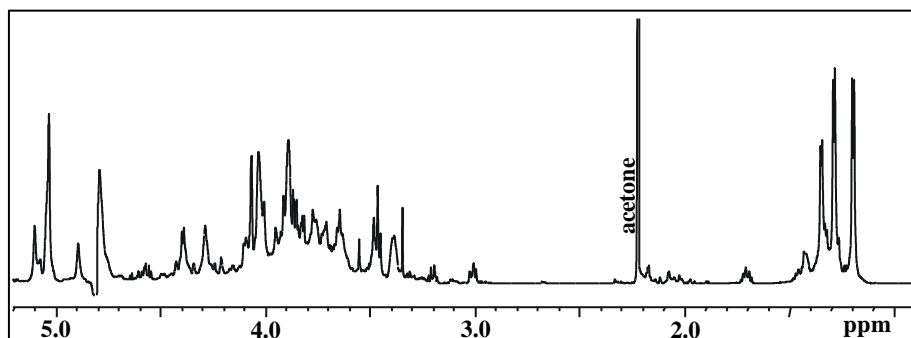


Figure 4.4: (600 MHz, 298K, D_2O) ^1H NMR spectrum of the *O*-Chain repeating unit of *S. maltophilia* BRT12.

Residue **A** was classified as α -Rha; the *manno* configuration explained the weak scalar correlation in the DQ-COSY spectrum relating H-2 to its vicinal protons (H-1 and H-3) and one strong between H-3 and H-4. C-2 (77.8 ppm) and C-4 (77.50 ppm) resonated in the down field region of HSQC (figure 4.5) spectrum and were identified as linked positions.

Signal at 5.04 ppm included both residues **B** and **C**, later identified as α -Rha and α -Fuc, respectively, on the basis of small value of $^3J_{H1-H2}$ of **B** and $^3J_{H3-H4}$ of **C**. In the DQ-COSY spectrum this signal presented two different correlations with H-2 of **B** and H-2 of **C** at 4.07 ppm and 3.90 ppm, respectively; starting from each H-2 proton, it was possible to discriminate between two residues. The α configuration of **A**, **B**, and **C** was inferred by the H-1 chemical shift and by comparing the C-5 chemical shift with respect to the standard value of methyl deoxypyranoside⁴. Therefore residue **B** was an α -Rha and comparison between its carbons chemical shifts and those reported in bibliography, proved that it was terminal in agreement with methylation analysis. Residue **C**, instead, was an α -Fuc and the low field shift of its C-3 signal (78.5 ppm) with respect to the standard value (72.3 ppm) proved glycosylation at this position (figure 4.5)⁴.

Residue **D** was identified as an α -Man on the basis of weak value of $^3J_{H1-H2}$ and $^3J_{H2-H3}$ coupling constants; complete assignation was possible analyzing TOCSY and COSY correlation and the low field shift of its C-3 (78.6 ppm) confirmed glycosylation in this position.

Oligosaccharide sequence was elucidated by the analysis of long range correlation; HMBC spectrum (figure 4.5 part a) showed these keys correlations: H-1 of residue **A** and C-3 of residue **D**, H-1 of **B** with C-3 of **C**, H-1 of **C** with C-2 of **A** and H-1 of **D** with C-4 of **A**.

These data, combined with the linkage analysis and with the analysis of carbon chemical shifts allowed elaboration of the structure of the repeating unit of the polysaccharide, reported in figure 4.1.

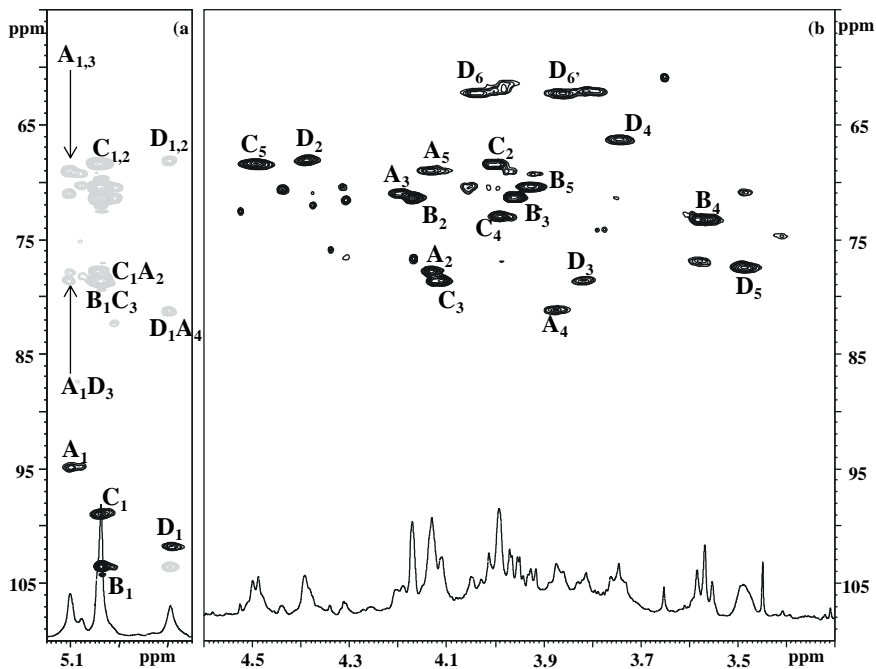


Figure 4.5: (600 MHz, D₂O, 298 K) Part a: Expansion of anomeric region of gHSQC spectrum (black) overlapped to HMBC spectrum (grey) of *O*-Chain repeating unit of LPS from *S. maltophilia* BRT12.

Part b: Part a: Expansion of gHSQC spectrum of *O*-Chain repeating unit of LPS from *S. maltophilia* BRT12.

Attribution of most of the cross peaks is indicated nearby the corresponding density. The structure of the *O*-Chain repeating unit is reported in Figure 4.1 together with the labels used.

		1	2	3	4	5	6	6'
A	¹ H	5.10	4.03	4.10	3.77	4.04	1.36	-
2,4-α-Rhap	¹³ C	94.8	77.8	70.9	77.5	69.1	18.3	-
B	¹ H	5.04	4.07	3.86	3.48	3.83	1.29	-
<i>t</i>-α-Rhap	¹³ C	103.5	71.4	71.3	73.2	70.3	17.9	-
C	¹ H	5.04	3.90	4.02	3.89	4.39	1.20	-
3-α-Fucp	¹³ C	98.9	68.4	78.5	73.0	68.3	17.8	-
D	¹ H	4.89	4.29	3.72	3.64	3.38	3.94	3.76
3-α-Man	¹³ C	101.6	68.1	78.6	66.3	77.4	62.1	-

Table 4.1: Proton (600 MHz) and carbon (150 MHz) chemical shifts at 298K in D₂O measured for *O*-Chain of *S. maltophilia*. Spectra were calibrated with respect to internal acetone (¹H: 2.225 ppm, ¹³C: 31.45 ppm). Structure of the repeating unit of the *O*-Chain is in figure 4.1

4.3 Isolation and purification of LPS from *Delftia acidovorans* CM30F

Delftia acidovorans is an aerobic, non-fermentative, Gram-negative bacterium involved in several diseases like corneal ulcers, infection of urinary tract and respiratory diseases⁵. The structure of *O*-antigen portions of the LPS produced by *Delftia acidovorans* strain CM30F was elucidated on the basis of chemical and spectroscopical analyses. This bacterium produces an *O*-chain constituted by D-glucose (D-Glcp), *N*-acetyl-D-glucosamine (D-GlcpNAc), and L-rhamnose (L-Rhap), linked as shown in figure 4.6.

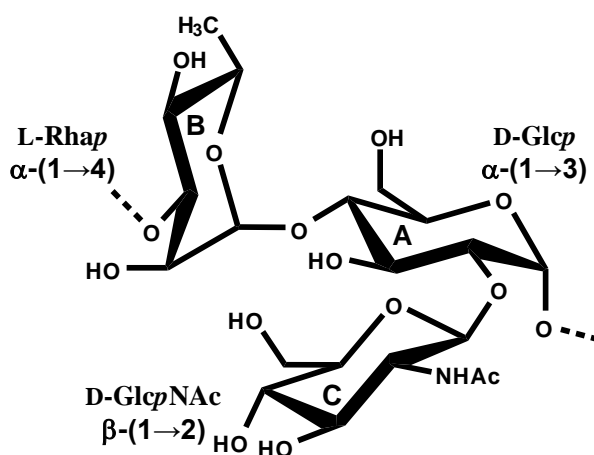


Figure 4.6: Structure of the repeating unit of the *O*-Chain of LPS from *D. acidovorans* 30F. Labels reflect those reported in Table 4.2.

The structure of Lipid-A was resolved on the basis of MALDI-TOF analysis and it presented a conserved biphosphorylated disaccharide backbone substituted by C8:0 (3OH) and C10:0 (3OH) as primary fatty acids substituted with a C12:0 and C16:0 (figure 4.10).

4.3.1 Chemical analyses of LPS

Cells of *Delftia acidovorans* CM30F were extracted according to hot water-phenol protocol and LPS was recovered in both phase; these were purified by enzymatic treatments and ultracentrifugation (section 6.2.3.3). Chemical analyses disclosed

the presence of D-Glcp, D-GlcpNAc, L-Rhap and Kdo. Methylation analysis detected, as main residues, 3-Rha, 2,4-Glc and t-GlcNAc². Fatty acid methyl esters analysis showed the presence of several fatty acids: 8:0 (3OH), 10:0 (3OH), 12:0, 14:0, 16:1⁹, 16:0, 18:1⁹, 18:0.

4.3.2 NMR analyses of LPS

¹H-NMR of O-chain spectrum (figure 4.7 part a) presents very broad signals; it is possible to indentify five anomeric signals, several overlapped signals at 1.3 ppm due to the methylenic groups of rhamnose units and a signals at ca. 2 ppm can be attributable to N-acetyl groups. gHSQC spectrum of O-chain (figure 4.9) contained a carbon signal of a hydromethylene group at 65 ppm and its protons were at 4.12 ppm and 4.54 ppm respectively, these proton and carbon chemical shifts value compared to typical value (60-62 ppm and 3.60-3.90 ppm) suggested the presence of an acetyl group on this carbon (¹H 2.05 ppm, ¹³C 23.0 ppm). Starting from this information, to simplify the spectrum attribution, O-Chain was deacetylated with NH₄OH (NH₃ 28%) and purified on a BioGel P-10 column using NH₄HCO₃ 50mM as eluent and a RID as detector. Deacetylated O-Chain was eluted in the void volume of column; it was collected, freeze-dried and analyzed by NMR (figure 4.7 part b).

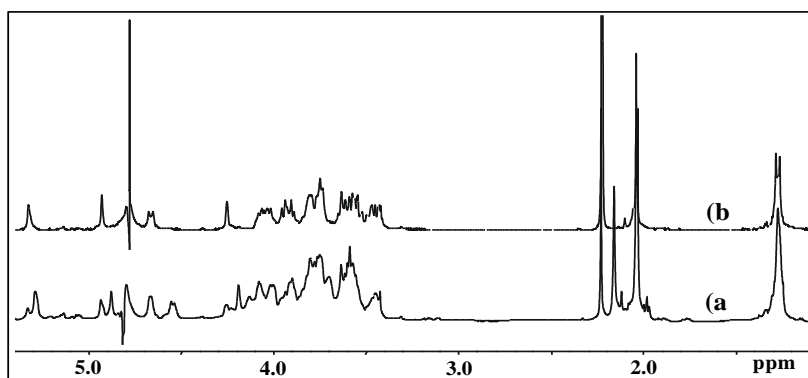


Figure 4.7: ¹H NMR spectra (600 MHz, 298K, D₂O) of pure O-Chain repeating unit of pure LPS produced by *Delftia acidovorans* 30F(part a) and of deacetylated O-Chain polysaccharide (part b).

¹H-NMR spectrum of deacetylated O-chain (figure 4.4 part b) contained the diagnostic signals relative to repeating unit of the O-Chain: three anomeric signals (5.20-4.80 ppm), and one doublet (1.27 ppm) attributable to the methyl group of rhamnose unit. All residues were labelled in order of decreasing chemical shift with letter (**A-C**), and the analysis of the 2D NMR spectra of the polysaccharide permitted the assignment of all proton and carbon chemical shifts (Table 4.2, structure in figure 4.6).

Residue **A** was identified as a 2,4- α -Glc on the basis of TOCSY and COSY correlations. H-1 of **A**, indeed, presented characteristic TOCSY correlations of a *gluco* configured residue. The α configuration was inferred on the basis H-1 chemical shift. HSQC spectrum (figure 4.8) analysis permits the attribution of all carbon and confirmed glycosylation in positions C-2 (84.4 ppm) and C-4 (76.1 ppm)².

Residue **B** was classified as 3- α -Rha; the *manno* configuration explained the weak scalar correlation in the DQ-COSY spectrum relating H-2 to its vicinal protons (H-1 and H-3) and one strong between H-3 and H-4. Complete residue assignment was possible analyzing NOESY, TOCSY and gHSQC spectra; chemical shift of C-3 confirmed glycosylation at this position. The α configuration of anomeric centre was deduced on the basis of chemical shift and comparing C-5 chemical shift with respect to the standard value of methyl deoxypyranoside (69.4)⁴. With regard of residue **C** it was classified as a *t*- β -GlcNAc; following COSY and TOCSY correlation was possible to assign all residue chemical shifts. gHSQC spectrum permitted to identify carbon chemical shift and confirm that C-2 (56.84 ppm) was a nitrogen bearing carbon³. The β configuration of anomeric centre was confirmed by chemical shift and by the *intra*-NOEs correlation of H-1 with H-3 and H-5. Repeating unit sequence was elucidated on the basis of NOESY correlations, which displayed these key correlations: H-1 of **A** with H-3 of **B**, H-1 of **B** with H-4 of **A**, H-1 of **C** with H-1 of **B**, suggesting an α -(1 \rightarrow 2)-linkage, and H-2 of **B**.

These data, combined with the linkage analysis and with the carbon chemical shift analysis, permitted the elaboration of the structure of the repeating unit of the polysaccharide, reported in figure 4.6.

Starting from information obtained by analysis of NMR spectra of deacetylated *O*-Chain was possible to resolve also structure of native *O*-Chain, gHSQC in figure 4.9. The presence of several anomeric signals suggested that GlcN's acetylation on carbon C-6 was not quantitative, integration of C-5 densities, indeed, of 6Ac-GlcN and GlcN (residues **E** and **F** respectively) suggested a substitution degree of 60%, and that repeating unit of *O*-Chain was composed of alternative acetylated and not acetylated forms.

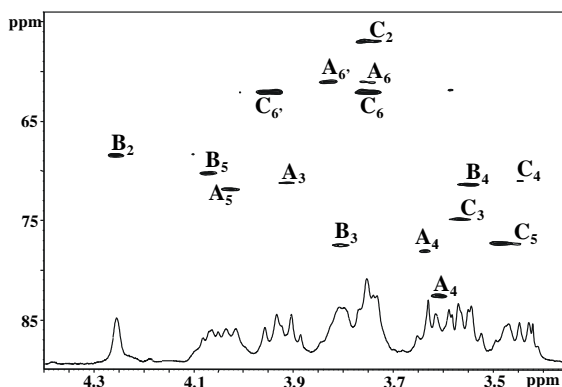


Figure 4.8: (600 MHz, D₂O, 298 K) Expansion of gHSQC spectrum of deacetylated *O*-Chain repeating unit of LPS from *D. acidovorans* 30F. Attribution of most of the cross peaks is indicated nearby the corresponding density. The structure of the *O*-Chain repeating unit is reported in Figure 4.6 together with the labels used.

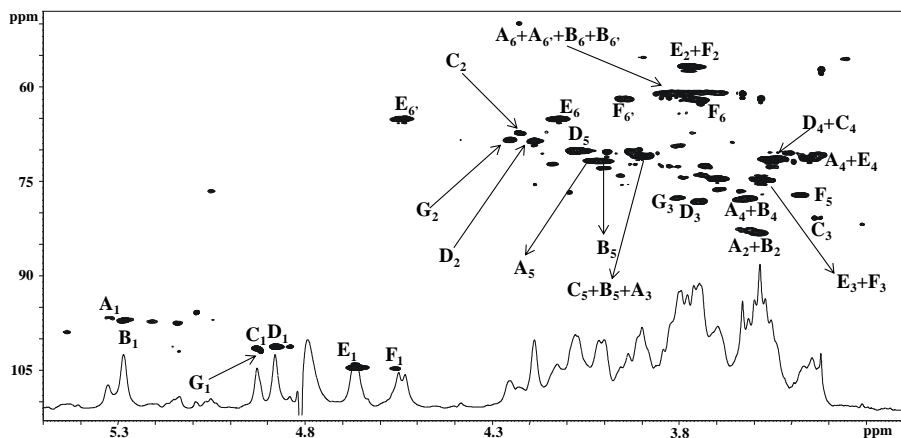


Figure 4.9: (600 MHz, D₂O, 298 K) Expansion of gHSQC spectrum of pure *O*-Chain repeating unit of pure LPS from *D. acidovorans* 30F. Attribution of most of the cross peaks is indicated nearby the corresponding density. Chemical shifts in table 4.3

		1	2	3	4	5	6	6'
A	¹ H	5.33	3.61	3.91	3.63	4.02	3.83	3.76
2,4-α-Glcρ	¹³ C	97.1	82.4	71.2	78.1	71.9	60.9	-
B	¹ H	4.92	4.26	3.80	3.54	4.06	1.27	-
3-α-Rhap	¹³ C	101.4	68.4	77.5	71.4	70.2	17.9	-
C	¹ H	4.67	3.75	3.57	3.44	3.45	3.95	3.77
<i>t</i>-β-GlcNρ	¹³ C	104.4	56.8	74.9	71.0	77.2	62.0	-

Table 4.2: Proton (600 MHz) and carbon (150 MHz) chemical shifts at 298K in D₂O measured for deacetylated *O*-Chain of LPS from *D. acidovorans*. Spectra were calibrated with respect to internal acetone (¹H: 2.225 ppm, ¹³C: 31.45 ppm). Structure of the repeating unit of the *O*-Chain is in figure 4.6

		1	2	3	4	5	6	6'
A	¹ H	5.23	3.60	3.1	3.64	4.10	3.84	3.79
2,4-α-Glcρ	¹³ C	96.54	82.7	71.0	78.0	71.8	61.4	-
B	¹ H	5.28	3.59	3.91	3.61	4.01	3.83	3.78
2,4-α-Glcρ	¹³ C	97.0	83.12	71.0	77.6	71.83	61.4	-
C	¹ H	4.92	4.23	3.44	3.49	3.94	1.29	-
3-α-Rhap (OMe)	¹³ C	101.7	67.3	80.8	71.4	70.3	17.6	-
D	¹ H	4.88	4.19	3.75	3.55	4.08	1.27	-
3-α-Rhap	¹³ C	101.3	68.6	78.2	71.4	70.1	17.9	-
E	¹ H	4.67	3.77	3.58	3.46	3.70	4.12	4.54.
<i>t</i>-β-6Ac-GlcNρ	¹³ C	104.4	56.7	74.8	71.4	74.5	65.1	-
F	¹ H	4.67	3.75	3.57	3.43	3.48	3.74	3.94
<i>t</i>-β-GlcNρ	¹³ C	104.4	56.9	74.6	70.8	77.2	62.0	-
G	¹ H	4.93	4.25	3.80	3.55	4.08	1.27	-
3-α-Rhap	¹³ C	107.8	68.4	77.6	71.42	70.15	17.9	-

Table 4.3: Proton (600 MHz) and carbon (150 MHz) chemical shifts at 298K in D₂O measured for pure *O*-Chain of LPS from *D. acidovorans*. Spectra were calibrated with respect to internal acetone (¹H: 2.225 ppm, ¹³C: 31.45 ppm). Structure of the repeating unit of the *O*-Chain is in figure 4.6

4.3.3 Structural characterization of Lipid-A

The Lipid A of *Delftia acidovorans* CM30F was structurally defined through MALDI-TOF mass spectrometry. Ion negative spectrum (figure 4.10) of Lipid A showed three main groups of signals labelled **A**, **B** and **C**; attributed to tetra-, penta- and hexa-acylated species of Lipid A respectively (composition in table 4.4). The base peak **C3** (m/z 1463.95) was composed of two C8:0(3-OH), two C10:0(3-OH), one C12:0 and one C16:0 and a phosphate group. This sample differed from

C4 for the lack of a second phosphate group, and to group of signals **C2** for the replacement of the C16:0 unit by one C14:0; while **C1** presented the replacement of the C12:0 by one C10:0(3OH).

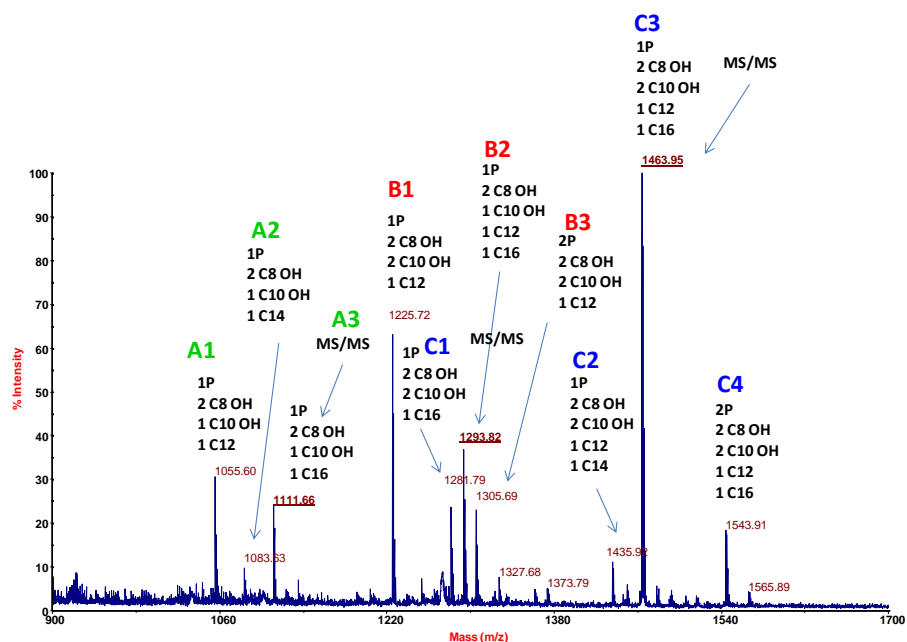


Figure 4.10: Linear ion negative MALDI-MS spectrum of Lipid A from *Deltia acidovorans* 30F. Peaks attribution is reported in table 4.3, structure in upper part of figure 4.12.

The structure of tetra-acylated Lipid-A was simply elucidated by the analysis of secondary fragmentations; in figure 4.11 is shown MALDI-MS-MS spectrum of **A3** (m/z 1111.66). This lipid-A was composed by three fatty acids 3OH, which had to be primary, and one 16:0. Position of different fatty acids was elucidated analyzing the ions originated by the second fragmentation. Most relevant fragmentations are ions at m/z 923.7, due to a cleavage of C10:0(3OH) from C-3 of GlcN-(II), and ion at m/z 855.6 due to a cleavage of 16:0 from C-3 of C8:0(3OH) N-linked to GlcN-(I).

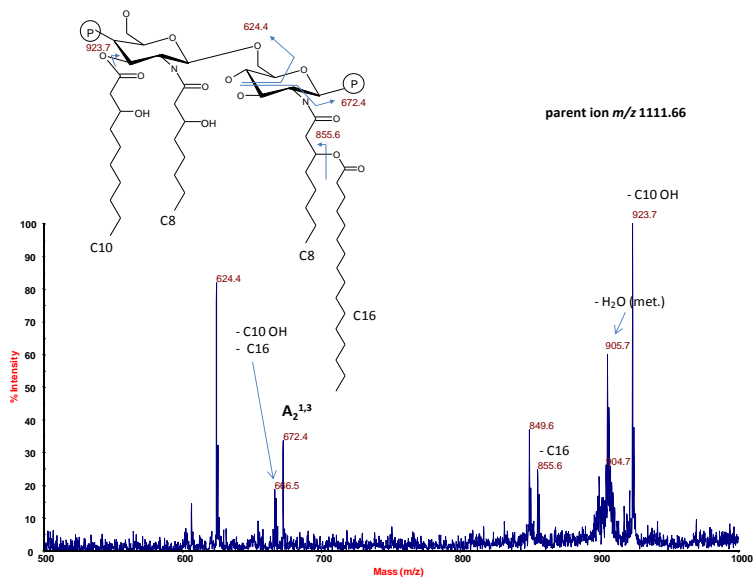


Figure 4.11: Linear ion negative MALDI-MS-MS spectrum of specie **A3** belonged to Lipid A from *Delftia acidovorans* 30F. Peaks attribution is reported in table 4.4.

These information together with analysis of FAME permitted to resolve MALDI-MS-MS spectrum of **C-3** (figure 4.12) and to identified structure of hexa-acylated Lipid-A.

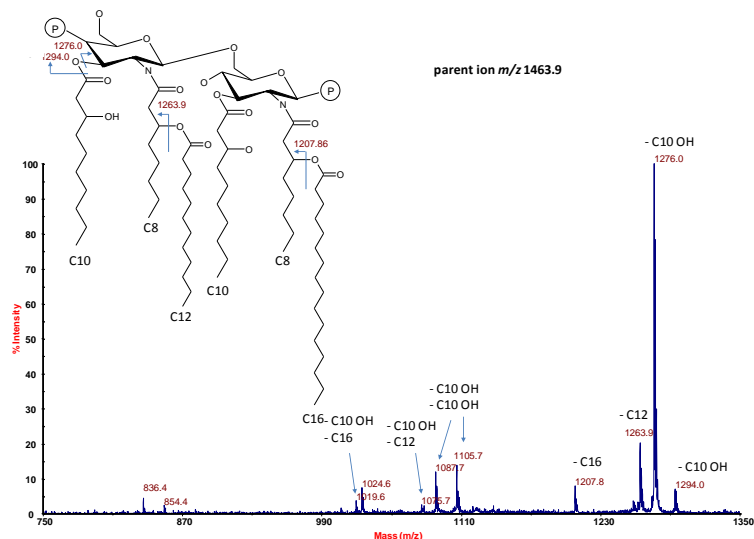


Figure 4.12: Linear ion negative MALDI-MS-MS spectrum of specie **C3** belonged to Lipid A from *Delftia acidovorans* 30F. Peaks attribution is reported in table 4.4.

Species	N acyl	Phosphate and fatty acids composition	Ion (m/z)
A1	4	2 x 8:0(3-OH), 10:0(3-OH), 12:0, <i>P</i>	1055.60
A2	4	2 x 8:0(3-OH), 10:0(3-OH), 14:0, <i>P</i>	1083.63
A3	4	2 x 8:0(3-OH), 10:0(3-OH), 16:0, <i>P</i>	1111.66
B1	5	2 x 8:0(3-OH), 2 x 10:0(3-OH), 12:0, <i>P</i>	1225.72
B2	5	2 x 8:0(3-OH), 2 x 10:0(3-OH), 16:0, <i>P</i>	1293.82
B3	5	2 x 8:0(3-OH), 2 x 10:0(3-OH), 12:0, 2 x <i>P</i>	1305.69
C1	6	2 x 8:0(3-OH), 2 x 10:0(3-OH), 16:0, <i>P</i>	1282.79
C2	6	2 x 8:0(3-OH), 2 x 10:0(3-OH), 12:0, 14:0, <i>P</i>	1345.92
C3	6	2 x 8:0(3-OH), 2 x 10:0(3-OH), 12:0, 16:0, <i>P</i>	1463.95
C4	6	2 x 8:0(3-OH), 2 x 10:0(3-OH), 12:0, 16:0, 2 x <i>P</i>	1543.91

Table 4.4: Tetra-, penta- and hexa-acylated species of Lipid A from *D. acidovorans* CM30F identified in the ion negative MALDI-TOF spectrum (figure 4.10). The two glucosamine units have been omitted for clarity.

4.4 Isolation and purification LPS from *Acinetobacter parvus* 11G

Acinetobacter parvus is a Gram-negative species associated with nosocomial infections. It is an opportunistic pathogen causing bacteremia, pneumonia, septic shock, and pyrexia in debilitated and immuno suppressed patients⁶.

The sequence of Core oligosaccharide of the LOS produced by *Acinetobacter parvus* strain 11G was resolved on the basis of chemical and spectroscopical analyses. This bacterium produces a branched oligosaccharide constituted by D-glucose (D-Glcp), D-galactose (D-Galp) D-glucosamine (D-GlcN), and 3-deoxy-manno-oct-2-ulosonic acid (Kdo) linked as shown in figure 4.13.

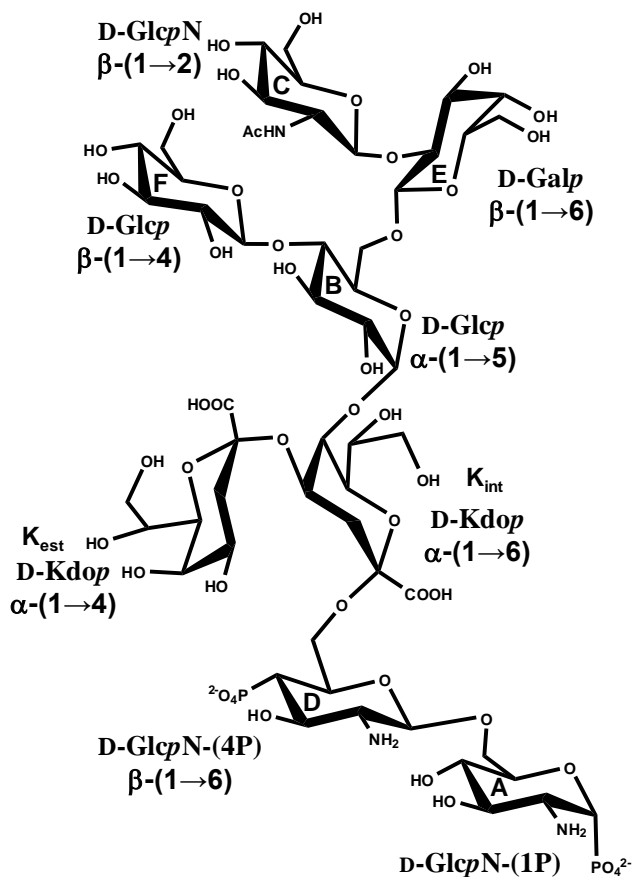


Figure 4.13: Complete structure of the Core oligosaccharide of LOS produced by *A. parvus* 11G. Labels reflect those reported in Table 4.5.

4.4.1 Chemical analyses of LPS

Acinetobacter parvus cells were extracted according to PCP method and LPS was found in the precipitate of PCP. Chemical analysis disclosed the presence of D-Glcp, D-Galp, D-GlcpN, and Kdo. Methylation analysis detected *t*-Glc, 4,6-Glc, 2-Gal and *t*-GlcN. Kdo substitution pattern was not determined by GC-MS analysis because the protocol used was not suitable for acid residues³.

Fatty acid methyl esters analysis (chromatogram figure 4.14) disclosed the presence of several fatty acids: 12:0, 12:0 (2OH), 12:0 (3OH), 16:1⁹, 16:0, 18:1⁹, and 18:0.

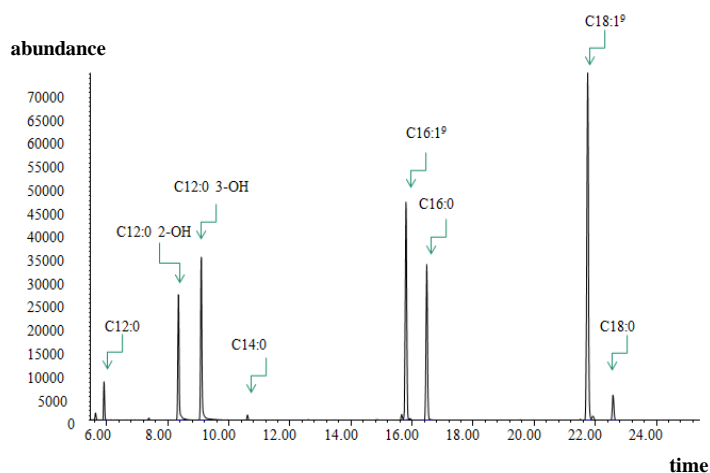


Figure 4.14: Fatty Acid Methyl Esters chromatogram for *Acinetobacter parvus* 11G.

4.4.2 NMR analyses of LPS

The complete structure of the Core oligosaccharide was deduced on the basis of the NMR spectroscopic data acquired for product isolated by alkaline degradation of LOS (section 6.8).

¹H-NMR spectrum of the delipidated LOS (figure 4.15) contained six anomeric signals, labelled in order of their decreasing chemical shift with letters (A-F), and three multiplets in the high field region of the spectrum due to two Kdo residues; labelled **K_{int}** and **K_{ext}**. The analysis of the 2D NMR spectra of the polysaccharide

permitted the assignment of all proton and carbon chemical shifts (Table 4.5, structure in figure 4.13).

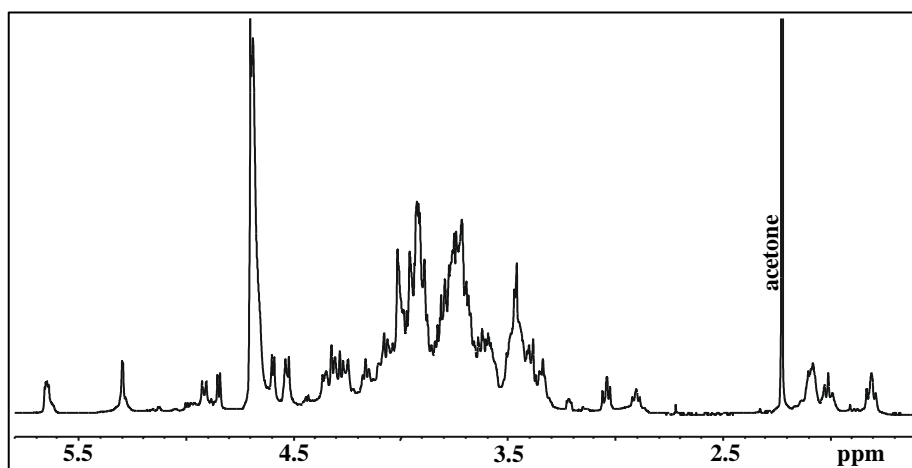


Figure 4.15: ^1H NMR spectrum (600 MHz, 308K, D_2O) of delipidated LOS from *Acinetobacter parvus*.

With regard to residues **A** and **D** their anomeric protons (5.65 and 4.86 ppm, respectively) showed six different correlations, characteristic of *gluco* configured residues, and on the basis of ring protons and carbon resonances these residues were recognised as the two glucosamines which composed the backbone of the Lipid-A moiety of LOS. Residue **B** was identified as a glucose and chemical shifts of C-4 (80.7 ppm) and C-6 (68.6 ppm) confirmed glycosylation at this residue; the α configuration of anomeric proton was confirmed on the basis of chemical shift. Anomeric proton at 4.91 ppm was attributed to residue **C**; it presented in TOCSY spectrum all *inter* residue correlations characteristic of a *gluco* configured ring; C-2 resonated at 58.3 ppm indicating a nitrogen bearing carbon. Therefore residue **C** was identified as a β -glucosamine. The methylation analysis, with the comparison between the carbons chemical shift and those reported in bibliography³, proved that this was a terminal residue. Residue **E** showed the classical behaviour of a galactose residue. H-1 had three TOCSY correlations with protons H-2, H-3 and H-4 respectively; complete assignation was possible by the analysis of T-ROESY spectrum and glycosylation at C-2 carbon was confirmed by the lowfield

displacement of its chemical shift (80.2 ppm). Analysis of the two Kdo residues started from diastereotopic methylenic protons H-3_{eq} and H-3_{ax} in the high field area of proton spectrum. Exploring scalar connectivities, for each Kdo, it was possible to identify only H-4 and H-5 due to the small coupling constant value $^3J_{H5,H6}$. Identification of H-6 proton was possible by analyzing T-ROESY spectrum, in which *intra* NOEs correlations H-5/H-6 and H-4/H-6 were present. Identification of protons H-7 and H-8, for each residue, was possible following scalar connectivities. gHSQC spectrum (figure 4.16) permitted attribution of all carbon chemical shifts and chemical shifts of C-5 (74.8 ppm) and C-4 (72 ppm) demonstrated that **K_{int}** was glycosylated at this position. C-4 chemical shift, in particular, compared to typical value (68-70 ppm) suggested a glycosylation with a ketose residue. The presence of an *inter*-residue NOE contact in 2D T-ROESY spectra between H-3_{eq} of **K_{int}** and H-6 of **K_{ext}** was diagnostic for a α -(2→4) linkage⁴.

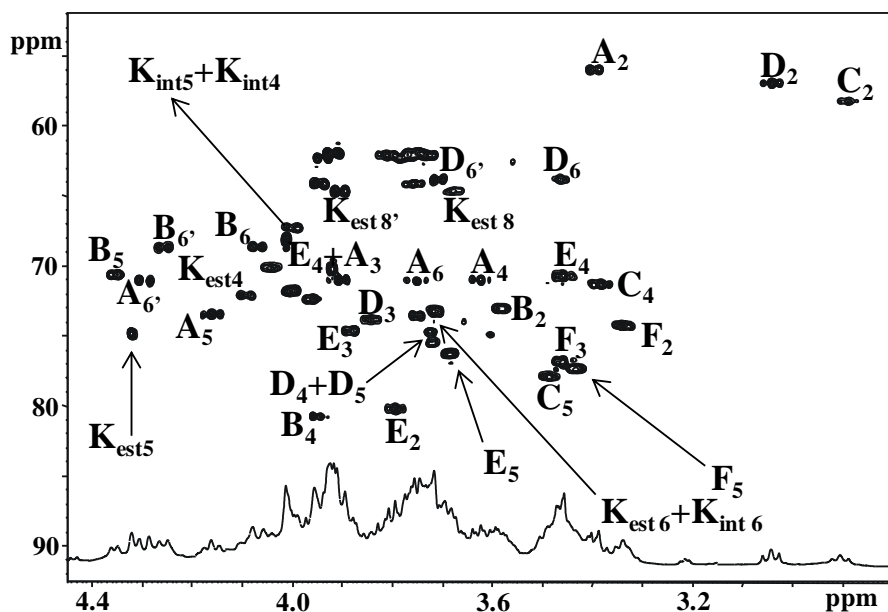


Figure 4.16: (600 MHz, D₂O, 298 K) Expansion of gHSQC spectrum of pure Core region of LPS from *A. parvus* 11G. Attribution of most of the cross peaks is indicated nearby the corresponding density. Chemical shifts in table 4.4

Complete sequence elucidation (figure 4.15) was possible by analyzing NOEs and long range correlations; HMBC spectrum (figure 4.17) showed the following key correlations: H-1 of **C** with C-2 of **E**; H-1 of **E** with C-6 of **B**; H-1 of **F** with C-4 of **B**; H-1 of **D** with C-6 of **A**, H-1 of **B** with C-5 of **K_{ext}**.

		1	2	3	4	5	6	6'
A	¹ H	5.64	3.93	3.91	3.62	4.16	3.75	4.30
6-α-Glc_pN-1P	¹³ C	91.7	55.9	70.9	70.9	73.4	71.1	-
B	¹ H	5.30	3.58	3.97	3.96	4.35	4.08	4.62
4,6-α-Glc_p	¹³ C	100.1	73.0	72.3	80.7	70.5	68.6	-
C	¹ H	4.91	2.91	3.61	3.38	3.48	3.77	3.94
<i>t</i>-β-Glc_pN	¹³ C	102.6	58.3	74.9	71.3	77.8	61.9	-
D	¹ H	4.86	3.04	3.84	3.73	3.72	3.46	3.70
6-β-Glc_pN-4P	¹³ C	100.9	56.9	73.7	74.7	75.5	63.8	-
E	¹ H	4.59	3.80	3.88	3.92	3.69	3.73	3.73
2-β-Gal_p	¹³ C	102.6	80.2	74.5	70.2	76.33	64.1	-
F	¹ H	4.53	3.34	3.46	3.46	3.44	3.75	3.92
<i>t</i>-β-Glc_p	¹³ C	104.1	74.3	76.9	70.7	77.3	61.9	-
		3	4	5	6	7	8	8'
K_{ext}	¹ H	1.81/2.08	4.00	4.01	3.72	4.00	3.77	3.94
<i>t</i>-α-Kdop	¹³ C	35.9	67.3	68.1	73.2	71.7	64.1	-
K_{int}	¹ H	2.01/2.10	4.10	4.32	3.75	4.04	3.67	3.90
5,4-α-Kdop	¹³ C	35.9	72.1	74.8	73.6	70.1	64.6	-

Table 4.5: Proton (600 MHz) and carbon (150 MHz) chemical shifts at 308K in D₂O measured Core oligosaccharide of LOS produced by *A. parvus* 11G. Spectra were calibrated with respect to internal acetone (¹H: 2.225 ppm, ¹³C: 31.45 ppm). Structure of the repeating unit of the *O*-Chain is presented in figure 4.6

4.5 Biological tests

Different tests were done to establish the biological activity of pure LOSs from different bacteria belonging to C.S.C.M. and to verify competition between different bacteria. Commercially available HEK293 hTLR4 cells were stably transfected with LPS-recognising molecular complex CD14, MD-2 and TLR-4 and have been stimulated with different concentration of LPSs (0.1, 0.5, 1, 10 and 100 ng/mL) from *Acinetobacter parvus* 11G, *Stenotrophomonas maltophilia* BRT12 and *Delftia acidovorans* CM30F. LPS produced by *E. coli* serotype O111:B4, that act as an antagonist on TLR4/MD2 was used at the same concentration as a positive control; while non-incubated HEK293 hTRL4 were used as a negative control. Analyses were performed monitoring activation grade of NF- κ B and cytokine CXCL8. The results (figure 4.18) showed that the two strains of *Acinetobacter* show a concentration dependent behavior similar to *E. coli*; in contrast, *S. maltophilia* and *D. acidovorans* did not show a potent immunostimulatory activity.

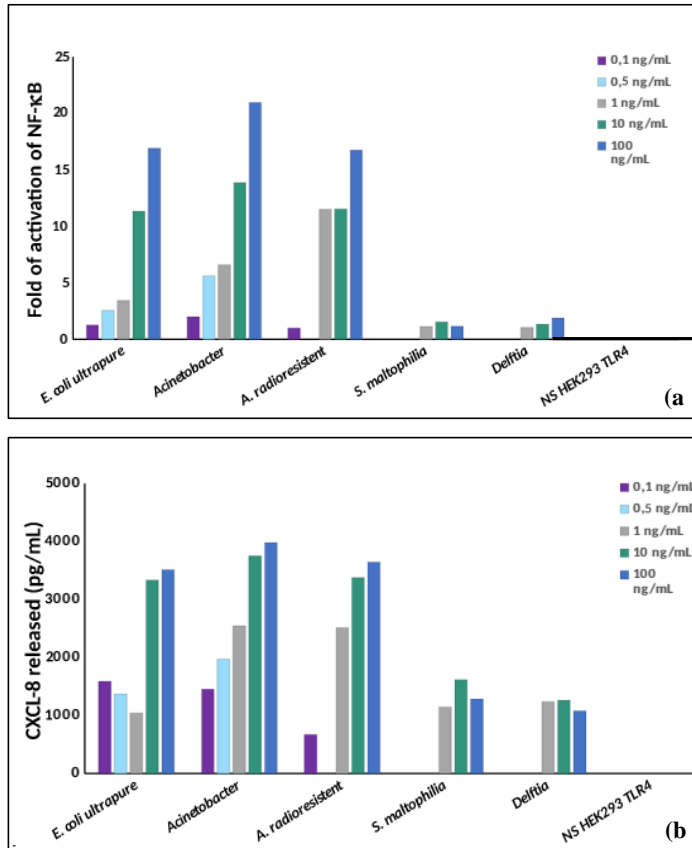


Figure 4.18: NF-κB and cytokine CXCL8 production of HEK293 hTLR4 stimulated with enhancing concentration of *A. parvus*, *S. maltophilia*, *D. acidovorans*. **Part a:** NF-κB activation upon stimulation of HEK293 hTLR4 after 4h with different LPSs concentration (0.1, 0.5, 1, 10 and 100 ng/mL) using hexa-acylated LPS from *E. coli* as positive test. **Part b:** CXCL-8 secretion after stimulation of HEK293 hTLR4 after 4h with different LPSs concentration (0.1, 0.5, 1, 10 and 100 ng/mL) using hexa-acylated LPS from *E. coli* as positive test. $p < 0.05$ after Student t-Test. Biological activity of *A. radioresistens* was also tested; complete structural analysis currently understudy. Biological tests were performed by Prof. M. L. Bernardini from department of Biology and Biotechnology of University of Rome “La Sapienza”.

These results suggest the possibility of the existence of a competition in the stimulation of the innate immune system between the different bacteria. It could be possible that *S. maltophilia* and/or *D. acidovorans* act antagonist of *Acinetobacter*. In this context competition tests were performed; in particular the activation grades of NF-κB and cytokine CXCL8 were monitored. Cells were incubated for 1h with different concentration of LOS from *A. parvus* (1, 10 and 100 ng/mL) and for 4 h

with 10 ng/mL of LPS from *S. maltophilia* or *D. acidovorans*. Results are showed in figure 4.19 and suggested that LPS from *S. maltophilia* could act as an antagonist of biological activity of LPS produced by *A. parvus*.

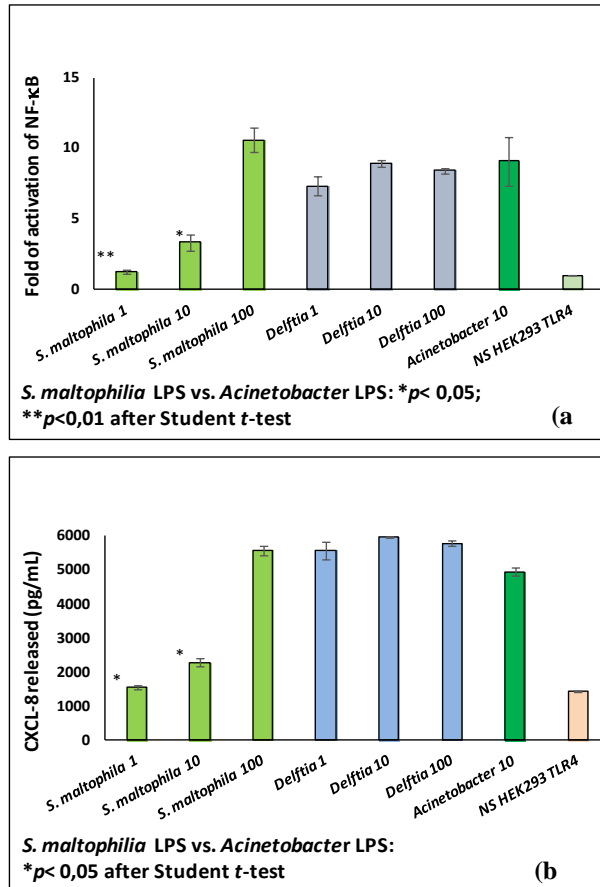


Figure 4.19: Fold NF-κB activation (part a): CXCL-8-release (part b) upon stimulation of HEK293 hTLR4 after 1h with 1, 10, 100 ng/mL of *A. parvus* LOS and the exposed with 10 ng/mL of LPS from *S. maltophilia* or *D. acidovorans* (4h).

Biological tests were performed by Prof. M. L. Bernardini from department of Biology and Biotechnology of University of Rome “La Sapienza”.

4.6 Conclusions

This work was conducted in collaboration with Prof. Sansonetti of Pasteur Institute, Paris, with the intent to characterize the cell membrane glycidic constituents produced by three bacteria isolated from mice intestinal crypt.

In this context lipopolysaccharides from *Stenotrophomonas maltophilia*, *Delftia acidovorans* and *Acinetobacter parvus* were extracted, purified and characterized by chemical and spectroscopical approaches.

With regards to *Stenotrophomonas maltophilia*, the repeating unit of *O*-Chain was resolved on the basis of chemical and spectroscopical analysis. This bacterium produced a branched polysaccharides composed by D-mannose (D-Man_p), L-rhamnose (L-Rhap), and L-fucose (L-Fuc_p) linked as showed in figure 4.1. FAME analysis revealed the presence of several fatty acids: 10:0, 12:0, 11:0 (3OH), 12:0 (3OH), 14:0, 13:0 (3OH), 15:0ⁱ, 15:0, 16:1⁹, 16:0, 17:0, 18:1⁹, 18:0 and 20:0.

Delftia acidovorans, instead, produced an *O*-Chain composed by D-glucose (D-Glcp), *N*-acetyl-D-glucosamine (D-GlcpNAc), and L-rhamnose (L-Rhap), linked as shown in figure 4.6. Lipid-A structure was elucidate by the analysis of MALDI-MS and MALDI-MS-MS. It presented a conserved biphosphorylated disaccharide backbone peculiarly substituted by C8:0 (3OH) and C10:0 (3OH) as primary fatty acids substituted with a C12:0 and a C16:0 (figure 4.10).

With regards to *Acinetobacter parvus* this bacterium produced a lipooligosaccharides and the structure of the Core region was resolved on the basis of chemical and spectroscopical analysis. This bacterium produces a branched oligosaccharide constituted by D-glucose (D-Glcp), D-galactose (D-Galp) D-glucosamine (D-Glc), and 3-deoxy-manno-oct-2-ulosonic acid (Kdo) as shown in figure 4.13. Fatty acid methyl esters analysis (chromatogram figure 4.14) showed the presence of several fatty acids: C12:0, C12:0 (2OH), C12:0 (3OH), C16:1⁹, C16:0, C18:1⁹, C18:0.

In order to verify if a competition existed between different bacteria in the stimulation of immune innate system receptors, biological tests were performed. Analyses were conducted monitoring activation grade of NF- κ B and cytokine CXCL8 in HEK293 hTLR4 cells. As shown in section 4.5, *S. maltophilia* and *D. acidovorans* did not show a concentration dependent immunostimulatory activity in contrast of LPS from *A. parvus*. Also, the competition assay performed indicated that there exists a competition in the biological activity between *A. parvus* and *S. maltophilia*.

References

- ¹ Pèdron T, Mulet C., Dauga C., Frangeul L., Chervaux C., Grompone G., and Sansonetti P.J.; “A Crypt-Specific Core Microbiota resides in the mouse colon”; *mBio*, **2012**, Vol.3, pp. 1-7.
- ² Looney W.J., Narita M., and Muhlemann K.; *Stenotrophomonas maltophilia*: an emerging opportunistic human pathogen; *Lancet infect dis.*; **2009**; Vol. 9; pp. 312-323.
- ³ De Castro, C., Parrilli, M., Holst, O., and Molinaro, A.; Chapter Five - Microbe-Associated Molecular Patterns in Innate Immunity: Extraction and Chemical Analysis of Gram-Negative Bacterial Lipopolysaccharides. *Methods in Enzymology* , 2010; Vol.480, pp. 89-115: Academic Press.
- ⁴ Bock K., and Pederden C.; Carbon-13 nuclear magnetic resonance spectroscopy of monosaccharides; *Adv. Carbohydr. Chem. Biochem.*; **1983**; Vol.41; pp 27-66.
- ⁵ Khan S., Sistla S., Dhodapkar R., and Parija S. C.; Fatal Delftia acidovorans infections in an immunocompetent patient with empyema; *Asian pacific journal of tropical biomedicine*; **2012**; Vol. 2 (11); pp. 923-924.
- ⁶ Turton J.F., Shah J., Ozongwu C., and Pike R.; Incidence of Acinetobacter species other than A. baumannii among clinical isolates of Acinetobacter: evidence for emerging species; *Journal of clinical microbiology*; **2010**; Vol. 48 (4). pp. 1445-1449.

Chapter V: Preparation of the building block for the synthesis of new glycoconjugates with potential activity against HIV-1

Introduction

The principal aim of this work is the preparation of building blocks for the synthesis of new aggregates having biological activity against HIV-1. Indeed, a monoclonal antibody named 2G12 was recently isolated that recognized mannose oligosaccharide repeating units present in glycoprotein *gp-120* which surrounds the capsid of surface of HIV-1 virus and inhibits its proliferation. Unfortunately this is originated only after the HIV infection¹.

The mature *gp120* is a glycosylated molecule containing high-mannose as well as hybrid and complex oligosaccharide structures, where it is possible to distinguish three different domains, referred to as D1, D2 and D3. (figure 2.1)².

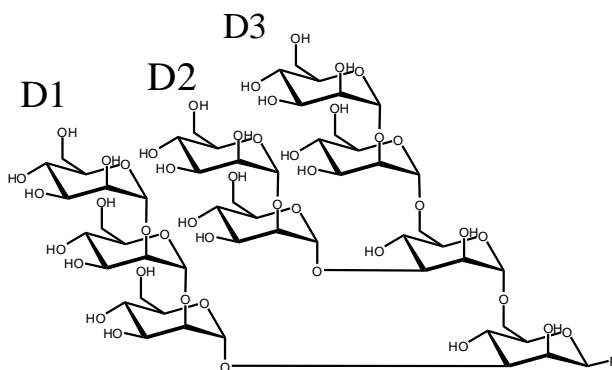


Figure 2.1. The cluster of terminal α -D-Man-(1 \rightarrow 2)- α -D-Man residues of the high mannose glycan displayed from *gp120* protein. The key part in the recognition process by mAb 2G12 is played from the D1 (mainly) and D3 arms.

2G12 interacts with the cluster of α -D-Man-(1 \rightarrow 2)- α -D-Man residues on *gp-120* and is able to act also on infected cells.

Indeed, these glycans may be used for the design of an HIV vaccine component to elicit “2G12-like” antibodies. This project is introduced in this context whose

principal goal is the preparation of building blocks for the synthesis of new glycodendrimers with potential activity against HIV-1 virus.

The focus is to link an oligosaccharide of mannose on a carrier of chitosan via click reaction in order to obtain a multivalent system that expose the mannose epitope and could stimulate biological activity of 2G12 antibody. Chitosan and mannose oligomers will be coupled using Huisgen reaction, a Cu(I) catalyzed 1,3-dipolar cycloaddition of azides and terminal alkynes to form 1,2,3-triazoles. This reaction was chosen because it is strongly selective and could be done in water solvent without any kind of protecting group on the reactives³. According to the strategy chosen, the azide carrier was a low molecular weight derivative of chitosan, while the alkyne derivative was prepared using yeast mannan as starting material.

Chitosan oligomers were chosen as carrier due to their biological activity and for the presence of several free amino functions, which can be converted to azides groups through diazo transfer reaction⁴.

Starting from chitosan polymer, pure chito-azidoligomers of different size were obtained. The reducing end of the chitoligomers was hydrogenated in the corresponding alditol to prevent collateral reactions at reducing end.

All reactions were done consecutively, without any intermediate or chromatographic purification of the sample. Chito-azide-oligomers mixture was directly purified via HPLC chromatography, yielding to the isolation of oligomers of different length and with different types of alditols units in pure form. It was possible to obtain a family of azide chito-oligomers, which are excellent precursors in click chemistry for the synthesis of new glycoconjugates

Manno oligosaccharides were obtained by extract from *S. cerevisiae*; this polysaccharide was chosen because it presents a backbone of α -(1 \rightarrow 6) residues decorated with α -(1 \rightarrow 2)-linked mono- to trisaccharide side chains, with a small percentage of α -(1 \rightarrow 3)-mannose units located at the terminal part of the longest branches⁵.

Starting from manna polysaccharide following a procedure of acetolysis and thio-glycosilation it was possible to obtain a mixture of mannose oligosaccharide presenting at pseudo-anomeric function and a propargyl moiety. This mixture was deacetylated by mild basic hydrolysis and purified following three different chromatographic procedures from which nine different mannose oligosaccharides with a length up to four units of mannose were obtained.

5.1 Preparation of a carrier of chitoazido oligomers⁶

Chitosan is a linear polymer of β -(1 \rightarrow 4)-linked 2-amino-2-deoxy-D-glucose and 2-acetamido-2-deoxy-D-glucose units in varying proportions. Although present in biomass, this polysaccharide is preferentially obtained by alkaline N-deacetylation of chitin (homopolymer of β -(1 \rightarrow 4) bound GlcNAc), a structural polysaccharide present in the exoskeleton of arthropods and in the cell-wall of many fungi's.

The peculiar physicochemical and biological properties confer to chitosan a vast range of applications in food, agriculture, medicine and drug delivery. However, its insolubility at neutral pH and its high viscosity in aqueous solution restrict its application. This problem is partially circumvented nowadays by making more soluble chitosan derivates or working with chitosan oligomers, which display interesting antibacterial, antitumorogenic and biological properties^{7,8,9}.

Indeed, reduction in chitosan's molecular weight facilitates its manufacture into various biomedical devices, thanks to its decreased viscosity; low molecular weight chitosan has been shown to effectively complex DNA and prevent nuclease degradation in addition to improving gene expression of luciferase plasmid.

In this frame, this work deals with preparation of chitosan oligosaccharides derivatives of defined length (figure 5.1), in pure form and functionalized with an azido function useful for further modification of the oligosaccharide scaffold according to the click chemistry approach¹⁰.

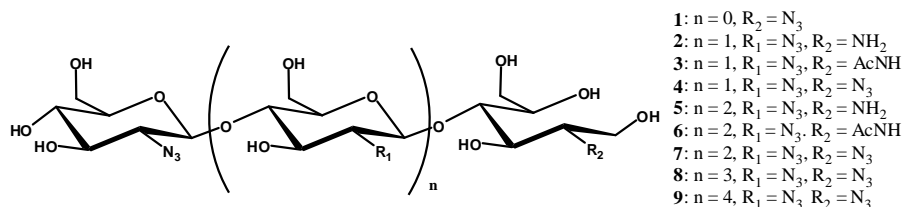


Figure 5.1: Different oligosaccharides obtained from chitosan later a treatment of acid hydrolysis, reduction, azidation and HPLC purification.

5.1.1 Hydrolysis of chitosan polymers and derivatization of free amino function with an azide group

Chitosan polysaccharide was partially depolymerized under acid conditions with concentrated HCl. Strong acid hydrolysis conditions were preferred to other approaches (nitrous acid or enzymatic treatments²) because in this case the resulting chito-oligomers possess a higher number of free amino functions. Chito-oligosaccharide mixture was isolated with cold acetone, centrifugation and freeze-drying. Figure 5.2 shows ¹H-NMR spectrum of acid treated chitosan; there were different diagnostic signals: at ca 2 ppm is possible to identify methyl signals of the N-acetyl groups, at ca. 3.2 and 3.4 the H-2 protons of the non acetylated GlcN; in the region between 3.40 and 4.20 ppm are located carbinolic protons, and in the region between 4.50 and 5.8 ca. are located anomeric protons. At this point the group of signals at 4.8 correspond to H-1 of non-reducing glucosamines while signals at 5.04, 5.40 and 5.53 were attributed to H-1 protons of reducing glucosamines. Comparing the signal's integration of H-2 of free Glc (0.09 and 0.01) with signal's integration of acetyl protons of GlcNAc (0.01) makes it possible to establish the percentage of free NH₂ groups:

$$NH_{2\text{-free}} = \left(\frac{I_{H-2(GlcN)}}{I_{H-2(GlcN)} + \left(\frac{1}{3}\right)I_{CH_3}} \right) = 97\%$$

Equation 1: percentage of free amino group in the chito-oligosaccharides mixture.

Similarly, by comparison of area of non reducing anomeric protons with reducing anomeric protons, applying equation 2, it is possible to establish the degree of polymerization (DP) of the oligosaccharide mixture:

$$DP = \left(\frac{I_{\text{non reducing protons}}}{I_{\text{reducing protons}}} \right) + 1 = 5$$

Equation 2: degree of depolymerisation of chitooligo mixture

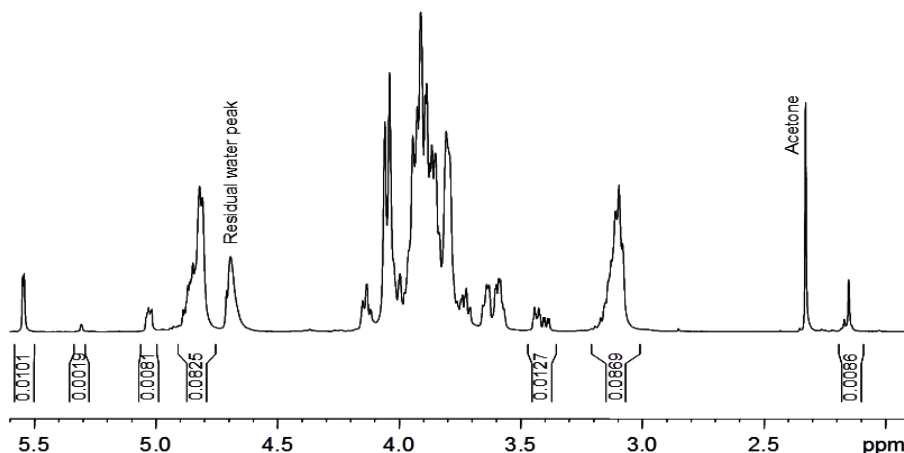


Figure 5.2: $^1\text{H-NMR}$ spectrum (600 MHz in D_2O , 318 K) of chito-oligomers obtained from hydrolysis with concentrated HCl ; integrals are reported for key protons and areas are used in formulas 1 and 2 to evaluate the acetylation and the depolymerization degrees, respectively.

To prevent parasite reactions at the reducing centre of the molecules, the mixture was treated with NaBH_4 in neutral conditions. The reaction was performed at $\text{pH}=7.0$, in a buffer AcOH/AcONa , to ensure the solubility of the substrate, which otherwise precipitated at the alkaline pH generated from the reducing reagent. Free amino groups of reduced chito-mixture were azidated with imidazol-1-sulfonylazide hydrochloride and sodium carbonate at $\text{pH}=7.0$ in phosphate buffer¹¹. Reaction was conducted for 3h, at room temperature and quenched with few drops of ethanolamine. The mixture was directly purified by HPLC chromatography.

5.1.2 Chromatographic purification of different chito-oligomers

The mixture of oligochitoazides was purified into its components via HPLC on octyl reverse phase using as eluent a solution composed by H₂O/CH₃OH (0.1% TFA) in gradient of methanol. Chromatographic profile, as shown in figure 5.3, confirms the presence of several peaks, which were collected and analyzed via ¹H-NMR spectrum. The fraction eluted within 5 minutes did not contain any material of interest as determined with ¹H-NMR analysis; these fractions contained mostly NMR silent products, as salts, and imidazol-1-sulphonyl azide hydrochloride related by products.

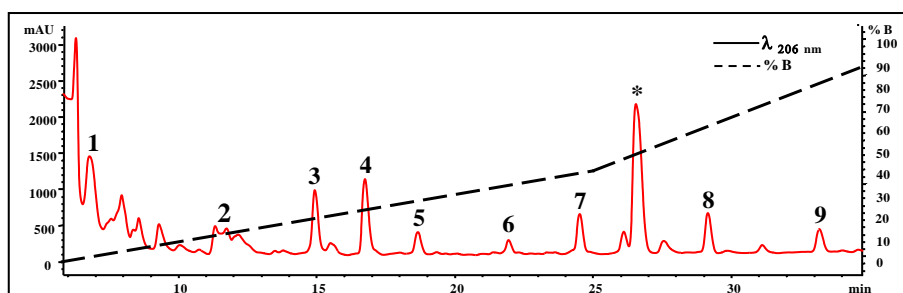


Figure 5.3: Expansion of RP8-HPLC profile measured at 206 nm (solid line) of the azide glucosamine oligoalditol mixture; separation was performed with 0.1% aqueous TFA–MeOH gradient (broken line); proton spectra were measured for all peaks and the most relevant ones are labeled with a number. *: byproduct from Stick reagent.

5.1.3 NMR analysis of different chito-oligomers

$^1\text{H-NMR}$ spectra for all HPLC fractions were recorded, as shown in figure 5.4, and peaks 1-9 were divided into three different subgroups on the basis of functional group linked on C-2 of alditol residue.

The first group comprehended oligosaccharides **1**, **4**, **7**, **8**, **9** (structure figure 5.1; spectrum figure 5.4); in contrast to other species, the NMR spectrum of these oligosaccharides does not present signal in the region between 4.2 and 4.5. These species, as showed by proton spectrum, were eluted in increasing order of length and were identified as fully azidates chitooligosaccharides.

In this contest, as example, is discussed attribution of product **4**; in the anomeric region two signals are present, at 4.64 ppm and 4.59 ppm, labelled with letter **A** and **B** respectively, attributable to two β anomeric signals on the basis of their chemical shift and their $J_{\text{H1-H2}}$.

Residue **A** was identified as a 4- β -GlcN₃ on the basis of TOCSY and COSY propagation and presents NOEs interactions between H-1 and H-3 and H-5 characteristic of a β configured sugar. HSQC spectrum (figure 5.5) analysis permits the attribution of all carbon and confirms the C-4 (78.9 ppm) was linked; C-2 chemical shift at 67 ppm instead at 58 ppm confirms that amino function was converted into an azide group. The same approach was followed in the attribution of residue **B** that was identified as a terminal GlcN₃.

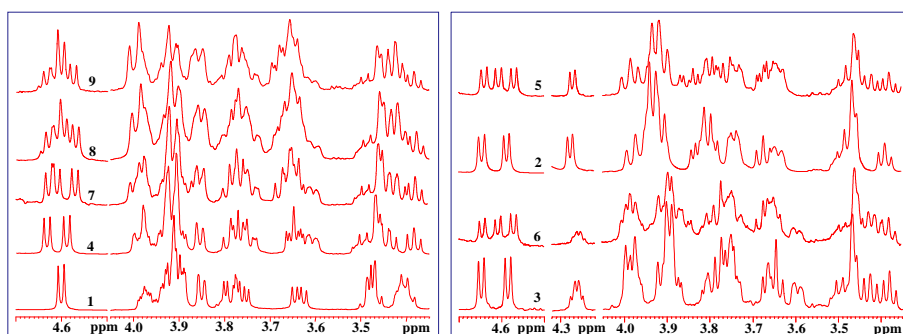


Figure 5.4: $^1\text{H-NMR}$ spectra of the three groups of chitoazide oligosaccharide alditols isolated

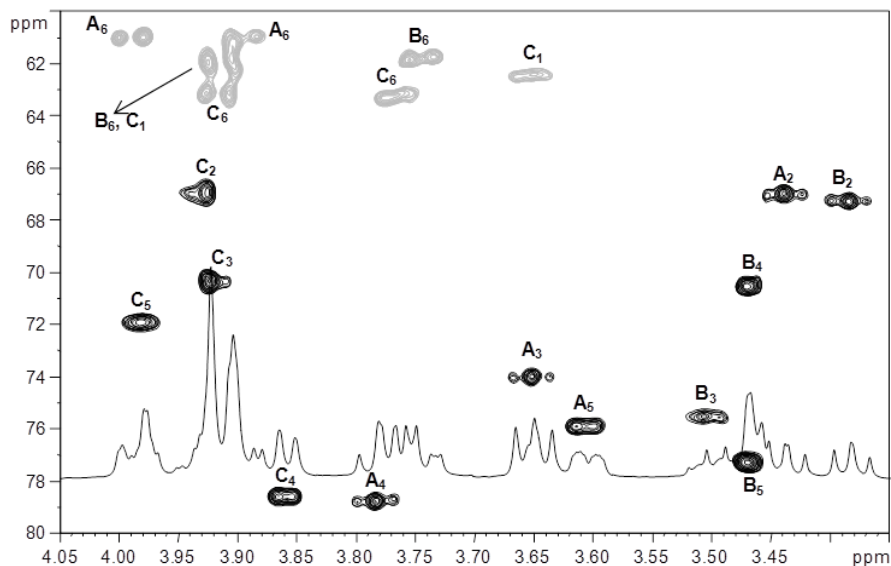


Figure 5.5: (^1H 600 MHz, ^{13}C 150 MHz) expansion of the HSQC spectrum measured at 305 K, in D_2O , of **4** (see structure in figure 5.1). The densities of the ring protons and carbons are attributed using the same labels of table 1.

Residue **C** was identified as alditol moiety and its attribution started from signal at 3.92 ppm and 66.9 ppm, which was recognized as H-2 because it is situated on an azide bearing carbon. This shows COSY correlation with methylenic protons at 3.91 ppm and 3.65 ppm generated by reduction of anomeric reducing function. Totally assignment (Table 5.1) and oligosaccharidic sequence was performed on the basis of TROESY and HMBC interactions: **B-A-C**.

Table 5.1: proton (600 MHz) and carbon (150 MHz) chemical shift of **4**, measured at 305 K. **A** and **B** residues are in the pyranosidic form and β configured at the anomeric centre. Spectra are calibrated with respect to internal acetone (^1H : 2.225 ppm, ^{13}C : 31.45 ppm). Residues sequence : **B-A-C**

		1	2	3	4	5	6
A	^1H	4.64	3.44	3.65	3.78	3.61	3.99; 3.89
4-β-GlcN₃	^{13}C	101.9	67.0	73.9	78.9	75.9	61.0
B	^1H	4.59	3.39	3.51	3.47	3.47	3.91; 3.74
t-β-GlcN₃	^{13}C	102.4	67.2	75.5	70.5	77.4	61.7
C	^1H	3.91; 3.65	3.92	3.92	3.86	3.98	3.76; 3.92
4-GlcN₃-alditol	^{13}C	62.4	66.9	70.4	78.6	71.9	63.2

A similar strategy was applied for the NMR attribution of products **1**, **7**, **8**, **9** which were identified as disaccharide-, tetrasaccharide-, penta-, and esaccharide-alditol respectively (figure 5.1).

The second group of samples comprehended **2** and **5** (structure figure 5.1; spectrum 5.4) that present as a common feature the occurrence of a doublet at 4.16 ppm, absent in the first group. Assignment of oligosaccharidic sequence started from anomeric signals and followed the same approach of the other group; with regard to residue **C** characterization started from signal at 4.16 ppm correlated with a carbon at 67.0 ppm, later identified as a C-3, which presents a COSY correlation with a nitrogen bearing proton at 3.74 ppm and 56.2 ppm. This last carbon was identified as a free amino group. Complete chemical shifts assignment and oligosaccharidic sequence was possible on the basis of TROESY and HMBC spectra. In this way samples **2** and **5** were identified as trisaccharide- and tetrasaccharide alditol, respectively.

		1	2	3	4	5	6
A	¹ H	4.65	3.47	3.67	3.80	3.64	3.98; 3.91
4-GlcN₃	¹³ C	102.1	66.8	74.1	78.5	76.0	60.8
B	¹ H	4.59	3.39	3.50	3.47	3.46	3.91; 3.74
t-GlcN₃	¹³ C	102.3	67.3	78.6	70.7	77.4	61.7
C	¹ H	3.94; 3.83	3.74	4.16	3.94	3.95	3.93; 3.80
4-GlcNH₂-alditol	¹³ C	60.2	56.2	67.0	79.0	71.5	63.1

Table 5.2: proton (600 MHz) and carbon (150 MHz) chemical shift of **2**, measured at 298 K. **A** and **B** residues are in the pyranosidic form and β configured at the anomeric centre. Spectra are calibrated with respect to internal acetone (¹H: 2.225 ppm, ¹³C: 31.45 ppm). Residues sequence : **B-A-C**

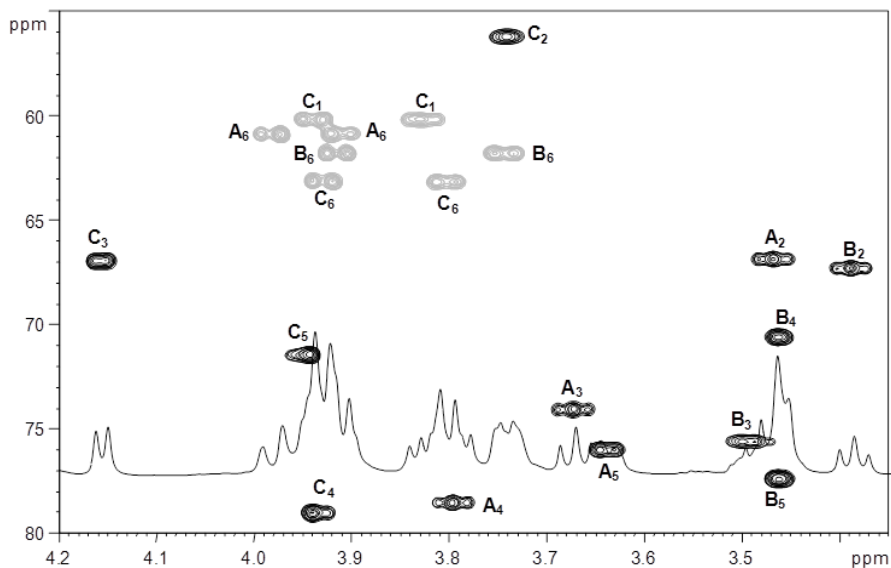


Figure 5.6: (^1H 600 MHz, ^{13}C 150 MHz) expansion of the HSQC spectrum measured at 298 K, in D_2O , of **2**. The densities of the ring protons and carbons are attributed using the same labels of table 5.2.

With regard to samples **3** and **6**, characteristic is the multiplet present at 4.3 ppm ca. attributable to H-2 of alditol moiety. This group of samples differs from previous because it presents on the alditol moiety a *N*-acetylated amino function. . Samples **3** and **6**, indeed, were identified as trisaccharide- and tetrasaccharide-alditol. Figure 5.7 and table 5.3 show HSQC and chemical shift of sample **3**.

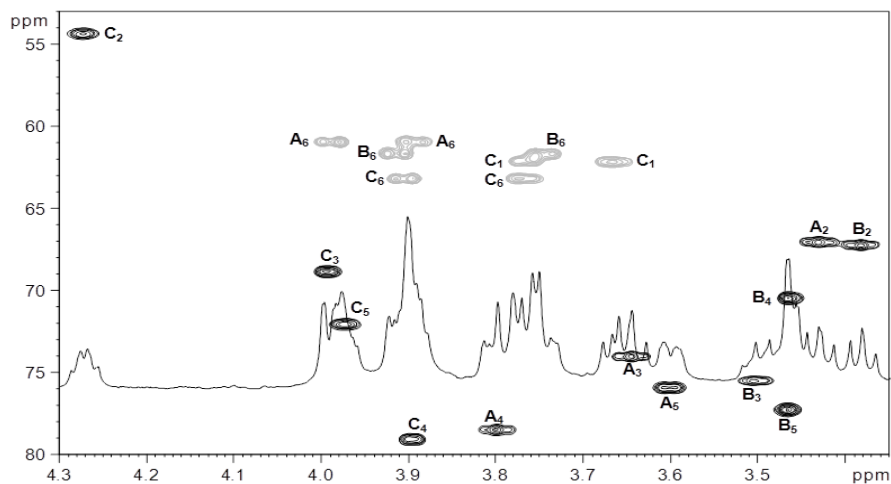


Figure 5.7: (^1H 600 MHz, ^{13}C 150 MHz) expansion of the HSQC spectrum measured at 288 K, in D_2O , of **3**. The densities of the ring protons and carbons are attributed using the same labels of table 5.3.

		1	2	3	4	5	6
A	^1H	4.65	3.43	3.65	3.80	3.60	3.99; 3.90
4-GlcN₃	^{13}C	101.9	67.1	73.9	78.4	75.8	61.0
B	^1H	4.59	3.50	3.50	3.47	3.46	3.91; 3.74
t-GlcN₃	^{13}C	102.2	67.2	75.5	70.5	77.1	61.6
C	^1H	3.70; 3.66	4.27	3.99	3.89	3.97	3.91; 3.77
4-GlcNAc_{-alditol}	^{13}C	62.8	54.3	68.9	79.1	72.1	63.2

Table 5.3: proton (600 MHz) and carbon (150 MHz) chemical shift of **3**, measured at 288 K. **A** and **B** residues are in the pyranosidic form and β configured at the anomeric centre. Spectra are calibrated with respect to internal acetone (^1H : 2.225 ppm, ^{13}C : 31.45 ppm). Residues sequence : **B-A-C**

5.2 Conversion of yeast mannan polysaccharide in mannose oligosaccharides with a thiopropargyl linker at anomeric position¹²

Saccharomyces cerevisiae belongs to the group of facultative fermenting yeasts. These yeasts exhibit alcoholic fermentation under oxygen-limited conditions. The ability of *S. cerevisiae* to ferment specific sugars is a major factor that differentiates it from other yeasts.

A polysaccharide, composed entirely of D-mannose, was extracted from the cell wall of yeast *Saccharomyces cerevisiae*¹² and found that its mannan is closely associated with cell wall protein. Several investigations on the structure of yeast mannan have been reported. Methylation studies show that the molecule is highly branched¹³, with one end group and one branch point for every three mannose units, and that the polysaccharide contains α -(1 \rightarrow 2), less α -(1 \rightarrow 3), and α -(1 \rightarrow 6) linkages. For these reasons, the mannan from *S. cerevisiae* was chosen as font of mannose α -(1 \rightarrow 2)-linked oligosaccharides.

Starting from yeast mannan polysaccharide; mannose oligosaccharides, having different length and functionalized with a propargyl linker were obtained, purified and characterized. Nine different oligosaccharides from mono- to tetrasaccharides presenting a propargyl linker were obtained and characterized (figure 5.8)

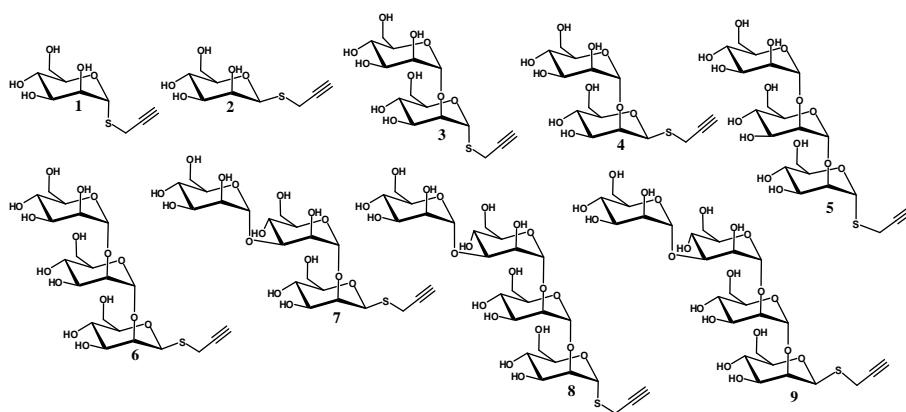


Figure 5.8: Oligosaccharides isolated after chemical manipulation of yeast mannan polysaccharide.

5.2.1 Acetolysis of yeast mannan

Yeast mannan was fully acetylated, then dissolved in acetic anhydride/acetic acid solution and cleaved with sulfuric acid. At the end of the treatment, the mixture was poured on ice, neutralized with solid sodium carbonate and extracted with chloroform. The organic layer was filtered on a small silica gel plug and volatiles were roto-evaporated. The mixture was directly used without any purification of the components.

5.2.2 Preparation of thiomannopropargyl-oligosaccharides

Propargyl appendage was linked to mannooligosaccharides acetylated mixture by a thioglycosidation¹⁴ (sections 6.15, 6.16 and 6.17). Fully acetylated mannose oligosaccharides mixture was at first converted in glycoside iodides and then in S-isothiuronium salt. This sample in presence of an alkyl bromide, in this case propargyl bromide, forms thioglycosides. As a result a complex mixture of fully acetylated thiopropargyl mannooligosaccharides was obtained. Purification of single components followed three different strategies: A) silica gel chromatography of the mixture, deacetylation and RP8-HPLC, B) deacetylation and RP8-HPLC, C) deacetylation, size exclusion chromatography and RP8-HPLC.

5.2.3 Purification of different mannose oligosaccharides

5.2.3.1 Silica gel chromatography of the fully acetylated mixture and RP8-HPLC purification of deacetylated fractions (**Method A**)

The crude mixture of acetylated thiothiopropargyl-oligosaccharides was purified on silica gel chromatography using a mixture of hexane/ethyl acetate in gradient of ethyl acetate yielding three different fractions: Fr-A, Fr-B and Fr-C. Each fraction was analyzed by $^1\text{H-NMR}$ spectrum and appeared as a mixture of products.

Each fraction was fully

deacetylated under mild alkaline conditions and each deacetylated fraction (labelled Fr-dA, Fr-dB and Fr-dC) was purified by HPLC chromatography using an octyl reverse phase (RP8) column, and a mixture of $\text{H}_2\text{O}/\text{MeOH}$ (95/5) as eluent (section 6.17.1).

Figure 5.9 shows chromatographic profile, recorded at $\lambda=206$ nm. This profile shows the occurrence of several peaks, which were collected and analyzed via $^1\text{H-NMR}$ (figure 5.12).

Fr-dA yielded oligosaccharides **1** and **2**; Fr-dB yielded **3** and **4** and Fr-dC yielded **4**, **5** and **6** Compound were collected and global yield, table 5.5 for each kind of purification, was compared to starting polysaccharide material: **1** (2.8%); **3** (12.8%), **4** (2.5%), **5** (9.5%), **6** (2.2%), figure 5.8.

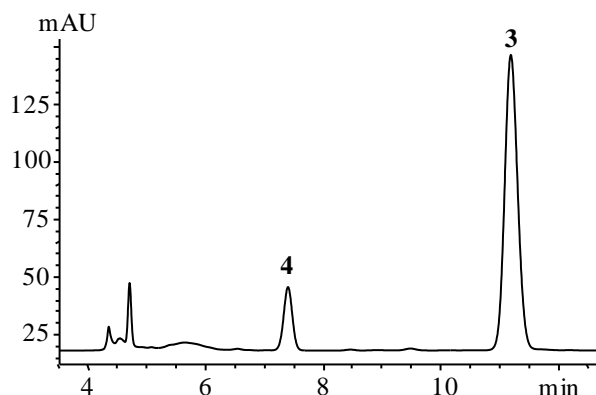


Figure 5.9: expansion of RP8-HPLC profile measured at 206 nm of deacetylated Fr-B; separation was performed with 95:5 v/v water/MeOH; peak labels correspond to the structures reported in figure 5.8.

5.2.3.2 Deacetylation of the oligosaccharide mixture and RP8-HPLC purification (**Method B**)

Fully acetylated mixture was deacetylated under mild conditions and deacetylated mixture was directly purified by RP8-HPLC chromatography using water as eluent. Chromatographic profile, figure 5.10, shows several peaks, which were collected and analyzed by $^1\text{H-NMR}$ (figure 5.12). As showed by chromatogram, this

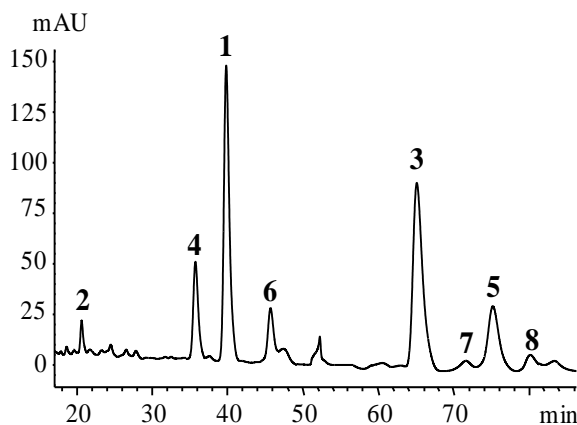


Figure 5.10. Expansion of RP8-HPLC profile measured at 206 nm of deacetylated oligosaccharide mixture; labels on the peaks correspond to the structures reported in figure 5.8

purification permits to isolate eight different species: **1** (9.6%), **2** (0.7%), **3** (13.0%), **4** (5.5%), **5** (8.2%), **6** (3.4%), **7** (0.7%), **8** (0.7%). Yields are scaled to the corresponding amount of starting material (Table 5.4).

5.2.3.3 Deacetylation, size exclusion chromatography and RP8-HPLC purification of oligosaccharide mixture (**Method C**)

Thiopropargyl-oligosaccharide mixture, after a deacetylation, was purified on a size-exclusion chromatography (Bio-Gel P-2) using water as eluent and a RID as detector. Chromatographic profile (figure 5.11) shows the occurrence of seven peaks (labeled D-L); these were collected, freeze-dried and analyzed via protonic spectrum. $^1\text{H-NMR}$ analysis was focused on the occurrence of the doublet at ca 3.5 ppm, characteristic of the methylene group of the propargyl glycoside. This was found in fractions F, G, H, containing a mixture of propargyl

mannooligosaccharides, and in Fr-I containing essentially α -thiopropargyldisaccharide **3** (figure 5.8) in 95% purity. On the contrary, fractions D and E did not show these signals and were not considered further.

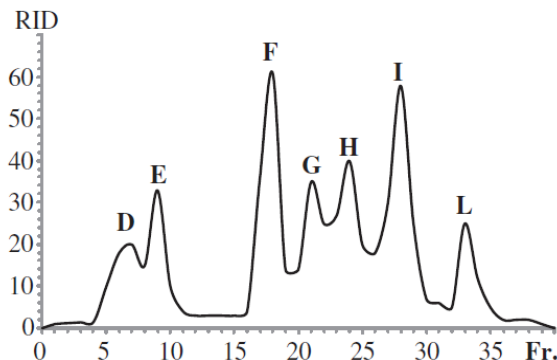


Figure 5.11: chromatographic profile of size exclusion purification profile of totally deacetylated mixture.

Other fractions were purified on by RP-8 HPLC using H₂O/MeOH (95/5 v/v) as eluent; Fr-F yielded sample **8** and **9**, Fr-G yielded **5**, **6** and **8**, Fr-H yielded **3**, **4**, **5** and **6**, Fr-L yielded **1** and **2**. Oligomers from different purification were pooled and the global yield (Table 5.4) scaled to corresponding amount of starting material: **1** (4.6%), **2** (0.3%), **3** (14.8%), **4** (2.5%), **5** (6.5%), **6** (3.1%), **8** (3.6%), **9** (1.5%).

Samples	Method		
	A	B	C
1	2.8	9.6	4.6
2	--	0.7	0.3
3	12.8	13.0	14.8
4	2.5	5.5	2.5
5	9.5	8.2	6.5
6	2.2	3.4	3.1
7	--	0.7	--
8	--	0.7	3.6
9	--	--	1.5

Table 5.4: Percent yields, scaled to the corresponding starting yeast mannan (w/w), observed for the thiopropargyl manno oligosaccharides **1-9** (Figure 5.8) using the three different purification protocols.

5.2.4 NMR analysis of different mannose oligosaccharides obtained

NMR spectra were recorded for all products isolated (figure 5.12 shows $^1\text{H-NMR}$ spectra for all samples). All spectra disclose a set of common signals: at 3.35 ppm ca. a multiplet attributable to the diastereotopic methylene protons of the thiopropargyl moiety, its carbon at 20 ppm; the sulfur-linked carbon atom at 84 ppm ca for both α and β -anomers and H-5 of the β -configured residues that resonate nearby the methylene protons of propargyl linker.

The complete characterization of all products, **1-9**, was possible on the basis of information from 2D NMR experiments (Table 5.5 reports protons and carbons chemical shifts for all samples) and the same approach was followed for all samples. The total characterization of sample **5** is discussed as follows.

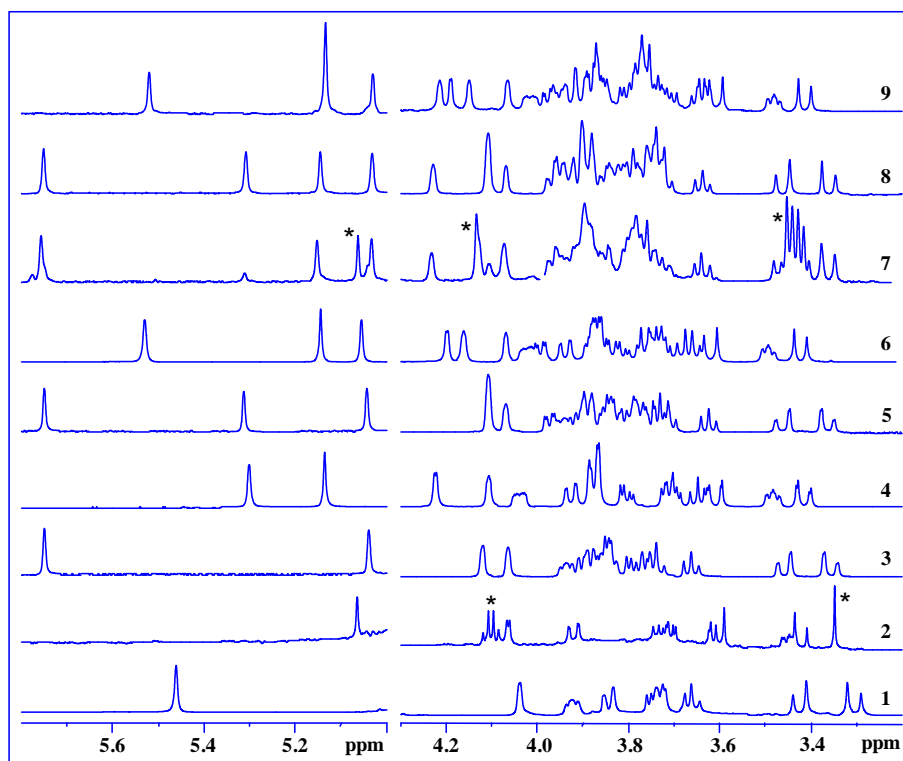


Figure 5.12: (600 MHz, 298K) $^1\text{H-NMR}$ spectra of the propargyl oligomannothioglycosides obtained in the course of this study. Structures are listed in figure 1. Signals with an asterisk are impurities

Product **5** presented three anomeric protons at 5.75, 5.31 and 5.04 ppm, which were labelled with letters **A**, **B** and **C**, respectively; each anomeric proton correlated in the HSQC spectrum with its carbon atom, and of relevance the highly shielded value of C-1 of **A** which was found at 83.9 ppm, characteristic of a sulfur-bearing carbon atom.

Starting from each anomeric proton, COSY spectrum returned a very weak correlation with the corresponding H-2, due to *manno* configuration of the sugar ring; starting from this proton TOCSY spectrum displayed all the correlations of the sugar ring protons. Indeed, COSY and TOCSY spectra interpretation led to assign all the proton chemical shift resonances for each residue. These data were integrated from the HSQC spectrum and analysis of the carbon chemical shifts disclosed that **C** was α -configured at the anomeric centre and terminally located, due to the agreement of its carbon chemical shifts with those reported for the α -methyl-mannopyranoside¹⁵. Similarly, **A** was α -configured and the low field value of its C-2 (81.2 ppm) with respect to the standard value (71.2 ppm), indicated that this residue was *O*-2 substituted. The same behaviour was found for **B** which appeared as a α -2 substituted mannose; C-2 79.9 ppm.

With regard to the propargyl moiety **D**, its methylene protons were found at 3.46 and 3.37 ppm and correlated with a carbon signal at 18.7 ppm; these H-1 protons were further correlated in the HMBC spectrum with the anomeric carbon of residue **A**, and importantly with the two carbons on the alkyne appendage, at 81.1 ppm and 73.2 ppm. This last signal was identified as the terminal alkyne carbon on the basis of literature data, and it was not detected in the HSQC spectrum (figure 5.13), due to chemical exchange of its proton with the deuterium of the NMR solvent.

Finally, HMBC and ROESY spectra confirmed the residue sequence, namely **C-A-B-D**.

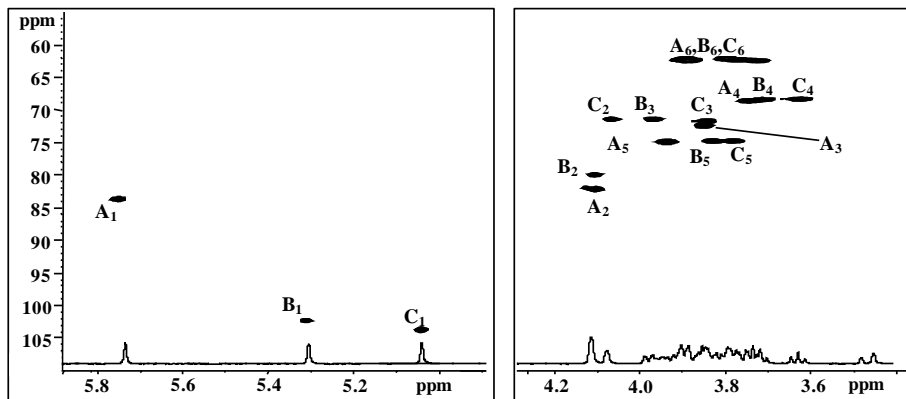


Figure 5.13: (^1H 600 MHz, ^{13}C 150 MHz) expansion of the HSQC spectrum measured at 298 K, in D_2O , of **5**. The densities of the ring protons and carbons are attributed using the same labels of table 5.5.

Unit	Position	1	2	3	4	5	6	7	8	9	
Linker	1	3.42;	3.62;	3.47;3.	3.62;	3.46;	3.61;	3.48;	3.46;	3.61;	
		3.31	3.35	37	3.43	3.37	3.44	3.37	3.36	3.42	
		18.7	19.1	18.8	19.2	18.7	19.3	18.8	18.8	19.1	
	2	--	--	--	--	--	--	--	--	--	--
		81.1	81.1	81.1	81.1	81.1	81.1	81.1	81.1	81.1	81.1
	3	--	--	--	--	--	--	--	--	--	--
		73.2	73.2	73.2	73.2	73.2	73.2	73.2	73.2	73.2	73.2
	Man^I	1	5.46	5.06	5.75	5.14	5.75	5.14	5.76	5.75	5.14
			85.0	84.6	83.6	83.9	83.5	83.9	83.2	83.3	83.4
		2	4.04	4.06	4.13	4.23	4.10	4.19	4.13	4.11	4.19
			72.7	73.1	81.7	79.4	81.5	79.9	81.7	81.7	80.0
		3	3.73	3.70	3.85	3.88	3.85	3.86	3.84	3.85	3.87
72.5			74.9	72.0	75.9	72.2	75.9	72.8	72.0	75.1	
4		3.67	3.61	3.75	3.65	3.75	3.65	3.75	3.74	3.64	
		68.3	67.8	68.5	67.9	68.4	68.1	68.4	68.2	68.1	
5		3.93	3.45	3.94	3.49	3.94	3.49	3.89	3.94	3.48	
		74.5	81.6	74.9	82.1	74.8	82.1	74.4	74.6	82.2	
6		3.74;	3.73;	3.80;	3.94;	3.91;	3.94;	3.86;	3.87;	3.71;	
		3.85	3.92	3.88	3.72	3.98	3.72	3.81	3.81	3.93	
		61.8	62.3	62.2	62.4	62.0	62.1	62.0	61.9	62.5	
Man^{II}		1	--	--	5.04	5.30	5.31	5.52	5.03	5.32	5.52
			--	--	103.8	102.8	102.1	101.4	103.7	102.0	101.4
		2	--	--	4.07	4.10	4.10	4.15	4.23	4.11	4.15
			--	--	71.3	71.4	79.9	79.6	70.9	79.8	79.8
		3	--	--	3.86	3.88	3.97	3.98	3.96	3.97	3.98
			--	--	71.9	71.5	71.4	71.4	79.4	71.0	71.3
		4	--	--	3.66	3.71	3.71	3.75	3.77	3.73	3.76
			--	--	68.1	67.7	68.2	67.9	67.5	68.1	67.8
		5	--	--	3.84	4.04	3.83	4.01	3.94	3.83	4.02
			--	--	74.6	74.6	74.5	75.8	74.7	74.4	74.5
		6	--	--	3.78;	3.88;	3.89;	3.86;	3.93;	3.90;	3.88;
	--		--	3.91	3.80	3.72	3.77	3.76	3.78	3.80	
	--		--	62.2	62.0	62.4	62.0	62.3	62.0	62.2	
	Man^{III}	1	--	--	--	--	5.04	5.05	5.15	5.03	5.03
			--	--	--	--	103.6	103.4	103.5	103.3	103.1
		2	--	--	--	--	4.07	4.07	4.07	4.22	4.22
			--	--	--	--	71.1	71.3	71.3	71.6	71.0
		3	--	--	--	--	3.84	3.84	3.89	3.95	3.95
--			--	--	--	71.6	71.6	71.5	79.0	79.2	
4		--	--	--	--	3.62	3.67	3.63	3.73	3.78	
		--	--	--	--	68.1	68.1	68.1	67.4	67.5	
5		--	--	--	--	3.78	3.73	3.79	3.80	3.76	
		--	--	--	--	74.5	74.3	74.5	74.5	74.5	
6		--	--	--	--	3.88;	3.86;	3.91;	3.92;	3.75;	
		--	--	--	--	3.72	3.75	3.78	3.73	3.91	
		--	--	--	--	62.4	62.1	62.1	62.2	62.4	

Man ^{IV}	1	--	--	--	--	--	--	--	5.15	5.14
		--	--	--	--	--	--	--	103.3	103.6
	2	--	--	--	--	--	--	--	4.07	4.07
		--	--	--	--	--	--	--	71.1	71.3
	3	--	--	--	--	--	--	--	3.88	3.87
		--	--	--	--	--	--	--	71.4	71.5
	4	--	--	--	--	--	--	--	3.63	3.63
		--	--	--	--	--	--	--	68.0	68.2
	5	--	--	--	--	--	--	--	3.77	3.79
		--	--	--	--	--	--	--	74.4	74.5
	6	--	--	--	--	--	--	--	3.99;	3.78;
		--	--	--	--	--	--	--	3.75	3.74
	--	--	--	--	--	--	--	62.1	62.1	

Table 5.5: (600 MHz, 298 K, D₂O) Proton and carbon chemical shift of **1-9**, spectra are calibrated with acetone (¹H: 2.225 ppm, ¹³C: 31.45 ppm) as internal standard. Mannose units in the mono- or oligosaccharides sequence are denoted with roman number superscript with Man^I as the pseudo-reducing unit linked at propargyl group via a thioglycosidic bond.

5.3 Conclusions

This part of the work was carried out to synthesize the building blocks for the preparation of new glycoconjugates having biological activity against the HIV-1. In particular, chemical procedures for preparation, purification and characterization of different chitoazidooligosaccharides and mannose alky- oligosaccharides having different length and different grade of functionalization were optimized.

An inexpensive and rapid method to obtain pure glucosamine oligomers of different size starting from chitosan polymer was developed. The free amino groups were transformed in azide by diazo transfer reaction without any kinds of protecting groups.

Mixture obtained was directly purified by HPLC using a RP-8 column and monitoring elution profile at 206 nm. In this way, it was possible to divide these molecules in three different groups on the basis of functional group linked at C-2 of glucitol extremity (figure 5.1).

All products obtained were analyzed by NMR spectroscopy and a valuable set of chemical shift were obtained. These molecules will be used as a carrier for mannose (1→2) oligosaccharides.

Mannose epitopes were obtained from mannan polymer, which were obtained from mannan yeast extract. This was depolymerized with an acetolysis treatment to obtain a mixture of peracetylated oligosaccharides which were used directly for the introduction of an iodide group at pseudo anomeric end. Glycosyl iodides obtained were treated with thiourea and the propargyl bromide, obtaining thiopropargyl glycosides with a length up to four units of mannose (figure 5.8).

The purification of mixture was done by three different chromatographic approaches yielding different oligosaccharides as showed in Table 5.4.

These molecules were analyzed by NMR spectroscopy and represent a good library of α -(1→2) mannoses with an alkyn group suitable in click chemistry.

References

- ¹ Scalan C.N., Pantophlet R., Wormald M.R., Saphire R., Wilson I.A., Katinger H., Dwek R.A., Rudd P.M., and Burton D.R.; The broadly neutralizing anti-human immunodeficiency virus type 1 antibody 2G12 recognize a cluster of $\alpha(1-2)$ mannose residue on the outer face of gp120; *Journal of virology*; **2002**; Vol.76; pp. 7306-7321.
- ² Calarese D.A., Scalan C.N., Zwick M.B., Deechongkit S., Mimura Y., Kunert R., Zhu P., Wormald M.R., Stanfield R.L., Roux K.H., Kelly J.W., Rudd P.M., Dwek R.A., Katinger H., Brton D.R., and Wilson I.A.; Antibody domain exchange is an immunological solution to carbohydrate cluster recognition; *Science*; **2003**; Vol. 300; pp. pp. 2065-2071.
- ³ Leoneti V.A., Campo V.L., Gomes A.S., Field R.A., and Carvalho I; Application of copper(I)-catalysed azide/alkyne cycloaddition (CuAAC) “click chemistry” in carbohydrate drug and neoglycopolymer synthesis; *Tetrahedron*; **2010**; Vol. 66 (49); pp. 9475-9492.
- ⁴ Trombotto S., Ladavière C., Delome F., and Domard A.; Chemical preparation and structural characterization of a homogeneous serie of chitin/chitosan oligomers; *Biomacromolecules*; **2008**; Vol.9; pp.1731-1738.
- ⁵ Bacon J.S.D, Farmer V.C., Jones D, and Taylor I.F.; The glucan components of the cell wall of baker’s yeast (*Saccaromyces cerevisiae*) considered in relation to its ultrastructure; *Biochem. J.*; **1969**; Vol. 114 (3); pp. 557-567.
- ⁶ Marzaioli A.M., Bedini E., Lanzetta R., Perino V., Parrilli M., and De Castro C. Preparation and NMR characterization of glucosamine oligomers bearing an azide function using chitosan; *Carbohydrate Polymers*; **2012**; Vol.90, pp. 847-852.
- ⁷ Lee M, Nah J.W., Kwon Y., Koh J.J., Ko K.S., and Kim S.W.; Water-soluble and low molecular weight chitosan-based plasmid DNA delivery; *Pharm Res.*; **2001**; Vol. 18 (4); pp. 427-31.
- ⁸ Richardson S.C., Kolbe F., and Duncan A., Potential of low molecular mass chitosan as a DNA delivery system: biocompatibility, body distribution and ability to complex and protect DNA. *Int. J. Pharm.*; **1999**; Vol. 178 (2); pp. 231-243.
- ⁹ Sato T., Ishii T., and Osahata Y.; In vitro gene delivery mediated by chitosan effect of pH, serum, and molecular mass of chitosan on the transfection efficiency; *Biomaterials*; **2001**; Vol. 22 (15); pp. 2075-2080.
- ¹⁰ Kulbokaite R., Ciuta G., Netopilik M., and Makuska R.; N-PEG’ylation of chitosan via “click chemistry” reactions; *Reactive & Functional Polymers*; **2009**; Vol. 69(10), pp. 771-778.
- ¹¹ Goddard-Borger E.D., and Stick R.V.; An efficient, inexpensive, and shelf diazotransfer reagent: Imidazole-1-sulfonyl azide hydrochloride; *Org. Lett.*, **2007**, Vol. 9 (19), pp. 3797–3800.

¹² Marzaioli A.M., Bedini E., Lanzetta R., Parrilli M., and De Castro C.; Conversion of yeast mannan polysaccharide in mannose oligosaccharides with a thiopropargyl linker at the pseudo-reducing end; *Carbohydr. Res.*; **2014**; Vol.383; pp.43-49.

¹³ Nakajuama T; and Ballou C.E.; Carbohydrate fragments obtained from *Saccaromyces cerevisiae* manna by alkaline degradation; *jbc*; **1974**; Vol.249; pp.7679-7684.

¹⁴ Valerio S., Iadonisi A., Adinolfi M., and Ravida A.; Novel approaches for the synthesis and activation of thio-and selenoglycoside donors; *J. Org. Chem.*; **2007**; Vol.72; pp. 6097-6106.

¹⁵ Bock K, and Pedersen C. 1983. Carbon-13 nuclear magnetic resonance spectroscopy of monosaccharides; *Adv Carbohydr Chem Biochem.*; Vol. 41; pp. 27–65.

Part III: Experimental

Chapter VI: Experimental method

6.1 General (ELECTROPHORESIS, NMR, MALDI; GC-MS, DLS, CHROMATOGRAPHIC PURIFICATION, HPLC)

Samples were run on discontinuous SDS-PAGE (Sodium Dodecyl Sulfate Polyacrylamide Electrophoresis) with the Mini Protean III Bio-Rad system run at 150 constant voltages. Samples were run on 5 % stacking gel and 15 % separating gel, using LPS of *E. Coli O55:B5* as standard. Gels were stained according to the silver stain procedure for Lipopolysaccharide¹, and Alcian blue fixative for negative charged polysaccharides².

NMR analyses of pure CPS were performed on a Bruker 400 MHz and on a Bruker 600 MHz equipped with a cryo-probe. Spectra were recorded at different temperatures depending on different samples and are reported in the corresponding section. Acetone was used as internal standard (¹H 2.225 ppm, ¹³C 31.45 ppm). 2D spectra (DQF-COSY, TOCSY, NOESY, gHSQC, gHMBC and HSQCTOCSY) were recorded using Bruker software (TopSpin 3.1). Homonuclear experiments were recorded using 512 FIDs of 2048 complex with 32 scans per FID and for TOCSY spectrum a mixing time of 120 ms was applied. HSQC and HMBC spectra were acquired with 512 FIDs of 2048 complex point and 40 scans per FID for HSQC and 50 scans per FID for HMBC.

Spectra were processed and analyzed using a Bruker TopSpin 3 program.

All GC-MS analyses were performed with a Hewlett–Packard 5890 instrument, equipped with a SPB-5 capillary column (Supelco, 30 m x 0.25 i.d. flow rate, 0.8 mL/min, He as a carrier gas). EI mass spectra were recorded with ionization energy of 70 eV and ionizing current of 0.2 mA. The temperature program used for the

analyses was the following: 150 °C for 5 min, 150→280 °C at 3 °C/min, 300 °C for 5 min.

DLS analysis were conducted using Laser quantum SMD 6000 working at $\lambda=5325$ Å and at 50 mW; analysis were conducted in a thermostatic bath at 25°C.

Analytical thin layer chromatographies (TLCs) were performed on aluminium plates pre-coated with Merck Silica Gel 60 F254 as adsorbent. TLCs were developed with 10% H₂SO₄ in EtOH and warmed up to 130 °C.

The chromatography column was loaded with Merck Kieselgel 60 (63–200 mesh). All chemicals were used as received.

HPLC purifications were performed on a octyl reverse phase (RP8) column (Supelco 59354-U, 25 cm 4.6 mm i.d.) mounted on an Agilent 1100 HPLC instrument, equipped with a binary pump and an UV/vis detector. Separation was achieved working at a flow rate of 0.8 mL/min, and monitoring the eluate reading at 206 nm. Elution conditions differed for the purification strategy selected are reported in the corresponding sections. Size exclusion chromatography was run using Biogel and Sephadex gels as adsorbent, as described in the respective sections, using a RID detector (Knauer 2310).

6.2 Cell membrane constituents extraction.

6.2.1 *Rhizobium rubi*^T

Rhizobium rubi^T DSM 6772 was grown in liquid shake culture in Nutrient Broth (NB No.4, SIGMA-ALDRICH, cod.03856) medium at 28°C for 40h. Cells were collected by centrifugation (8000 rpm, 4°C, 15 min) and freeze-dried (yield 0.13% g/l).

Cells (3.1g) were extracted according to ether petroleum:chloroform:phenol 90% (8:5:2 v:v:v)³ method. Cells were suspended in the PCP solution at room

temperature for 1 hour; mixture was centrifuged (8000 rpm, 4°C, 15 min) in order to separate supernatant from pellet. This procedure was repeated three times.

After removal of the volatile solvents under vacuum, LOS was precipitate with water. Precipitate was dialyzed (cut-off 12000 Da) against water and freeze-dried (2.3% yield $\text{g}_{\text{LOS}}/\text{g}_{\text{cells}}$).

The remaining pellet was extracted following hot water:phenol (1:1 v:v) extraction⁴, pellet was suspended in 40 mL of water and an equal volume of 90% phenol mixture was incubated at 70°C, with stirring, for 1 hour. Phenol-water separation was performed by spinning at 4°C. Phenol phase was extracted two more times with hot water. To eliminate phenol all phases were dialyzed against water (cut-off 12000 Da) and finally freeze-dried. LOS was recovered only in the PCP phase.

6.2.1.1 De-O-acylation of LOS from *Rhizobium rubi*^T

LOS from *Rhizobium rubi*^T was de-O-acetylated with dry hydrazine. 70 mg of dry LOS were suspended in dry hydrazine (25 mg/mL) stirred at 37°C for 1 h. De-O-acetylated LOS was recovered by precipitation with cold acetone. Supernatant was separated from precipitate by centrifugation (8000 rpm, 4°C, 15 min) and precipitate was dried under air flux at 37°C; subsequently it was washed again with acetone (this procedure was repeated for tree times). At the end precipitate was suspended in 200 μl of water and precipitated again with cold acetone, centrifuged and freeze-dried; 41 mg (58% yield $\text{g}_{\text{de-O-LOS}}/\text{g}_{\text{LOS}}$) of de-O-acetylated were obtained.

6.2.2 *Acinetobacter baumannii* clinical isolates A74, D36, D78, D46 , F4

Acinetobacter baumannii A74, D36, D78, D46 and F4 are multidrug resistant (MDR) clinical isolates representative of a clonal lineage causing nosocomial infections on immune compromise people. These strains were isolated from different Australian hospitals.

They were cultivated in Luria Broth (LB) for 16 h at 37°C and cells were collected by centrifugation(8000 rpm, 4°C, 30 min). The cell pellet was resuspended in 0.9% saline, autoclaved and then freeze-dried (average yield ca 0.3 g/l for all strains).

Isolation of LOS was performed on dry cells, by PCP extraction (section 8.2.1) (A74 yield 0.16 % , D36 yield: 0.05% $\text{g}_{\text{LOS}}/\text{g}_{\text{cells}}$; D78 yield: 0.17% $\text{g}_{\text{LOS}}/\text{g}_{\text{cells}}$; D46 yield: 0.18% $\text{g}_{\text{LOS}}/\text{g}_{\text{cells}}$; F4 yield: 0.05% $\text{g}_{\text{LOS}}/\text{g}_{\text{cells}}$). The remaining pellets were extracted according to hot water: phenol extraction (section 8.2.1) and for all strains preliminary electrophoresis and chemical analyses showed the presence of polysaccharidic material attributable to a capsule polysaccharide in the water phases (A74 yield : 15% $\text{g}_{\text{CPS}}/\text{g}_{\text{cells}}$, D36 yield: 14% $\text{g}_{\text{CPS}}/\text{g}_{\text{cells}}$; D78 yield: 12% $\text{g}_{\text{CPS}}/\text{g}_{\text{cells}}$; D46 yield: 19% $\text{g}_{\text{CPS}}/\text{g}_{\text{cells}}$; F4 yield: 14% $\text{g}_{\text{CPS}}/\text{g}_{\text{cells}}$), phenol phases were not investigated.

CPSs were purified from nucleic acids, proteins and LOS by enzymatic treatment and, except for A74 and D36, ultracentrifugations.

Water phase was solved in the digestion buffer (100 mM TRIS, 50 Mm NaCl, 10 mM MgCl_2 , buffer at pH 7.5) at a concentration of 5 mg/mL, and treated with DNase (2 % $\text{w}_{\text{enzyme}}/\text{w}_{\text{crude CPS}}$, SIGMA-ALDRICH cod. DN25) and RNase (2% $\text{w}_{\text{enzyme}}/\text{w}_{\text{crude CPS}}$, SIGMA-ALDRICH cod. R5503) at 37°C, with stirring, over night. Subsequently, Proteinase K (1% $\text{w}_{\text{enzyme}}/\text{w}_{\text{crude CPS}}$, SIGMA-ALDRICH cod. P5147) was added and solution was heated at 60 °C for 10 hours. After dialysis (cut-off 12000 Da) the sample was freeze-dried (ca 50 % yield $\text{g}_{\text{CPS}}/\text{g}_{\text{water phase}}$ for each sample)

After dialysis, enzyme treated water phase, was solved in distilled water and ultracentrifuged (30000 rpm, 4°C, 3h), precipitate was separated from supernatant. The CPS-containing supernatant were pooled and ultracentrifuged again (30000 rpm, 4°C, 16h). Pure-CPS was found for some bacteria in supernatant but also in some case in the precipitate; as described in the respective sections (A74 yield: 8.3% $\text{g}_{\text{pure-CPS}}/\text{g}_{\text{cells}}$; D36 6.6% $\text{g}_{\text{pure-CPS}}/\text{g}_{\text{cells}}$; D78 7.1% $\text{g}_{\text{pure-CPS}}/\text{g}_{\text{cells}}$; A388 6.8% $\text{g}_{\text{pure-CPS}}/\text{g}_{\text{cells}}$; D46 4.7% $\text{g}_{\text{pure-CPS}}/\text{g}_{\text{cells}}$; F4 5.5% $\text{g}_{\text{pure-CPS}}/\text{g}_{\text{cells}}$).

6.2.3 *Acinetobacter parvus 11G*, *Stenotrophomonas maltophilia (BRT112)*, *Delfia acidovorans (30F)*

6.2.3.1 *Acinetobacter parvus 11G*

Acinetobacter 11G cells (8.0 g) were extracted according to PCP and hot water/phenol (1/1 v/v) extractions (section 8.2.1). LOS 62 mg (0.8 % yield $\text{g}/\text{g}_{\text{cells}}$) was found in PCP phase. Remaining pellet was extracted via hot water/phenol extraction; obtaining 1.225 g (15.2% yield $\text{g}/\text{g}_{\text{cells}}$) from the water phase and 405 mg (5.1 % yield $\text{g}/\text{g}_{\text{cells}}$) from phenol phase. Since preliminary analysis showed that LOS with a good degree of purification was found only in PCP precipitate only this sample was used for the chemical and spectroscopic analyses.

6.2.3.2 *Stenotrophomonas maltophilia (BRT112)*

Stenotrophomonas maltophilia (BRT112) cells (11.5 g) were extracted according to PCP and hot water:phenol methods (8.2.1). In the PCP phase were obtained 70 mg (0.6 % yield $\text{g}/\text{g}_{\text{cells}}$) of LPS (precipitation of LPS in this phase could be related to

its lipophilic nature). Remaining pellet was extracted by hot water:phenol extraction. In this case it was not possible to separate water phase from phenol phase; mixture was dialyzed, freeze dried and 1.613 g (14.1 % yield g/g_{cells}) were obtained. Since preliminary analyses showed the presence of LPS, this sample was centrifuged (8000 rpm, 4°C, 20 min) and precipitate (544 mg 4.7% yield g/g_{cells}) was separated from supernatant. This was ultracentrifuged (30000 rpm, 4°C, 1h) obtaining 254 mg of precipitate (2.2 % yield g/g_{cells}) while supernatant was ultracentrifuged again (40000 rpm, 4°C, O.N.). 657 mg (5.7 % yield g/g_{cells}) of supernatant and 190 mg (1.6 % yield g/g_{cells}) of precipitate were obtained. All samples were analyzed by SDS page and LPS was found in the last precipitate.

6.2.3.3 *Delftia acidovorans* (30F)

Delftia acidovorans (30F) cells (13.7 g) were extracted according to PCP extraction and hot water/phenol protocols (8.2.1). LOS was not found in PCP phase. The remaining pellet was then extracted by hot water:phenol extraction obtaining 0.460 mg (3.6 % yield g/g_{cells}) from water phase and 850 mg (6.2% yield g/g_{cells}) from phenol phase. Preliminary SDS-PAGE and ¹H-NMR analyses showed the presence of LPS contaminated by a large amount of nucleic acids and proteins in both phases.

Crude material present in water phase was purified by enzymatic treatment (section 8.2.2) and 127 mg of LPS (0.9 % yield g/g_{cells}) were obtained.

Crude material from phenol phase, was also purified via enzymatic hydrolysis. After dialysis, enzyme treated phenol phase was solved in distilled water and centrifuged (8000 rpm, 4°C, 15 min); precipitate (28 mg , 0.20% yield g/g_{cells}) was separated from supernatant. The latter was ultracentrifuged (30000 rpm, 4°C, 1h) obtaining 54 mg of precipitate (0.4 % yield g/g_{cells}), while supernatant was further ultracentrifuged (30000 rpm, 4°C, 5h); supernatant (170 mg, 1.2% yield g/g_{cells})

was then separated from precipitate (71 mg, 0.5% yield g/g_{cells}). To obtain LPS with a high grade of pureness, precipitate was suspended in ca 2 mL of water and ultracentrifuged again (40000 rpm, 4°C, O.N.) to obtain 61 mg of precipitate (0.4% yield g/g_{cells}) and 8 mg of supernatant (0.05% yield g/g_{cells}). All the samples obtained from this purification were analyzed by SDS-PAGE.

6.3 Methyl glycosides acetylated M.G.A. and fatty acid methyl esters F.A.M.E⁵.

Total fatty acid content and monosaccharide composition were determined by treating the crude material obtained by extractions (1 mg) with methanolic HCl 1 M at 80 °C for 16 h. The solution was extracted three times with an equal volume of *n*-hexane; the top layers (*n*-hexane) were combined and dried. Fatty acids methyl esters (FAME) were analyzed directly by GC-MS. The bottom layer (methanol) was dried and the *O*-methyl glycosides were acetylated with dry pyridine (100 µl) and Ac₂O (50 µl) at 80 °C for 20 min. The mixture of acetylated *O*-methyl glycosides was analysed by GC-MS.

6.4 Partially methylated alditol acetates A.A.P.M⁵.

Glycosyl-linkage analysis was performed derivatizing monosaccharides as partially methylated alditol acetates (PMAA) and analysed by GC-MS⁶, 1-2 mg of sample was solubilized in dry DMSO (1 mL) and then powdered NaOH (100 mg) was added to promote the sugars deprotonation (3 h, 25 °C). Solution was treated with 200 µl of iodomethane (from 0°C to 25 °C, 16 h) and per-*O*-methylated lipopolysaccharide was extracted by adding water and chloroform to the reaction mixture. The organic layer was washed with 50 mL of water, dried under vacuum,

dissolved in 2 M TFA. After 1 h at 120 °C, it was dried and acid traces were removed by isopropanol washing and drying. Partially methylated monosaccharides were converted in alditols by reduction with NaBD₄ in ethanol (1 h, 25 °C), followed by borates treatment with methanol and AcOH. Methylated alditols were finally acetylated (150 μ l of Pyr, 150 μ l of Ac₂O, 80 °C, 30 min.) and salts removed with water-chloroform extraction.

6.5 Octyl glycosides acetylated

The absolute configuration was determined by GC-MS analysis of the chiral 2-octyl⁷ derivatives. Starting from M.G.A., samples were treated with 200 μ l of 2-(-)-octanol and 14 μ l of CH₃COCl at 60°C over night. Excess of octanol was eliminated under air flux; then octyl glycosides were acetylated with 200 μ l of Pyr and 100 μ l of acetic anhydride at 80°C for 30 minutes. The mixture of octyl glycosides acetylated was analyzed by GC-MS.

6.6 Mild acid hydrolysis of CPSs

Protonic spectra of pure CPSs from *A.baumannii* A74, D36 and D78, as showed in figure 3.3 part a, in figure 3.7 part a, and in figure 3.21 part a, returned very broadly signals. In order to obtain structures easier to be analyzed by NMR, pure CPSs were depolymerised by mild acid treatment.

6.6.1 Mild hydrolysis and purification of CPS from *Acinetobacter baumannii* A74

Purified CPS (10 mg) was hydrolyzed in aq. 1% AcOH (100°C, 2 h). The precipitate was removed by centrifugation and the supernatant was lyophilized and purified by size exclusion liquid chromatography run in water on a BioGel P-10 column (Bio-Rad, flux = 14 mL h⁻¹, d = 1.5 cm, h = 110 cm), the eluate was monitored by an on-line refractive index detector (Knauer K-2301) and fractions were pooled according to the chromatographic profile recorded. CPS (6.3 mg, 63 % yield $\frac{g_{\text{hydrolyzedCPS}}}{g_{\text{pureCPS}}}$) was recovered in the void volume of the column and used for NMR analysis, while Pse5Ac7Ac monosaccharide was eluted later⁸.

6.6.2 Mild hydrolysis and purification of CPS from *Acinetobacter baumannii* D36

Pure CPS (10 mg) was hydrolyzed with 1mL of aq. acetic acid 6% (5 h, 100°C). The precipitate was removed by centrifugation and supernatant was firstly freeze dried and then purified on BioGel P-10 gel (Bio-Rad, flux = 10 mL h⁻¹, d = 1.5 cm, h = 100 cm) using ammonium bicarbonate 50 mM as eluent. Chromatographic profile was monitored by an on-line refractive index detector (Knauer K-2301) and fractions were pooled according to chromatographic profile. CPS (1.5 mg, 15 % yield $\frac{g_{\text{hydrolyzedCPS}}}{g_{\text{pureCPS}}}$) was recovered in the void volume of column while a monosaccharide mixture (1 mg, 63 % yield $\frac{g_{\text{hydrolyzedCPS}}}{g_{\text{pureCPS}}}$) containing L-glycero-L-althro-5,7-diacetammido-3,5,7,9-tetraoxo-2-nonulosonic acid was recovered later⁹.

6.6.3 Mild hydrolysis and purification of CPS from *Acinetobacter baumannii* D78

Enzyme treated CPS (18 mg) was hydrolyzed with 1 mL of TFA 0.1M (2 h, 100°C). The precipitate was removed by centrifugation and supernatant was firstly freeze dried and then purified on BioGel P-10 gel (Bio-Rad, flux = 10 mL h⁻¹, d = 1.5 cm, h = 60 cm) using water as eluent. Chromatographic profile was monitored by an on-line refractive index detector (Knauer K-2301) and fractions were pooled according to chromatographic profile. CPS (6.0 mg, 33 % yield $\frac{g_{\text{hydrolyzedCPS}}}{g_{\text{pureCPS}}}$) was recovered in the void volume of column.

6.7 Computational analysis

Molecular Mechanic calculations were performed using MM3* force field implemented on Maestro 9.0. MM3* force field was chosen because when compared to regular MM3, it performs the treatment of electrostatic interaction in terms of charge-charge interaction instead of dipole-dipole interactions¹⁰. The molecular mechanic approach was used to optimize dihedral angles, Φ and Ψ , for each glycosidic junction. For each disaccharide entity, both Φ and Ψ were varied incrementally using a grid step of 20°. Φ is defined as H₁-C₁-O-C_{aglycon} and Ψ as C₁-O-C_{aglycon}-H_{aglycon}. Calculation was done using a dielectric constant ϵ , of 80, to mime water solvent. Flexible maps were calculated employed DRIVE utility (modulated with a DEBG option 150, which causes the program to start each minimization from the initial input file).

Different flexible maps were obtained for each glycosidic junction using 2D-plot function implemented in Maestro program. The conformation ensemble generated during the process of flexible map construction was used to calculate the simulated

intra and *inter* NOEs and the averaged distances, by using the program NOEPROM.

6.8 Total delipidation of different LPSs

In order to obtain oligosaccharidic part of LOS from *Acinetobacter 11G*, LOS was totally delipidated. The de-*O*-acylation of LOS (40 mg) was performed suspending sample in dry hydrazine (25 mg/mL) stirring at 37°C for 1h. De-*O*-acylated LOS was recovered by precipitation with cold acetone. The precipitate was centrifuged (8000 rpm, 4°C, 15 min), washed twice with cold acetone, dissolved in water and freeze-dried (35% yield). The sample was de-*N*-acylated with 4 M of KOH (10 mg/mL) for 16h at 120°C and after neutralization was desalted by gel permeation chromatography on a Sephadex G-10 (Pharmacia, 1.5 x 75 cm, eluent water, flow 12.5 mL/h) column¹¹. De-acylated oligosaccharide (4 mg, 10 % yield $\frac{g_{\text{delipidatedLPS}}}{g_{\text{pureLPS}}}$) was eluted in the void volume and was directly used for spectroscopical analyses.

6.9 Isolation of Lipid A and O-Chain from different bacteria

To obtain O-specific chain and Lipid-A, LPSs from *Stenotrophomonas maltophilia* (*BRT112*) and *Delftia acidovorans* (*30F*) were hydrolyzed with AcOH. 6 mg of samples were suspended in 600 μ l of AcOH 1% and heated at 100°C in order to promote the hydrolysis of linkage between Kdo and GlcN II of lipid-A. Heated was continued until the formation of white precipitate was observed (2h for *Stenotrophomonas* and 6h for *Delftia*). Lipid-A (1.1 mg 18% yield $\frac{g_{\text{lipidA}}}{g_{\text{pureLPS}}}$ for *Stenotrophomonas*, 1.0 mg 16.6 % yield $\frac{g_{\text{lipidA}}}{g_{\text{pureLPS}}}$ for *Delftia*) was obtained as precipitate after a centrifugation (8000 rpm, 4°C, 15 min) while O-chain was

found in the supernatant (2.1 mg 34.7 % yield $\frac{g_{O-chain}}{g_{pureLPS}}$ for *Stenotrophomonas*, 1.0 mg 10 % yield $\frac{g_{O-chain}}{g_{pureLPS}}$ for *Delftia*).

6.10 Preparation of Liposomes ToThyRu/POPC/LOS

Liposomes were prepared using lipid film procedure¹².

Partially delipidated LOS was dissolved in a mixture of chloroform, methanol and water (15:8:2 v:v:v) at a concentration of 1 mg/mL. Dissolution is slow and requires a gentle warming (40°C) and a 30 min sonication treatment. Appropriate amounts of this solution were transferred in round-bottom glass tubes and added to ToThyRu and POPC dissolved in chloroform. A thin film of the lipid was produced by evaporating the solvent with dry nitrogen gas. Final traces of solvent were removed by subjecting the sample to vacuum desiccation for at least 3h. The samples were then hydrated with H₂O and vortexed. The obtained suspension was sonicated for 3–4 h and repeatedly extruded through polycarbonate membranes of 100 nm pore sized. Hydration step was performed also in fetal serum bovine (Sigma-Aldrich F0804) in order to verify the stability of liposomes in serum.

6.11 Hydrolysis of chitosan polymer and reduction of anomeric function

Chitosan (230 mg, 1.43 mmol of GlcN, Sigma–Aldrich 448869, deacetylation degree 10%, MW 612 kDa) was dissolved in 12.5 M aqueous HCl (2.3 mL, Fluka 96208); the solution was kept at 70 °C in a thermostatic oil-bath and after 150 min the reaction vessel was cooled at room temperature, treated with 3 volumes of ice cold acetone. Chitosan oligosaccharides were recovered by centrifugation (5000 rpm, 4°C, 15 min), washed three times with cold acetone and dissolved in water;

the resulting solution was neutralized adding few drops of 5 M aqueous NaOH and freeze-dried (179 mg, 1.11 mmol of GlcN, 77.9% yield)¹³.

To reduce anomeric function chito-oligosaccharides (50 mg) were dissolved in 0.5 M AcOH/AcONa buffer (5.0 mL, pH 7.0) and reduced with NaBH₄ (3 mg) at room temperature over night; the reaction was quenched by adding with few drops of HCl 1 M and water was roto-evaporated adding MeOH.

6.12 Azidation of chitosan free amino function

Reduced chito-oligosaccharide mixture (50 mg, 0.310 mmol) was dissolved in 10 mL of phosphate buffer 1M together with K₂CO₃ (72.4 mg, 1.7 eq.), CuSO₄·5H₂O (0.77 mg, 0.01 eq.), and imidazole-1-sulfonyl azide hydrochloride (78.1 mg, 1.2 eq; Stick reagent). The mixture was stirred at room temperature for 3 hours, and the excess of Stick reagent was quenched with few drops of ethanol-amine¹⁴. The solution was directly purified by HPLC chromatography.

6.13 Chromatographic purification chito oligomers

Chromatographic separation of the mixture was achieved using an RP-8 column, working at a flow rate of 0.8 mL/min, and using a water-methanol gradient (in both solution we introduced 0.1% v/v of TFA 99% Sigma-Aldrich 411564), eluent B (methanol) changed from 5% to 40% in 30 minutes, then immediately reached and stayed at 100% for 20 minutes to return then to 5%, the initial injection conditions. Fractions were collected from column, and freeze-dried after that methanol was removed with rotary evaporator. After ¹H NMR investigation, the following products were indentified (figure 6.1) and these yields were observed: **1** (6.8 mg,

yield 13.60%), **2** (1.6 mg, 3.2%), **3** (4.3 mg, 8.6%), **4** (5.0 mg, 10%), **5** (2.8 mg, 5.6%), **6** (2.2 mg, yield 4.4%), **7** (4.8 mg, 9.6%), **8** (3.0 mg, 6.0%), **9** (3.3 mg, 6.6%)¹⁵ structure of different oligomers is reported in figure 5.1.

6.14 Acetolysis of mannan polymer

Vacuum dried mannan (574 mg) from *Saccharomyces cerevisiae* (M7504 Sigma-Aldrich) was acetylated stirring overnight at 100°C in pyridine (20 mL) and acetic anhydride (20 mL). Solvents were removed under vacuum, and brown oil was obtained (840 mg). α -(1→6)-bonds were then cleaved dissolving the crude acetylated polysaccharide in acetic anhydride (20 mL) with acetic acid (20 mL) and concentrated sulfuric acid (2 mL). The solution was stirred at 40°C overnight, poured on ice, then CHCl₃ (approx. 100 mL) was added and the slurry was neutralized with powdered NaHCO₃ until no effervescence was observed. The organic layer was concentrated and discolored by filtration on a small silica plug (about 10 grams), eluted with 95:5 v/v CHCl₃/MeOH. At this stage, a mixture of O-acetylated oligosaccharides (840 mg) was obtained and used for the successive reaction without any further purification.

6.15 Preparation of thiomannopropargyl-oligosaccharides

840 mg (1.2 mmol considering a medium DP=2 with molecular weight of 678 g/mol) of O-acetylated oligosaccharides were dissolved in CH₂Cl₂ (5.0 mL) and treated with 487 mg (1.9 mmol, 1.6 eq.) of I₂ (57652 Sigma-Aldrich), and 303 μ l (1.9 mmol, 1.6 eq.) of Et₃SiH (230197 Sigma-Aldrich). The reaction was stirred at room temperature and monitored by TLC eluted with 1:2 v/v hexane/ethyl acetate;

glycosyl iodides spot on TLC was UV-visible, while unreacted acetylated oligosaccharide, when present in the reaction mixture, gave a TLC spot visualized only by charring the silica plates with 10% H₂SO₄ in ethanol. The reaction was complete after 6 h and then the solution was diluted to 50 mL with CH₂Cl₂ and washed with aqueous sodium carbonate containing sodium thiosulfate. The organic phase was washed with water, dried over anhydrous Na₂SO₄, filtered and concentrated.

The resulting mixture of acetylated glycosyl iodides was dissolved in CH₃CN (5.0 mL) and then treated with 137 mg (1.8 mmol, 1.5 eq) of thiourea (T8656 Sigma-Aldrich), and the solution was heated at 60°C and stirred at this temperature for 3.5 h. TLC showed the formation of polar products which did not migrate in the condition reported above, confirming the consumption of the glycosyl iodide. The solution was cooled to RT and treated with 267 µl (2.4 mmol, 2 eq.) of CHCCH₂Br (P51001 Sigma-Aldrich, 80% w/v in toluene) and 669 µl (4.8 mmol, 4 eq.) of Et₃N (T0886 Sigma-Aldrich). The mixture was stirred for 2h at room temperature and TLC, eluted with 1:2 v/v hexane/ethyl acetate and charred with 10% H₂SO₄ in ethanol, showing three different products¹⁶.

6.16 Purification of different mannose oligosaccharides¹⁷

6.16.1 Silica gel chromatography of the fully acetylated mixture and RP8-HPLC purification of deacetylated fractions

The crude reaction mixture (150 mg) was purified by silica gel chromatography (hexane/ethyl acetate mixture from 4:1 to 1:4 v/v) to afford three fractions containing the alkyl thioglycosides, named Fr-A (10.2 mg; 6.7%), Fr-B (26 mg; 17.3 %), and Fr-C (41 mg; 27.3%). Fractions were deacetylated by treatment with

MeOH/H₂O/NH₄OH (1:0.9:0.1 v/v/v) at 37°C for 2h. Volatiles were roto-evaporated and the products were recovered freeze drying the remaining water.

Deacetylated fractions Fr-dA, Fr-dB, and Fr-dC were purified via RP8-HPLC; the column was equilibrated and run isocratically with 5% MeOH in water; each sample was dissolved in water (10 mg/mL), centrifuged (5000 rpm, 10 min.), and passed through 0.2 µm filters; 100 µl, equivalent to 1 mg, was injected during each run.

After freeze-drying, the following yields, scaled to the amount of the starting polysaccharide, were observed (Figure 6.8, **1** (3.1 mg, 2.8 %), **3** (14.1 mg, 12.8 %), **4** (2.8 mg, 2.5 %), **5** (10.4 mg, 9.5 %), **6** (2.4 mg, 2.2 %).

6.16.2 Deacetylation of the oligosaccharide mixture and RP8-HPLC purification

The crude reaction mixture (20 mg) was deacetylated as above (11.3 mg) and directly purified via RP8-HPLC; the sample was dissolved in water (1 mg/mL), centrifuged (5000 rpm, 10 min.), and passed through 0.2 µm filters; 100 µl, equivalent to 100 µg, was injected each run.

Chromatographic profile (Figure 5.10) showed the occurrence of several peaks, which were collected and analyzed via ¹H NMR in order to identify the thiopropargyl oligosaccharides.

This purification allowed the isolation of most of the thiopropargyl oligosaccharides; after freeze-drying the following yields, scaled to the amount of the starting polysaccharide, were observed (structures in figure 5.8): **1** (1.4 mg, 9.6 %), **2** (0.1 mg, 0.7 %), **3** (1.9 mg, 13.0 %), **4** (0.8 mg, 5.5 %), **5** (1.2 mg, 8.2 %), **6** (0.5 mg, 3.4 %), **7** (0.1 mg, 0.7 %), **8** (0.1 mg, 0.7 %).

6.16.3 Deacetylation, size exclusion chromatography and RP8-HPLC purification of oligosaccharide mixture

The crude reaction mixture (120 mg) was deacetylated as described above. The mixture (65 mg) was first purified on a Biogel P-2 column where seven fractions were obtained (Figure 6.5) :Fr-I contained **3** (11 mg) with a good grade of purity, Fr-D and Fr-E did not contain propargyl-derived oligosaccharides while for the other fractions the HPLC purification was needed.

Fr-F, G, H and L were purified via RP8-HPLC using 5% MeOH in water as eluent. Each sample was dissolved in water (10 mg/mL), centrifuged (5000 rpm, 10 min.), and passed through 0.2 μ m filters; 100 μ l, equivalent to 1 mg, was injected each run.

This procedure afforded products (Figure 5.8): **1** (4.0 mg, 4.6 %), **2** (0.3 mg, 0.3 %) **3** (13.0 mg, 14.8 %), **4** (2.2 mg, 2.5 %), **5** (5.7 mg, 6.5 %), **6** (2.7 mg, 3.1 %), **8** (3.2 mg, 3.6 %), **9** (1.3 mg, 1.5 %), with yields scaled to the amount of the starting polysaccharide.

References

- ¹ Kittelberger R., and Hilbink F.; Sensitive silver-staining detection of bacterial Lipopolysaccharides in polyacrylamide gels. *J. Biochem. Biophys. Meth.*; **1993**; Vol.26 (1);pp. 81-86.
- ² Min H., and Cowman M.K.; Combined Alcian blue and Silver staining of Glycosaminoglycans in polyacrylamide gels: application to electrophoretic analysis of molecular weight distribution. *Anal. Biochem.*; **1986**; Vol. 155 (2);pp. 275-285.
- ³ Galanos C., Luderitz O., and Westphal O.; A new method for the extraction of R Lipopolysaccharides; *Eur. J. Biochem.*; Vol. 9 (2); pp. 245-249.
- ⁴ Westphal O., and Jann K.; Bacterial lipopolysaccharides. Extraction with phenol-water and further applications of the procedure. *Meth. Carbohydr. Chem.*; **1965**; Vol.5;pp. 83-91.
- ⁵ De Castro C., Parrilli M., Holst O., and Molinaro A.; Chapter Five - Microbe-Associated Molecular Patterns in Innate Immunity: Extraction and Chemical Analysis of Gram-Negative Bacterial Lipopolysaccharides; *Methods in Enzymology*; **2010**;Vol.480; pp. 89-115: Academic Press.
- ⁶ Ciucanu i., and Kerek F.; A simple method for permethylation of carbohydrates; *Carbohydr. Res.*; **1984**; Vol.131 (2); pp.801-1808.
- ⁷ Leontein K., Lindberg B., and Lonngren J.; Assignment of absolute configuration of sugars by g.l.c. of their acetylated glycosides formed from chiral alcohols. *Carbohydr. Res.*; Vol.62 (2); pp. 359-362.
- ⁸ Kenyon J.J., Marzaioli A.M, Hall R.M., and De Castro C.; Structure of the K2 capsule associated with the KL2 gene cluster of *Acinetobacter baumannii*; *Glycobiology*; **2014**; Vol. 24 (6), 554-563.
- ⁹ Kenyon J. J., Marzaioli A. M., De Castro C., and Hall R. M.; 5,7-di-N-acetyl-acinetaminic acid: A novel non-2-ulosonic acid found in the capsule of an *Acinetobacter baumannii* isolate; *Glycobiology*; **2015**; doi: 10.1093.
- ¹⁰ Allinger N.L., Yuh Y.H., Lii J.H.; Molecular mechanics. The MM3 force field for hydrocarbons. *J. Am. Chem. Soc.*; **1989**; Vol. 111 (23), pp. 8551-8560.
- ¹¹ Gargiulo V., Garozzo D., Lanzetta R., Molinaro A., Sturiale L., De Castro C., and Parrilli M.; *Rhizobium rubi*^T: a gram-negative phytopathogenic bacterium expressing the Lewis B epitope on the outer core of its lipooligosaccharide fraction. *Chembiochem.*; **2008**; Vol. 9 (11); pp. 1830-1835.
- ¹² D'Errico G., Silipo A., Mangiapia G., Vitiello G., Radulescu A., Molinaro A.,Lanzetta R., and Paduano L.; Characterization of liposomes formed by lipopolysaccharides from *Burkholderia cenocepacia*, *Burkholderia multivorans* and *Agrobacterium tumefaciens*: from the molecular structure to the aggregate architecture; *Physical Chemistry Chemical Physics*; **2010**; Vol. 12; pp.13574-13585.

- ¹³ Trombotto S., Ladaviere C., Delome F., and Domerd A.; Chemical preparation and structural characterization of a homogeneous series of chitin/chitosan oligomers; *Biomacromolecules*; **2008**; Vol.9 (7); pp.1731-1738.
- ¹⁴ Borger E.D., and Stick R.V.; An efficient, inexpensive and shelf-stable diazotransfer reagent: imidazole-1-sulfonyl azide hydrochloride; *Org. Lett.*; Vol. 9 (19); **2007**; pp. 3797-3800.
- ¹⁵ Marzaioli A.M. , Bedini E. , Lanzetta R. , Perino V. , Parrilli M., De Castro C.; Preparation and NMR characterization of glucosamine oligomers bearing an azide function using chitosan; *Carbohydrates Polymers*; **2012**; Vol.90; pp. 847-852.
- ¹⁶ Valerio S., Iadosini A., Adinolfi M., and Ravidà A., Novel approaches for the synthesis and activation of thio- and selenoglycoside donors; *J. Org. Chem.*; **2007**; Vol.72, pp. 6097-6106.
- ¹⁷ Marzaioli A.M., Bedini E., Lanzetta R., Parrilli M., and De Castro C.; Conversion of yeast mannan polysaccharide in mannose oligosaccharides with a thiopropargyl linker at the pseudo-reducing end; *Carbohydr. Res.*; **2014**; Vol. 383; pp. 43-49.